Feasibility Study and Performance Evaluation of Vehicle-to-Everything (V2X) Communications Applications

Junsung Choi

Dissertation submitted to the Faculty of
Virginia Polytechnic Institute and State University
in partial fulfillment of the requirement for the degree of

Doctor of Philosophy
in
Electrical Engineering

Carl B. Dietrich, Chair
Alan T. Asbeck
Harpreet S. Dhillon
Jeffrey H. Reed
Yaling Yang

July 24, 2018
Blacksburg, VA

Keywords: DSRC, V2R,V2T, LTE, V2X, C-V2X, WiFi, propagation channel characteristics, adjacent channel interference, ITS band

Feasibility Study and Performance Evaluation of Vehicle-to-Everything (V2X) Communications Applications

Abstract

Junsung Choi

Vehicular communications are a major subject of research and policy activity in industry, government, and academia. Dedicated Short-Range Communications (DSRC) is currently the main protocol used for vehicular communications, and it operates in the 5.9 GHz band. In addition to DSRC radios, other potential uses of this band include Wi-Fi, LTE-V, and communication among unlicensed devices. This dissertation presents an architecture and a feasibility analysis including field measurements and analysis for vehicle-to-train (V2T) communications, a safety-critical vehicular communication application. The dissertation also presents a survey of research relevant to each of several possible combinations of radio-spectrum and vehicular-safety regulations that would affect use of the 5.9 GHz band, identifies the most challenging of the possible resulting technical challenges, and presents initial measurements to assess feasibility of sharing the band by DSRC radios and other devices that operate on adjacent frequencies using different wireless communication standards.

Although wireless technology is available for safety-critical communications, few applications have been developed to improve railroad crossing safety. A V2T communication system for a safety warning application with DSRC radios can address the need to prevent collisions between trains and vehicles. The dissertation presents a V2T early warning

application architecture with a safety notification time and distance. We conducted channel measurements at a 5.86–5.91-GHz frequency and 5.9-GHz DSRC performance measurements at railroad crossings in open spaces, shadowed environments, and rural and suburban environments related to the presented V2T architecture. DSRC systems can provide good communication range; however, the range is likely to be reduced in the presence of interference and / or Non-Line-of-Sight (NLoS) conditions. Such environmental factors are the major influence on DSRC performance. By knowing the relationship between DSRC and environmental factors, DSRC radios can be set up in a way that promotes good performance in an environment of interest. Although independent, the DSRC performance measurements and propagation channel characteristic measurements were conducted in the same locations and share the same distance parameters. Results of linear regression to analyze the relationship between DSRC performance and propagation channel characteristics indicate that additional data are required to enable robust statistical modeling. However, the DSRC links performed well in V2T measurements conducted near rural and suburban railroad crossings with varying numbers and types of obstacles to the radio signals. These results provide a strong indication that the DSRC protocol can be adapted to serve the purpose of a V2T safety warning system.

Several stakeholders, including traditional mobile operators, unlicensed Wi-Fi proponents and Cellular-Vehicle-to-Everything (C-V2X) proponents, are seeking access to the 5.9 GHz band currently used by DSRC. The FCC and National Highway Traffic Safety Administration (NHTSA), the two major organizations that are responsible for regulations related to vehicular communications, have not finalized rules regarding this band. The relative merits of the above mentioned wireless communication standards and coexistence

issues between these standards are complex. There has been considerable research devoted to understanding the performance of these standards, but in some instances there are gaps in needed research. We have analyzed regulation scenarios that FCC and NHTSA are likely to consider and have identified the technical challenges associated with these potential regulatory scenarios. The technical challenges are presented and for each a survey of relevant technical literature is presented. In our opinion for the most challenging technical requirements that could be mandated by new regulations are interoperability between DSRC and C-V2X and the ability to detect either adjacent channel or co-channel coexisting interference. We conducted initial measurements to evaluate the feasibility of adjacent channel coexistence between DSRC, Wi-Fi, and C-V2X, which is one of the possible regulatory scenarios. We set DSRC at Channel 172, Wi-Fi at Channel 169 for 20 MHz bandwidth and at Channel 167 for 40 MHz, and C-V2X at Channel 174 with almost 100% spectrum capacity. From the measurements, we observed almost no effects on DSRC performance due to adjacent channel interference. Based on our results, we concluded that adjacent channel coexistence between DSRC, C-V2X, and Wi-Fi is possible.

Feasibility Study and Performance Evaluation of Vehicle-to-Everything (V2X) Communications Applications

General Audience Abstract

Junsung Choi

Researchers and regulators in industry, government, and academic institutions are interested in vehicular communications. Dedicated Short-Range Communications (DSRC) is currently the standard protocol for communication between vehicles, including for safety applications, and operates in the band of radio frequencies near 5.9 GHz. In addition to operators of DSRC radios, other potential users are interested in using the 5.9 GHz band. This dissertation presents an architecture and a feasibility analysis including field measurements for vehicle-to-train (V2T) communications, a safety-critical vehicular communication application. The dissertation also identifies major technical challenges that could become important in the future for users of the 5.9 GHz band. The challenges will be different depending on what decisions government regulators make about the types of radios and communication protocols that are allowed in the 5.9 GHz band and about which types of radios should be used for vehicular safety.

Although wireless technology is available for safety-critical communications, few applications have been developed to improve railroad crossing safety. To prevent collisions between trains and vehicles, we present a vehicle-to-train (V2T) communication system that uses DSRC radios to provide safety warnings to motorists. Although the term V2T is used, the emphasis is on communication from the train to vehicles. We present a high-level design, or architecture, of the warning system that includes goals for safety notification time and

distance. We conducted measurements of radio channels near 5.9 GHz as well as measurements of 5.9 GHz DSRC radio link performance at the same locations (railroad crossings in open spaces, shadowed or obstructed environments, and rural and suburban environments). The measurements were performed to help decide whether the V2T warning system architecture would work.

A DSRC system can provide good communication range; however, that range could be reduced if the DSRC system experiences interference from other radios or if the signal is partially blocked due to objects between the DSRC radios. The environmental factors are the most important influence on DSRC performance. By knowing the relationship between DSRC and environmental factors, manufacturers and operators can set up the radios to perform well in environments of interest. Although DSRC performance and radio channel characteristics were measured separately, they were measured in the same locations near railroad crossings. This made it possible to perform a statistical analysis of the relationship between DSRC performance and propagation channel characteristics. This analysis indicated that additional measurements will be required to collect enough data to develop robust statistical models that relate DSRC performance directly to measured channel characteristics. However, the results of the V2T measurements that we conducted near rural and suburban railroad crossings with varying numbers and types of obstacles to the radio signals provide a strong indication that DSRC can be used for to provide V2T safety warnings.

The 5.9 GHz band has been sought after by several stakeholders, including traditional mobile operators and others who support use of the band for DSRC, unlicensed Wi-Fi, and Cellular-Vehicle-to-Everything (C-V2X) communication. The FCC and National Highway Traffic Safety Administration (NHTSA), the two major organizations that are responsible for

regulations related to vehicular communications, have not finalized the rules regarding this band. The relative merits of the above mentioned communication standards and coexistence issues between these standards are complex. There has been considerable research devoted to understanding the performance of these standards, but in some instances there are gaps in needed research. We have analyzed regulation scenarios that FCC and NHTSA are likely to consider and have identified the technical challenges associated with these potential regulatory scenarios. The technical challenges are presented and for each a survey of relevant technical literature is presented. In our opinion for the most challenging technical requirements that could result from new regulations are interoperability between DSRC and C-V2X and the ability to detect either adjacent channel or co-channel coexisting interference. We conducted initial measurements to evaluate the feasibility of adjacent channel coexistence between DSRC, Wi-Fi, and C-V2X, which is one of the possible regulatory scenarios. From the measurements, we observed almost no effect on DSRC performance when other types of radios used frequencies adjacent to the frequencies used by the DSRC radios. Based on our results, we concluded that adjacent channel coexistence between DSRC, C-V2X, and Wi-Fi is possible.

Acknowledgements

I really thank God for my 13 years of successful study abroad since high school. I appreciate my parents, Dr. Yongseok Choi and Eunkyung Choi, and my sister, Jinyoung Choi, for their support and prayers from South Korea at the opposite side of the Earth.

I highly appreciated my advising professor, Dr. Carl B. Dietrich, for his advice and support for my career since undergraduate research. Also, I appreciate Dr. Jeff Reed, Dr. Harpreet S. Dhillon, Dr. Alan Asbeck, and Dr. Yaling Yang for being my committee members.

I acknowledge Dr. Christopher R. Anderson, Dr. Vuk Marojevic, Dr. Xiaofu Ma, Dr. Seungmo Kim, Biniyam Zewede, and Aakanksha Sharma for co-authorships on several publications, guidance about how to research, and many hours to discuss research topics. For my research, I appreciate the Federal Railroad Administration and Ford Motor Company for providing funding and opportunities for conducting the research. Other than researches, I could not get through living in Blacksburg and finish degrees for the past nine years without my dearest friends, Dr. David Park, James Nutter, and Taekyoung Oh. I hope their careers in the future will go well.

It was great being a Hokie for 9 years!

No temptation has seized you except what is common to man. And God is faithful; he will not let you be tempted beyond what you can bear. But when you are tempted, he will also provide a way out so that you can stand up under it.

1 Corinthians 10:13

Contents

List of Figures

List of Tables

Abbreviations

1G	first generation
3GPP	3rd Generation Partnership Project
4G	4th generations
5G	5th generations
BPSK	Binary Phase Shift Keying
BSM	Basic Safety Message
C-V2X	Cellular Vehicle to Everything
CCH	Control Channel
CDF	Cumulative Distribution Function
CH	Channel
DAV	Detect and Vacate
DL	Downlink
DSRC	Dedicated Short Range Communications
DSSS	Direct Sequence Spread Spectrum
EMI	Electro-Magnetic Interference
FCC	Federal Communications Commission
GPS	Global Positioning System
GSM-R	Global System for Mobile Communication - Railway
ICWS	Intersection Collision Warning System
IoT	Internet of Things
IoV	Internet of Vehicles
IP	Internet protocol

ITS	Intelligent Transportation Systems
LCX	Leaky Coaxial Cables
LoS	Line of Sight
LTE-R	LTE-Railroad
LTE-U	LTE Unlicensed
LTE-V	LTE for Vehicles
LTE	Long-term evolution
NHTSA	National Highway Traffic Safety Administration
NLoS	Non Line of Sight
NPRM	Notice of Proposed Rulemaking
OBU	Onboard Unit
OFDM	Orthogonal Frequency Division Multiplexing
PDP	Power Delay Profile
PDR	Packet Delivery Ratio
PER	Packet Error Rate
PL	Path Loss
QAM	Quadrature Amplitude Modulation
QoS	Quality of Service
QPSK	Quadrature Phase Shift Keying
RF	Radio Frequency
RMa	Rural Macro
RMS	Root Mean Square
RoF	Radio Over Fiber
RSU	Roadside Unit

Rx	Receiver
SAE	Society of Automotive Engineers
SCH	Service Channel
SINR	Signal to Interference plus noise Ratio
SMa	Suburban Macro
SPS	Semi Persistent Scheduling
SVRR	Shenandoah Valley Railroad
TDD	Time Division Duplex
TTCI	Transportation Technology Center, Inc.
Tx	Transmitter
U-NII	Unlicensed National Information Infrastructure
UL	Uplink
UMa	Urban Macro
V2I	Vehicle to Infrastructure
V2P	Vehicle to Pedestrian
V2R	Vehicle to Railroad
V2T	Vehicle to Train
V2V	Vehicle to Vehicle
V2X	Vehicle to Everything
WIMAX	Worldwide Interoperability for Microwave Access

Chapter 1 Introduction

1.1 Vehicle-to-Everything (V2X) Communication

Commercial cellular wireless communication systems evolved from analog first generation (1G) cellular systems to the current fourth generation (4G) and long-term evolution (LTE), which is intended to promote further continuous evolution. Fifth-generation (5G) wireless systems are expected to extend and improve current 4G LTE cellular systems. As 5G becomes more flexible in the future, it will develop the capability to support a wide range of services: gigabit per second data throughput and low latency will enable 5G systems to support such applications as smart city cameras, self-driving cars, augmented reality, etc.

Self-driving cars, a 5G application, can be developed with a technology called connected car or the Internet of Vehicles (IoV), which is a combination of Internet of Things (IoT) and intelligent transportation systems (ITSs). Dedicated short-range communications (DSRC) is a current standard for ITS applications, so it is a natural candidate for use in IoV systems. DSRC uses center frequencies near 5.9 GHz, and it is closely related to WiFi. DSRC has been deployed to the market and its usage is slowly growing.

The distinctive end users of IoV will be vehicles and drivers, but IoV also has the potential to enable communications between road vehicles and pedestrians, trains, ships, airplanes, unmanned aerial vehicles, and much more. This is referred to as vehicle-to-everything (V2X). V2X enables numerous convenient, but not necessarily time-critical applications and services. Because V2X applications do not rely on classical vehicular communication, sufficient validation of the feasibility of these applications is required. Therefore, V2X system designs must be proven effective for desired applications.

Within V2X communications, we consider and provide contributions in three important areas: vehicle-to-train (V2T) communication, also referred to as vehicle-to-railroad (V2R), cellular vehicle-to-everything (C-V2X) communication, and propagation channels for vehicular communication.

1.2 V2T Communications

A collision between a train and a vehicle happens about once per 90 minutes in the US [1]. These accidents, which lead to injury and death, are mainly caused by drivers' lack of awareness about approaching trains. Most accidents happen near railroad-grade crossings [1, 2]. Despite efforts, like by Operation Lifesaver, installing safety related features at grade crossings, more than 80% of U.S. crossings are considered as "unprotected," meaning the crossing has no safety devices such as lights, warnings, or gates [1]. In addition, during January–December 2012, about 10% of reported train accidents were V2T collisions, accounting for almost 95% of reported train accident fatalities [2].

Through direct communication between vehicles and trains or indirect communication with the aid of a relay, V2T communication comprising the transmission and reception of warning messages will be possible. Unlike typical vehicle-to-vehicle (V2V) or vehicle-to-infrastructure (V2I) communications, the presented system is transmitting warning of an approaching train that is running on a known and fixed track. Therefore, the focus of a V2T communication application would be different from V2V or V2I communication. Because DSRC is currently used for communication among vehicles and between vehicles and roadside infrastructure, the new V2T application requires a proper feasibility study and performance evaluation in typical railroad environments.

1.3 C-V2X Communications

On February 20, 2013, the Federal Communications Commission (FCC) issued a notice of proposed rulemaking (NPRM) regarding the potential use of the 5.9-GHz DSRC spectrum by Unlicensed National Information Infrastructure (U-NII) devices. According to FCC Docket ET 13-49 [3], the FCC is considering the sharing of the 5.85–5.925-GHz spectrum between DSRC and unlicensed devices. The 5.85–5.925-GHz spectrum was originally used for DSRC with seven different channels, each with a 10-MHz bandwidth. The proposed U-NII-4 Channel 163, with a center frequency at 5.815 GHz, will correspond to the 160-MHz bandwidth. Meanwhile, the proposed U-NII-4 Channel 171, with a center frequency at 5.855 GHz, will correspond to 80 MHz, and the proposed U-NII-4 Channel 175, with a center frequency at 5.875 GHz, will correspond to 40 MHz. Finally, the proposed U-NII-4 Channel 177, with a center frequency at 5.885 GHz, will correspond to 20 MHz. As shown in the proposed U-NII-4 channel allocation in Figure 1, the lower 45-MHz bandwidth of the DSRC band may be allocated for co-channel existence or adjacent channel existence with unlicensed devices. The primary unlicensed devices could be 802.11ac or LTE devices. If LTE is used for vehicular communication and a substitute DSRC application, LTE for vehicular communication will be termed C-V2X. If 802.11ac uses the spectrum, both U-NII-4 devices and DSRC will be categorized as WiFi devices. To inform the FCC decision about permitting C-V2X or WiFi in DSRC spectrum bands, it is necessary to characterize performance of DSRC in the presence of co-channel interference and adjacent channel interference due to C-V2X and due to WiFi.

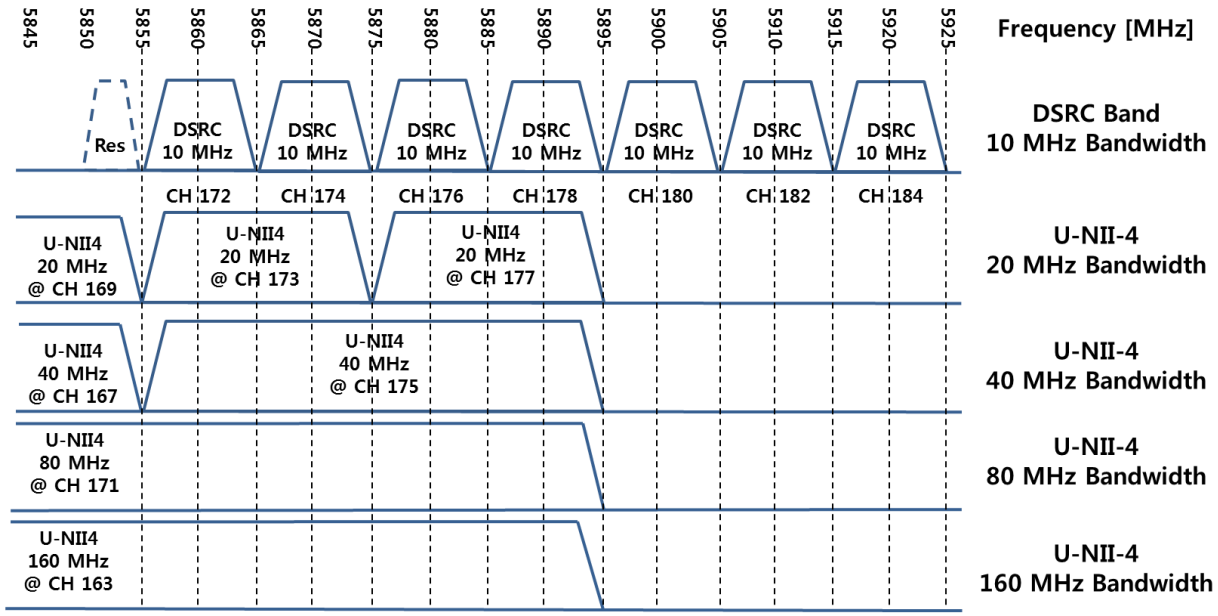

Figure 1 DSRC and proposed U-NII-4 spectrum bands

1.4 Propagation Channels for Vehicular Communications

A DSRC system has a communication range of up to 1.0 km with strong line-of-sight (LoS) communication and no interference. However, the range of communication is highly relying on the surrounded environment, and it is possible to significantly reduce due to the existence of any surrounding interference sources or non-line-of-sight (NLoS). DSRC radios and protocols already contain mechanisms that allow reliable communication in typical vehicular environments. However, the reliability is also affected by interference at the same time. Propagation channel parameters, such as root mean square (RMS) delay spread, Ricean-K factor, and path loss exponent, can represent the conditions of the surrounding propagation environment. Use of the same physical setup for DSRC radio measurements and propagation measurements can provide instantaneous numeric DSRC performance values and propagation

statistics at the same time. The relationship or correlation between propagation channel statistics and DSRC performance can be found using the same physical setting for the two types of measurements. By knowing the relationship between DSRC performance and propagation channel statistics, when a service provider is planning to implement a vehicular communication-related application in a certain place, it can estimate the DSRC performance, reducing the need for field testing. Therefore, validating the relationship between DSRC performance and propagation channel statistics reduces the cost of deploying a new DSRC infrastructure and applications.

1.5 Overview of Dissertation

The vehicular communication field is a focus of industrial and academic research and will be a major 5G wireless research area. For future research in the field, vehicular communication requires contributions from industry, the academy, and government. Their interests in vehicular communication will be different: companies must fulfill customers' needs, academic researchers seek technical advances for the field and future works, and government must ensure that development of vehicular communication is safe and protects citizens' lives. Therefore, this dissertation presents one type of vehicular communications as a critical safety application, considers upcoming regulation issues and associated technical and research challenges that would result from possible regulatory decisions, and presents measurements that evaluate feasibility of adjacent-channel band sharing between vehicular communications and other wireless technologies.

Chapter 2 Summary of Contributions

This research presents three major contributions:

1. A V2T communication feasibility study and performance evaluation
2. A strategic survey of literature related to potential regulatory decisions that identifies technical challenges associated with several possible decisions and summarizes relevant research to date related to these challenges. The results of this study can be used to set a research agenda in vehicular communications.
3. An experimental evaluation of DSRC performance in the presence of adjacent channel interference from Wi-Fi, LTE, and C-V2X signals.

2.1 V2T Communication Feasibility Study Performance Evaluation, and Statistical Analysis

The first contribution of this research is a feasibility study of V2T communication in wide-open space and shadowing environments and a performance evaluation of a DSRC radio for V2T communication in wide-open space, shadowing, rural, and suburban environments. The key aspects of the research are described below:

- This work presented a V2T communication scenario for broadcasting warning messages, which is a new type of application for V2X communication.
- This work presented the numeric requirements for and a feasibility study of V2T communications with DSRC, which is differs from prior works.
- It proposed and implemented a measurement methodology for the feasibility study and performance evaluation, which only able to find simple methods from prior works.

- It provided a recommended configuration of hardware tools used for measuring propagation channel statistics and a DSRC performance evaluation measurement.
- It characterized the impact of the propagation environment, modulation schemes, transmit power level, and antenna types on the performance of DSRC for V2T communication.
- It presented tools for propagation channel measurements and a DSRC performance measurement, similar to that presented for Contribution 1.
- It provided a measurement methodology to align two independent measurement results.
- It presented results showing propagation channel statistics relative to positions in locations shared with a DSRC performance evaluation.
- It presented a linear regression model among propagation channel statistics, the Packet Error Rate (PER), and the relative distance from a train to a crossing.
- It compared the observed models from previous works.

2.2 ITS Band Regulatory Survey

The second contribution of the research is a regulatory contingency study for FCC and NHTSA's possible spectrum sharing plan at ITS bands, presented potential technical challenges, and technical surveys related to presented technical challenges.

- FCC and NHTSA's 5.9 GHz ITS band possible scenarios are presented
- The ITS band sharing scenarios can be adaptable for sharing spectrum in other bands
- Based on technical surveys, more papers were found that related to usage of DSRC or C-V2X only than papers related to coexistence

- Technical challenges/research priorities identified for multiple regulatory contingencies
- If mandated, interoperability between DSRC and C-V2X would be the most difficult technical challenge

2.3 Adjacent Channel Interference Evaluation

The third contribution of the research is a performance evaluation of DSRC (5.855–5.865 GHz) with the existence of C-V2X, which acts as adjacent channel interference (5.865–5.875 GHz and 5.875–5.885 GHz). The outcomes of the research to date are described below:

- It provided tools not yet deployed in the actual market for measurements relevant to broadcasting DSRC-deployed technology in the spectrum band and broadcasting Wi-Fi, LTE, and modified C-V2X signals at adjacent channels.
- It provided a measurement methodology to evaluate DSRC performance by setting the adjacent interference sources at desired spectrum bands.

It provided results about the impact of adjacent channel interference from Wi-Fi, LTE, and C-V2X on DSRC performance.

Chapter 3

V2T Communication Feasibility Study and Performance Evaluation

3.1 Introduction

Collisions between trains and vehicles that lead to injury or death are mainly caused by a driver's lack of awareness of an approaching train. According to reference [2], most accidents happen near railroad-grade crossings. Efforts such as Operation Lifesaver to implement safety related features at crossings improved the safety at many grade crossings, but about 80% of U.S. crossings are still considered as *unprotected*, meaning the crossing has no lights, warnings, or gates [4]. In addition, in 2016, about 95% of all reported railroad accidents were due to V2T collisions [2].

For ITSs, DSRC [4] is the major recommended protocol for V2V and V2I communications. DSRC's center frequency is at 5.9 GHz, with seven 10-MHz channels between 5.850 and 5.925 GHz. One feature of DSRC is an early warning system to avoid a potential vehicle collision [5].

Unlike typical V2V or V2I, V2T collisions feature several different aspects. The usual communication environment near a crossing is similar to an intersection on a vehicle road; however, the visibilities of trains and vehicles are different. At typical vehicle intersections, drivers are able to view the other vehicles at the other points of the intersection, as well as to prepare for a potential accident, to an extent. However, drivers find it hard to prepare for oncoming trains due to a blocked view or the fact that it is difficult for a vehicle to stop once

the driver notices an oncoming train. In addition, the time to stop is different; trains take much longer than a vehicle to stop, and vehicle drivers are able to react faster to avoid collisions. Therefore, the safety warning applications used for trains must differ from those used for vehicles.

In this section, the V2T communications architecture for an early warning application is presented. Because it is more difficult for a train driver to react than for a vehicle driver, the train's role is always transmitter and the vehicle's role is receiver in the architecture. The designed system targets messages transmitted from a train approaching a crossing and running on a known track. The DSRC receivers in the road vehicles near the crossing determine whether to trigger a warning based on the location difference between the oncoming train and the position of the vehicle.

We measured the DSRC performance, as well as the wireless propagation environment, under a variety of operational conditions. The measurements used place at crossings of the Transportation Technology Center, Inc. (TTCI) at Pueblo, Colorado, and the Shenandoah Valley Railroad (SVRR) at Staunton, Virginia.

We presented a V2T communications architecture for early warning systems with scenarios and safety requirements related to train and vehicle speeds and stopping distances. Through the DSRC performance measurements, we evaluated the feasibility of adapting DSRC to the proposed V2T communications architecture to enable a warning application that meets the safety requirements, such as packet reception within the stopping distance, to prevent collisions. From the wireless propagation measurements, we compared the propagation channel characteristics of our measurements and characteristics of V2V or V2I cases from previous works to identify near environments.

The setups for DSRC radios can be defined into regulatory parameters which are fixed and selective by the environments that radios face and the setup is highly effective by environmental parameters which are flexible and easily different by where the radio will deploy. By knowing the expected DSRC performance under certain combinations of environmental parameters, DSRC can select the setup based on fixed regulatory parameters and provide the best performance under the environment. Table I showed the types of environmental parameters, values for DSRC, and considerable environmental parameters.

Within the considerable parameters, we selected propagation channel characteristics to evaluate the relationship between the parameters and DSRC performance. For generating the models, the estimation methods are mainly using in the process. The estimation methods used are 1) finding mean and variance for finding one independent value at the certain setup of an experiment, 2) finding a linear model by applying linear regression models where independent and dependent aspects existing at the certain setup of the experiment.

By knowing the relationship between DSRC performance and propagation channel statistics, when a service provider is planning to implement a vehicular communication related application to a certain place, they can estimate the DSRC performance, reducing the need for field testing. Therefore, validating the relationship between DSRC performance and propagation channel statistics reduce the cost of deploying new DSRC infrastructure and applications.

Table I Regulatory and Environmental parameters

Parameter type	Parameter name	Value

Regulatory Parameter	Available BW	75 MHz (10 MHz x 7 ch + 5 MHz extra) @ 5.9 GHz
	Coexisting Technologies	Co-channel, adjacent channel
	User multiplexing schemes	TDM only
	Data channel coding	Convolutional
	Resource Selection	CSMA-CA
	Modulation support	Up to 64QAM
	Waveform	OFDM
	Transmission period	Once every 100ms/50ms
	MIMO support	No
	Data messages	50 symbols
	CP	1.6 us
	Subcarrier spacing	156.25 kHz
	Flexibility	Flexible number of OFDM symbols
Environmental Parameter	# of vehicles/km^2	
	Traffic speed	<25mph, 25~45 mph, 65mph<
	Vehicle spacing	<2m, <15m, <50m, <100m
	Terrain	Rural: wide open space, one or two low height building Suburban: more number of low height buildings
	CH condition	LOS

3.2 Related Works

Researchers have studied use of Wi-Fi-based and LTE-based systems for warning applications such as V2V and Vehicle to Pedestrian (V2P). In [6], the authors combined IEEE 802.11p-based multi-hop clustering and a 4G cellular system. Similar to the concept in [6], [7] presented Wi-Fi-associated warning applications; the difference from [6] was they focused on the performance of a single device. In [8], the authors compared the performance between IEEE 802.11p and LTE for vehicles (LTE-V) under the intersection collision warning system (ICWS), which is an environment similar to our warning application, a crossing. Moreover, we observed a similarity in the architecture in the use of a roadside unit (RSU) placed near the intersection and acting as a relay. The concept is also shown in [9], which presented a V2V relay network in an obstructed environment. The authors of [10] presented a warning application for pedestrians, named V2P. In the presented system, the minimum notification distance was represented, and our architecture has the minimum notification time and distance for safety, as well. As shown in [6]–[10], we observed a warning application representing methodologies by showing the major components, architecture, and minimum requirements for using the application, and some were similar to the methodology used to represent our architecture.

There are studies on train communications services using advanced wireless technologies, such as LTE and Global System for Mobile Communication - Railway (GSM-R). In [11], the author presents an LTE-railroad (LTE-R) testbed with an Internet protocol (IP)-based network architecture. The authors demonstrate the performance of the testbed and confirm that reliable communications and multimedia services that require high data rates are feasible. In [12], the authors propose a feasible quality-of-service (QoS) management scheme for

control train traffic using a conventional LTE system. In [11], the authors presented a GSM-R-based train-related monitoring system for the entire rail network in the UK. The authors of [14] presented technical surveys of possible candidates for railroad technologies, including GSM-R, Wi-Fi, Worldwide Interoperability for Microwave Access (WIMAX), LTE-R, Radio Over Fiber (RoF), Leaky Coaxial Cables (LCX), and cognitive radio. They concluded that WIMAX and LTE could be the best technologies for train-related communications; interestingly, the authors did not consider DSRC a candidate. We presented train communication using a DSRC protocol, one that was not considered by the authors of [11]–[13].

The concept of V2T communications was introduced in [15], which describes a vehicle-to-train early warning system that are designed and managed for trains and vehicles near railroad crossings in Australia [15]. In [15], the authors were more focused on the warning architecture and the degree of noticing warnings than the reception performance of the radio communications; without considering the reception performance, the noticing performance can differ in the various conditions in which the application will be implemented. In addition, there have been many related theoretical studies and measurement campaigns. In [16] and [17], the authors explore the antenna criteria for a railroad crossing safety application and derive an optimal antenna pattern for practical installation. While [16] and [17] present theoretical antennas, [16] presents empirical models and measurement results for 5.8-GHz propagation channels in train environments. The authors of [19] introduce a V2T early warning system architecture, and they present their DSRC performance and propagation channel measurements at the measurement sites. In [16]–[19], DSRC performance and propagation channels are measured. This paper extends our prior work in [16], [17], and [19]. In those works, DSRC technology was proven to have the potential to offer a cost-effective

approach to the deployment of an early warning system to avoid V2T collisions. We presented a more detailed V2T early warning system architecture with safety requirements and DSRC performance evaluations in six more crossings than in [19]; the results that will be presented in later sections are an extension of the studies in [16]–[19].

Studies on 5.9-GHz or vehicular communication environment propagation channel characteristics are presented in [20]–[25]. The authors of [20] measured and analyzed the propagation channel measurements at 930 MHz in a practical high-speed railway and provided a Ricean K-factor and path loss equation with the relative distance and height of a viaduct. In [21], the authors presented a path loss exponent from the measured path loss values of urban and suburban scenarios at 5.9 GHz with transmitter antenna heights of 1.5 and 3.5 m. The measurements were performed at 5.6 GHz. Also, the authors compared measured results between time- and frequency-varying K-factor in [22] and delay and Doppler spreads in [23]. Similarly, the authors of [24] and [25] measured the propagation channel at 5.9 GHz and presented a delay spread and Doppler spread in rural, urban, and highway environments. The methodology of [18] and [25], using the PDP, is used for our analysis method. From our measurement results at 5.9 GHz, including those extended from [18] and [19], we compared the values in [20]–[25] to evaluate the measurement site types and how the V2T propagation channel differs from that of V2V or V2I

3.3 V2T Communication Scenarios and Requirements

The considered V2T communication scenario comprises an oncoming train, vehicles approaching to crossing, and an infrastructure transceiver, such as a light signal or a signal

pole near the crossing. The possible early warning system for V2T communication scenarios comprises a *direct* case and *indirect warning* cases. The scenarios are shown in Figure 2.

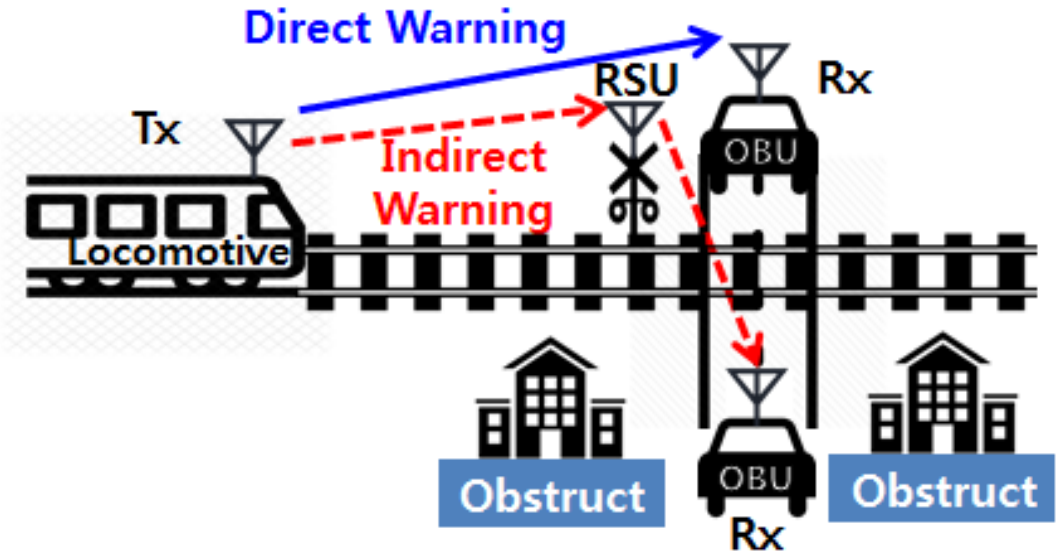

Figure 2 V2T communication scenario

For *direct warning*, the driver of vehicles receives the message about warning directly from the transmitter in the train. This scenario is preferred at low vehicle speeds and where the radio channel between the train and vehicle is a strong LoS condition.

For *indirect warning*, the train is broadcasting messages of warning to the infrastructure transceiver which placed near the crossing, a RSU, and it retransmits the messages to the on-board unit (OBU) on the vehicles; the RSU has a role of a relay. The *indirect warning* is preferable when the speed of the vehicle is higher and the propagation channel between the infrastructure and when the train has a stronger LoS component than that between the train and the vehicle.

As shown in Table I, the difference in stopping time for a slower speed, e.g., 25 mph, and a faster speed, e.g., 65 mph, is about 3 s. The difference is more critical for the train to make a decision regarding when to transmit the message; in 3 s, the train moves 13 m at a low velocity of 10 mph and 105 m at a high velocity of 79 mph. Another important aspect when deciding the boundary is the minimum notification time, which is the time when the warning message needs to be received by the vehicle driver. It should account for the recognition time about warning, reaction time after notifying the warning, and stopping time. By knowing when the driver must be notified, the distance when the train needs to broadcast the warning message can be determined. The message needs to be received so the driver can stop the car before the crossing. The time of the warning is a function of the train and car speed and the reaction time. From Table I, the minimum notification time can be acceptable at 10 s, while 15 s can provide more time to take action. With the given notification time from Table I, the car driver must receive the message when the train is at least at the distance shown in Table II. The differences due to different train and vehicle speeds and notification time requirements require a proper warning message schedule as a function of the speeds, geometry, communications, and other delays.

Table II Vehicles' Average Stopping Distance With Related to Speed [26]

Vehicle Speed (mph)	Vehicle Speed (m/s)	Stopping Distance on Dry (m)	Stopping Time on Dry (s)	Stopping Distance on Wet (m)	Stopping Time on Wet (s)
25	11.11	25.5	2.3	51.3	4.62

35	15.55	41.4	2.66	82.8	5.32
45	20	59.1	2.96	118.2	5.91
55	24.44	79.8	3.27	159.3	6.52
65	28.89	103.2	3.57	206.7	7.15

Table III Notification Distances for Different Locomotive Speeds

Locomotive Speed (mph)	Locomotive Speed (m/s)	Notification Time (s)	Notification Distance (m)
10	4.44	10	44.4
		15	66.6
20	8.88	10	88.8
		15	133.2
50	22.22	10	222.2
		15	333.3
79	35.11	10	351.1
		15	526.7

3.4 Measurements Characteristics

3.4.1 Measurement Category

We took two major measurements: the DSRC performance measurement and radio frequency (RF) propagation characterization measurement. Both measurements shared the same crossing points and same locomotive; however, the tools differed.

1) DSRC Performance Measurement

The purpose of DSRC performance measurements is to evaluate the performance of V2T communication to determine whether the performance can cover the minimum notification distance for both the locomotive and the vehicle. The performance metric of DSRC is the PER, within a certain distance window, 20 m, related to the distance to the crossing point. The distance values are calculated between the crossing and instantaneous Global Positioning System (GPS) locations. The PER was calculated from the post-process by comparing the received packets and the transmitted packets.

2) RF Propagation Characterization

The RF propagation characterization measurements' purpose is to measure the propagation channel characteristics parameters for the area close to the train tracks where DSRC performance measurements were taken. Because of the DSRC performance measurements used (5.875–5.885 GHz and Channel 176), the RF propagation characterization measures the 5.86–5.91-GHz frequency range, which covers the measuring spectrum bands, with the direct sequence spread spectrum (DSSS) channel sounder [26]. The channel sounder [26] that we used transmitted a continuous waveform with a 2,047-m long sequence-spreading code, which is clocked at the rate of 25 MHz; using 50 MHz RF bandwidth. Both radios used a GNU Radio program and USRP B210. The data were scanned and saved at intervals of 0.5 s.

3.4.2 Measurement Parameters/Settings

1) DSRC Radios

For the DSRC performance measurements, Cohda MK5 DSRC radios for both the OBU and RSU [27] are used. For both the TTCI and SVRR tracks, one DSRC OBU, which acted as the transmitter, was installed on the locomotive engine and it used Channel 174 (center frequency of 5.87 GHz). The OBU antenna was placed on top of the train's long hood, right after the engineer's cab; the height from the ground to the tip of the antenna, including the height of the train, was approximately 5 m. The antenna installation is shown in Figure 3. For both the TTCI and SVRR tracks, the radios on the vehicles or the infrastructures acted as the receiver.

2) DSRC Radio Displacements

For both the TTCI and SVRR tracks, the DSRC OBU that performs as the receiver is on the roof of a bucket truck, which is about 1.7 m in height, as shown in Figure 4(b) and Figure 5(a) for the TTCI track and Figure 5(b) for the SVRR track. For the TTCI track wide-open space, named the railroad test track (RTT) setup, the DSRC OBU is placed about 50 m away from the crossing. For the TTCI track artificial shadowing, named the precision test track (PTT) setup, the DSRC OBU is placed about 3 m away from the railroad cargos, and the cargos were about 2 m away from the operating track. The displacements of the cargos are shown in Figure 6. The DSRC RSUs are placed about 6–7 m from the ground, as shown in Figure 4(a) and (b). For the SVRR track, the DSRC OBU at Crossing #2 is about 42 m away from the track, and at Crossing #5, it is about 36 m away from the track. For the DSRC RSU that performs as a receiver, the radio is hanged on the tip of a 3-m-tall tripod, as shown in Figure 5(c), and it is placed about 4–7 m away from the crossing.

Figure 3 Antenna installations for TTCI

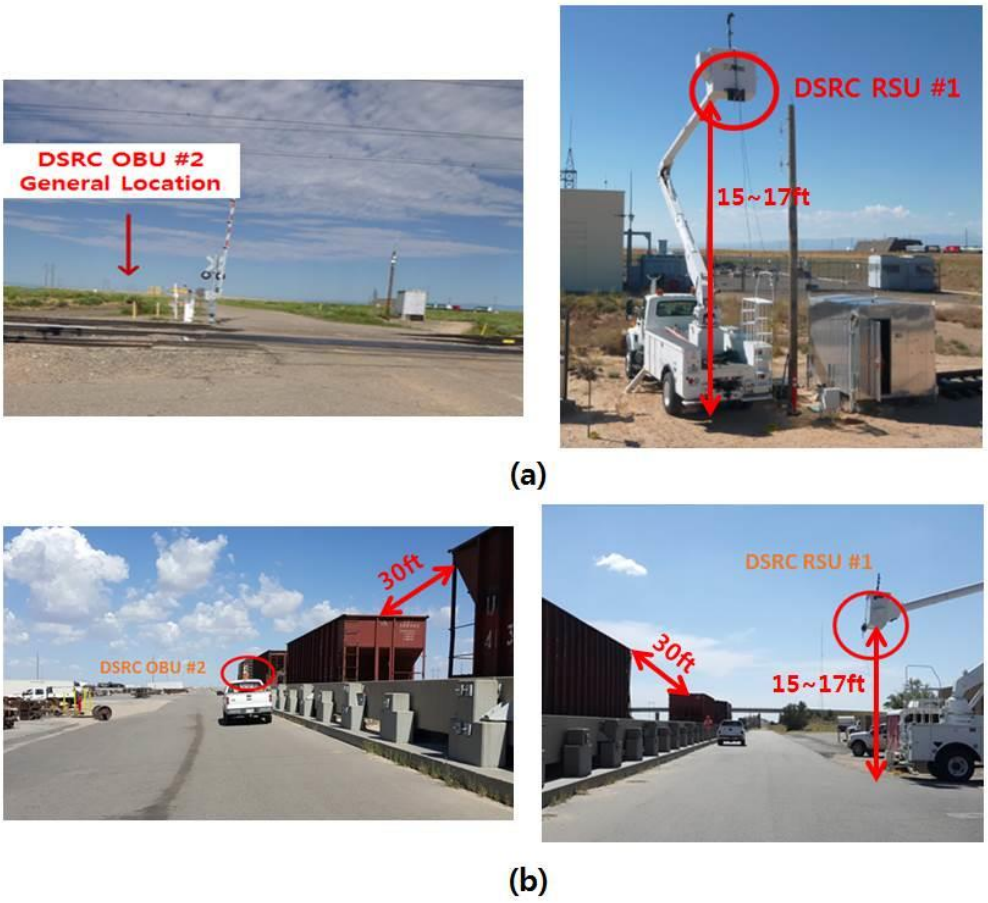

Figure 4 (a) DSRC OBU and RSU displacement for wide-open space TTCI, (b) DSRC OBU and RSU displacement for artificial shadowing TTCI

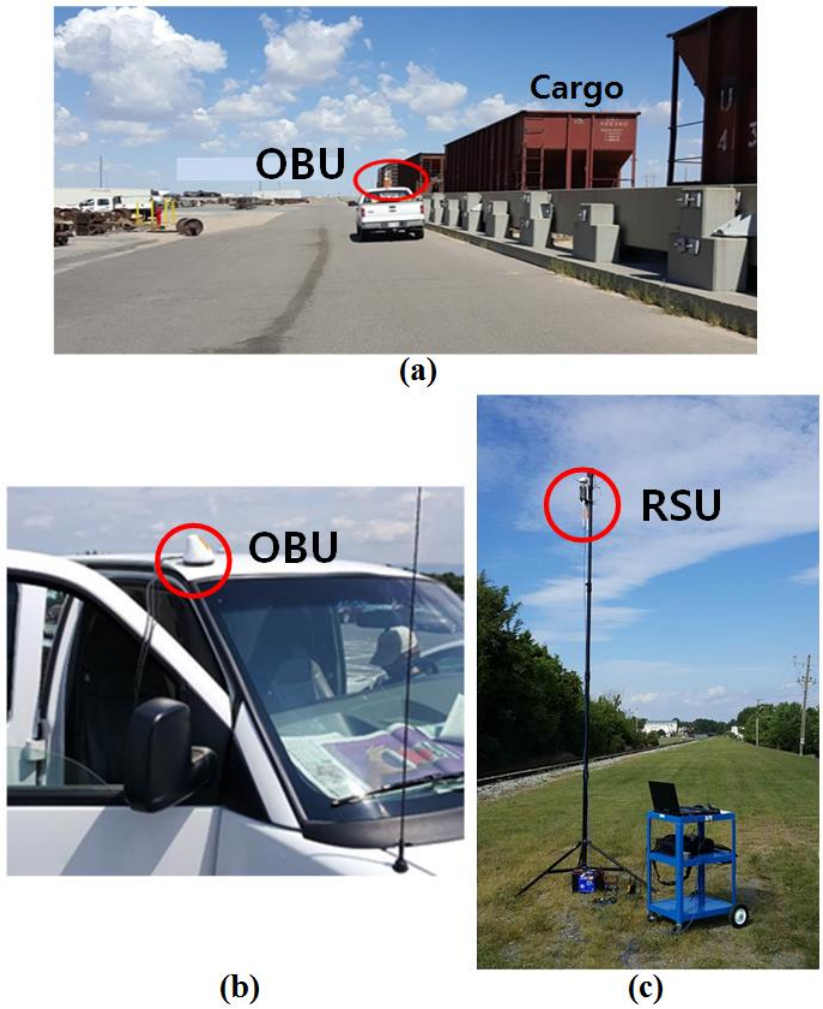

Figure 5 (a) DSRC OBU installation for shadowing TTCI, (b) DSRC OBU installation for SVRR, (c) DSRC RSU installation for SVRR

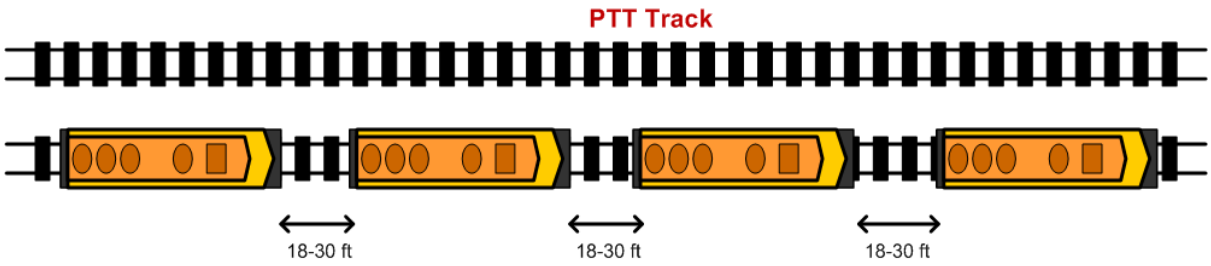

Figure 6 Displacement of the cargos for the TTCI track

3) Channel Sounder Radio Displacements

For both the TTCI and SVRR tracks, the receiver is on top of the train engine, where the DSRC transmitter is placed. For the TTCI track, the channel sounder transmitter is hanged about 10 m from the ground and placed at the end of the track; the channel sounder antenna is placed above the DSRC RSUs. For the SVRR track, the channel sounder transmitter is hanged on the tip of 3-m-tall tripod, similar to the DSRC RSU, and it is placed about 4–7 m away from the crossing.

4) Configurations

For both the TTCI and SVRR tracks, the DSRC OBU and RSU as receivers used a 6-dBi omnidirectional antenna [28]; the antenna pattern is shown in Figure 7(a) and (b). The transmitter for the TTCI track used a 12-dBi omnidirectional antenna [28] with a 23-dBm power level; the antenna pattern of the 12-dBi omnidirectional antenna [28] is the same as that of the 6-dBi antenna. The transmitter for the SVRR track used a 12-dBi omnidirectional and 12-dBi bi-directional antenna [29] with power levels of 11 and 23 dBm, respectively; the antenna pattern of the bi-directional antenna is shown in Figure 7(c) and (d). The installed omnidirectional antenna is shown in Figure 8, and the installed bi-directional antenna is shown in Figure 9. The modulation scheme for the TTCI track is QPSK, while the modulation schemes for the SVRR track are BPSK, QPSK, and 16 QAM. The hardware configuration is shown in Table IV.

Table IV Hardware Configurations

Parameter	Configuration

Antenna Type	12dBi Omnidirectional [28]/ Bi-directional [29] (Transmitters) 6dBi Omnidirectional [28] (Receivers)
Transmit Power	11 / 23 dBm
Modulation	BPSK, QPSK, 16QAM

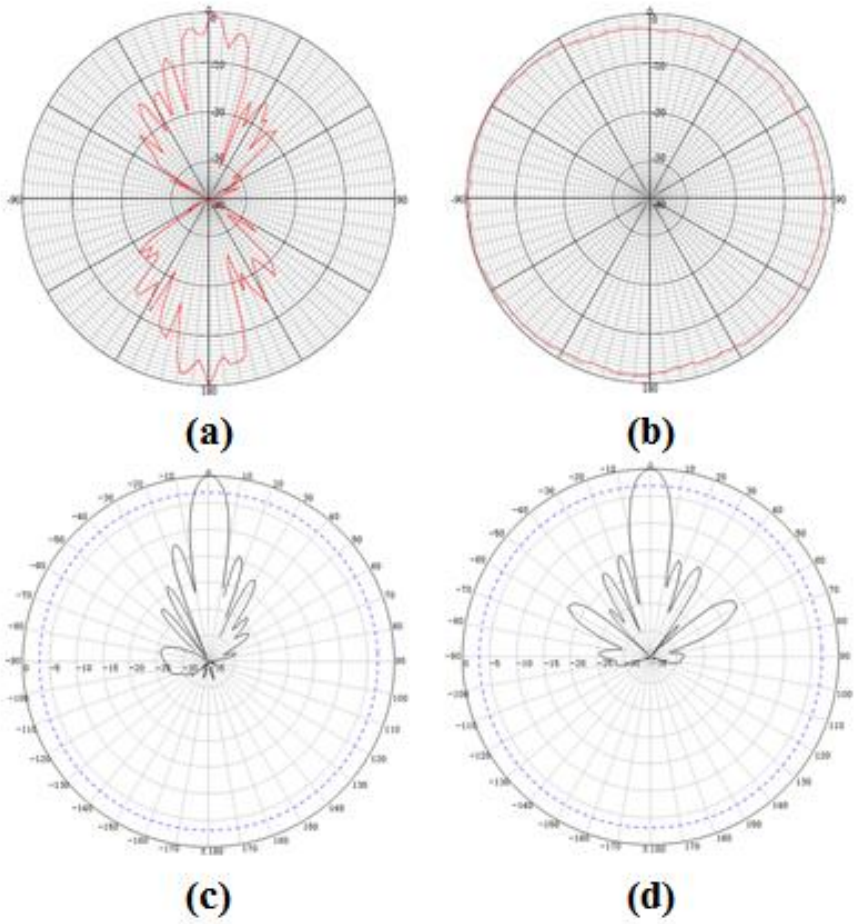

Figure 7 (a) Omnidirectional antenna's elevation pattern, (b) horizontal pattern, (c) bidirectional antenna's elevation pattern, (d) horizontal pattern

Figure 8 Omnidirectional antenna

Figure 9 Bi-directional antenna

5) Train Operations

For both the TTCI and SVRR tracks, the train made a “pass” through the measurement region. For each pass, the train started 1 km for the TTCI track and 300–400 m for the SVRR track before the crossing and it accelerated until hits the desired test speeds of 20, 50, and 79 mph for the TTCI track and 10 mph for the SVRR track. The rate of 79 mph is the highest speed a locomotive can run in the US, and 10 mph is the maximum speed allowed due to the SVRR’s track regulations. For all cases, the locomotive maintained a constant speed through the test area and then decelerated after the train passed a certain distance beyond the crossing.

3.5 Data Analysis Methods

Because V2T communication is for safety-critical applications, the performance metric should be related to the distance between the locomotive and the crossing. To be effective, the system must provide a reliable warning signal at/before the minimum notification distance for the driver to be able to react and safely stop the vehicle before the crossing.

With the different regions of interest, the evaluations of performance should be highlighted in the region; performance beyond the region may also be important because of the potential for applications other than V2T communication. If the performance is good enough within the regions, we could assume the driver is able to receive the warning messages within the minimum notification time, preventing a potential collision.

3.5.1 DSRC Data Analysis

For the DSRC performance measurements, the application named basic safety message (BSM) which using a packet size of 99 bytes was used. Each packets are continuously transmitted every 0.05 s. The PER is calculated by comparing the transmitted and received packets within

a 20-m range window. The number of transmitted packets' average is 94 within the 20-m range window, and we decided the threshold about packet reception as should receiving more than 10 packets in the window range, which represents at least one packet captured per 2-m range. With the threshold, we decided that if less than 10 packets were received within the window ranges, we would consider this to mean reliable communication was not achieved. When the PER is equal to or less than 0.9, we consider the DSRC performance as having *satisfied* the minimum requirement for safety and succeeded in receiving the warning message. PER can be given by:

$$\mathrm{PER} = 1 - \frac{Number\ of\ Received\ Packets}{Number\ of\ Transmitted\ Packets} \quad (1)$$

3.5.2 Propagation Data Analysis

With the recorded data from the channel sounder, we created the power delay profile (PDP) to evaluate the propagation channel characteristics. The PDP contains one bin per 65 ns of delay, which is the shortest time delay we can evaluate.

With the created PDP, we calculated the propagation channel characteristics. The path loss exponent, RMS delay spread, and Ricean K-factors are post-processed with the recorded data. We calculated Ricean K-factors by the ratio between the LoS, a dominant path signal power, to the multipath signal power. Ricean K-factors were calculated with the following equation:

$$\mathrm{K} = \frac{Specular\ Power}{Nonspecular\ Power} \quad (2)$$

We considered the specular power as the LoS power and the non-specular power as the reflected power in the PDP.

We calculated the RMS delay spread (τ_{rms}) and the path loss exponent (n) by comparing the LoS signal and the multipath signal. The RMS delay spread (τ_{rms}), defined as the square root of the second central moment of the PDP, is:

$$\tau_{rms} = \sqrt{\overline{\tau^2} - \bar{\tau}^2} \tag{3}$$

The second moment is given by:

$$\overline{\tau^2} = \frac{\sum P(\tau_i)\tau_i{}^2}{\sum P(\tau_i)} \tag{4}$$

The first moment of the PDP, mean excess delay, is given by:

$$\bar{\tau} = \frac{\sum P(\tau_i)\tau_i}{\sum P(\tau_i)} \tag{5}$$

$P(\tau_i)$ is the power level observed in the PDP.

The path loss exponent (n) is defined by:

$$\mathrm{n} = \frac{-(P_t - P_r + 10log_{10}K_0)}{10log_{10}d} \tag{6}$$

K_0 is the free-space path loss at the reference point where the transmitter is placed, and K_0 is given by:

$$\mathrm{K_0} = 20log_{10}\frac{4\pi}{\lambda} \tag{7}$$

where d is the distance between the channel sounder transmitter (the crossing) and the receiver (the train). With these calculations, the channel characteristic parameters can be obtained from the PDP. All calculations were done with the relative position of the train from the crossing.

For DSRC measurements, we used (1) for packets within a 20-m distance window and evaluated the performance by a metric of the PER related to distances. With the threshold of the PER at 0.9, we define whether the performance can be considered to *satisfy*. For propagation channel characteristic measurements, we used (2), (3), and (6) for the same distance window as the DSRC measurement, and we averaged the total value.

3.6 TTCI Results/Evaluations

The TTCI track tests evaluated the DSRC performance for possibly the best- and worst-case scenarios a train can face. Two scenarios are a wide-open space without any interference sources near a crossing and an artificial shadowing environment, as shown in Figure 10 and Figure 11. DSRC performance was measured in each of these environments in terms of PER as a function of the distance of the train from the crossing.

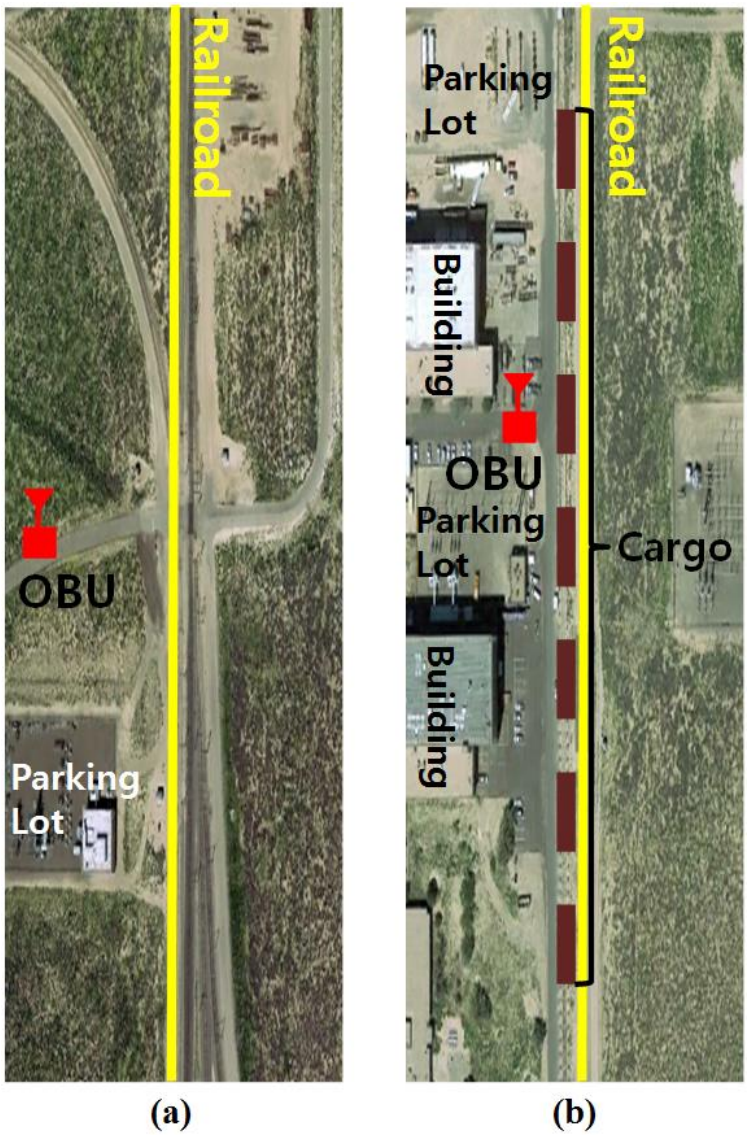

Figure 10 TTCI Tracks: (a) wide-open space and (b) artificial shadowing environment and radio displacement

Figure 11 TTCI tracks: Test site 1 (wide-open space) and test site 2 (artificial shadowing)

3.6.1 TTCI Sites

The TTCI track's environmental setups are different. As shown in Figure 10(a), the first setup is a wide-open space with no existence of any potential reflection or fading sources near the track. As shown in Figure 10(b), the second setup is an artificial shadowing environment. We artificially set seven railroad cargos, approximately 4 m in height and 10 m in length, between the track and DSRC radio, as shown in Figure 4(b). The railroad cargos are displaced between the track and DSRC receiver, so shadowing is generated.

With these two different scenarios, we evaluated the feasibility of DSRC radios for V2T communication with possibly the best- and worst-case scenarios in communications: a wide-open space and a shadowing environment.

For the TTCI track, the DSRC OBU was placed 50 m away from the track, which can be represented as a 25-mph stopping distance. The locomotive operated at speeds of 20, 50, and 79 mph. The minimum notification time of 10 s is enough time for a 25-mph speed scenario;

therefore, the regions of interest for different speeds are 88.8, 222.2, and 351.1 m before and after the crossing; these values are from Table III.

3.6.2 Propagation Channel Measurements

The propagation channel parameters, average Ricean K-factor (K_{avg}), RMS delay spread (τ_{rms}), path loss exponent (n), and its standard deviation (σ) for the wide-open space and artificial shadowing scenarios are shown in Table V. We find that the Ricean K-factors are generally consistent across the entire track, but the difference appears in different speeds; therefore, we calculated average Ricean K-factors for both tracks' PDPs with different speeds. In addition, the path loss exponents are not relevant to the different train speeds; therefore, we calculated the value for each setup. More detailed evaluations and figures are shown in Appendix A.

Table V Propagation Channel Parameters for Wide-open Space and Artificial Shadowing

Scenario	Train Speed (mph)	Train Speed (m/s)	Propagation Channel			
			K_{avg} (dB)	τ_{rms} (ns)	n	σ
Wide-open Space	20	8.88	10.9	<1	2.7	5.5
	50	22.22	9.8	8		
	79	35.11	11.3	14		
Shadowing	20	8.88	10.9	3	2.7	3.1
	50	22.22	9.8	9		
	79	35.11	11.3	4		

Interestingly, the propagation channel parameters for both tracks are similar. The delay spreads are different; however, because the unit is ns, the values are still low enough. Furthermore, the differences in the delay spreads for the different speeds are small. We expect the reason to be that the two setups have similar propagation channel parameters due to the significant height of the channel sounder transmitter. The height of the channel sounder transmitter is higher than the blocked railroad cargos; therefore, the channel sounder transmitter and receiver have clean sight and they are minimally affected by the cars. In addition, two buildings placed beside the tracks for the artificial shadowing scenario may have a minor effect.

We observe Ricean K-factors in the range of 9.76–11.31, and [22] provided 14.2 as a rural and 14.6 as an on-bridge value. Other than these two cases, the measured Ricean K-factor is higher than any values from other previous works. For the path loss exponent, we observe it near 2.8, while [21] measured it as 1.12 for suburban and 1.98 for urban regions; we can assume V2T communication faces a higher path loss exponent than the vehicle communication environment. The measured RMS delay spread is much lower than any cases shown in [23]–[25]. Therefore, under the assumption of operating in a rural environment, V2T will face a similar fading environment and greater power degradation due to a higher path loss exponent, but a lower effect from multipath components.

3.6.3 DSRC Performance Measurements

To evaluate DSRC performance, we used 1-PER to see the distribution and cumulative distribution function (CDF) of the received packets. Using these plots, we can evaluate

whether the performance can be defined as *satisfactory* in the proper regions. For a proper comparison, we choose OBU results instead of comparing both the OBU and RSU results because of a different displacement of RSU for the wide-open space and artificial shadowing environments. The results of RSU for both scenarios are shown in Appendix B.

Figure 12 shows the results of the DSRC performance for the wide-open space scenario. We can identify the DSRC performance by the PER within the region, as shown in Figure 12(a). The proper regions for speeds of 20, 50, and 79 mph are +/- 88.8, 222.2, and 351.1 m with the center at the crossing and a minimum notification time of 10 s. For the wide-open space scenario, the best environment a locomotive can face, we can identify that the performance can be *satisfied* for all three different speeds. The coverage range after the crossing is shorter than that before the crossing; we assume the existence of a blockage after the position of the antenna degraded the transmitted power, causing the results. Interestingly, we observe that the performance of DSRC might not be affected by speed in the wide-open space scenario, as shown in Figure 12(b). The coverage region seems to make a huge difference (100-m difference between each speed), but when we compare the overall packet distribution, 50% of packets were received approximately 200 m before the crossing.

Figure 13 shows the DSRC performance results for the artificial shadowing environment setup. As shown in Figure 13(a), we are able to observe the effect of shadowing. For all speeds, we observe a certain gap range, where 1-PER equals 0, and the reason for the event is due to the shadowing by the railroad cars. The DSRC performance can be identified as *satisfied* for all speeds at the minimum notification distances. The interesting aspects of the artificial shadowing environment are that the performance can be identified as *satisfied* whenever a weak signal is captured and the effect of shadowing is lesser for a faster speed.

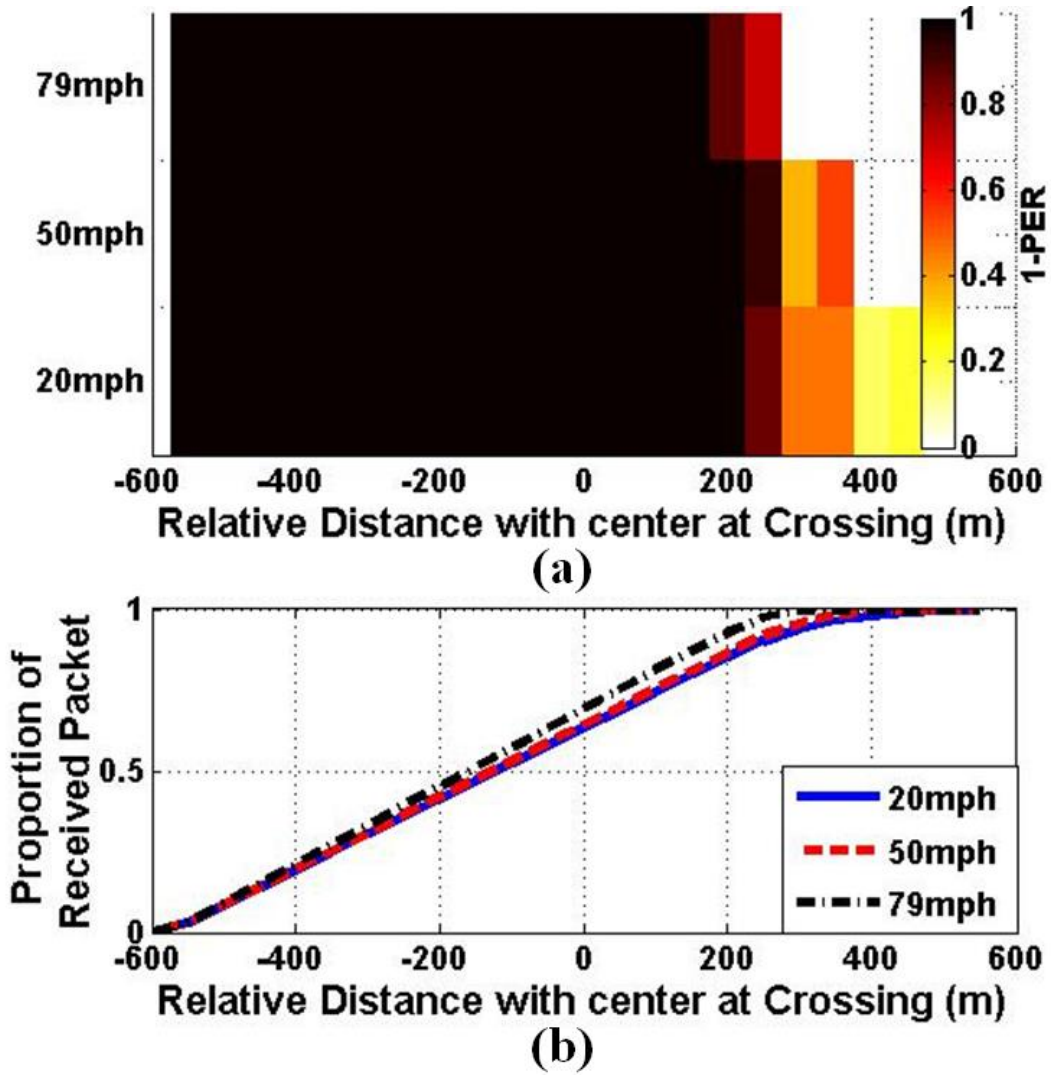

Figure 12 DSRC performance with different speeds for the wide-open space (a) distribution of the DSRC performance (1-PER), (b) proportion of received packets

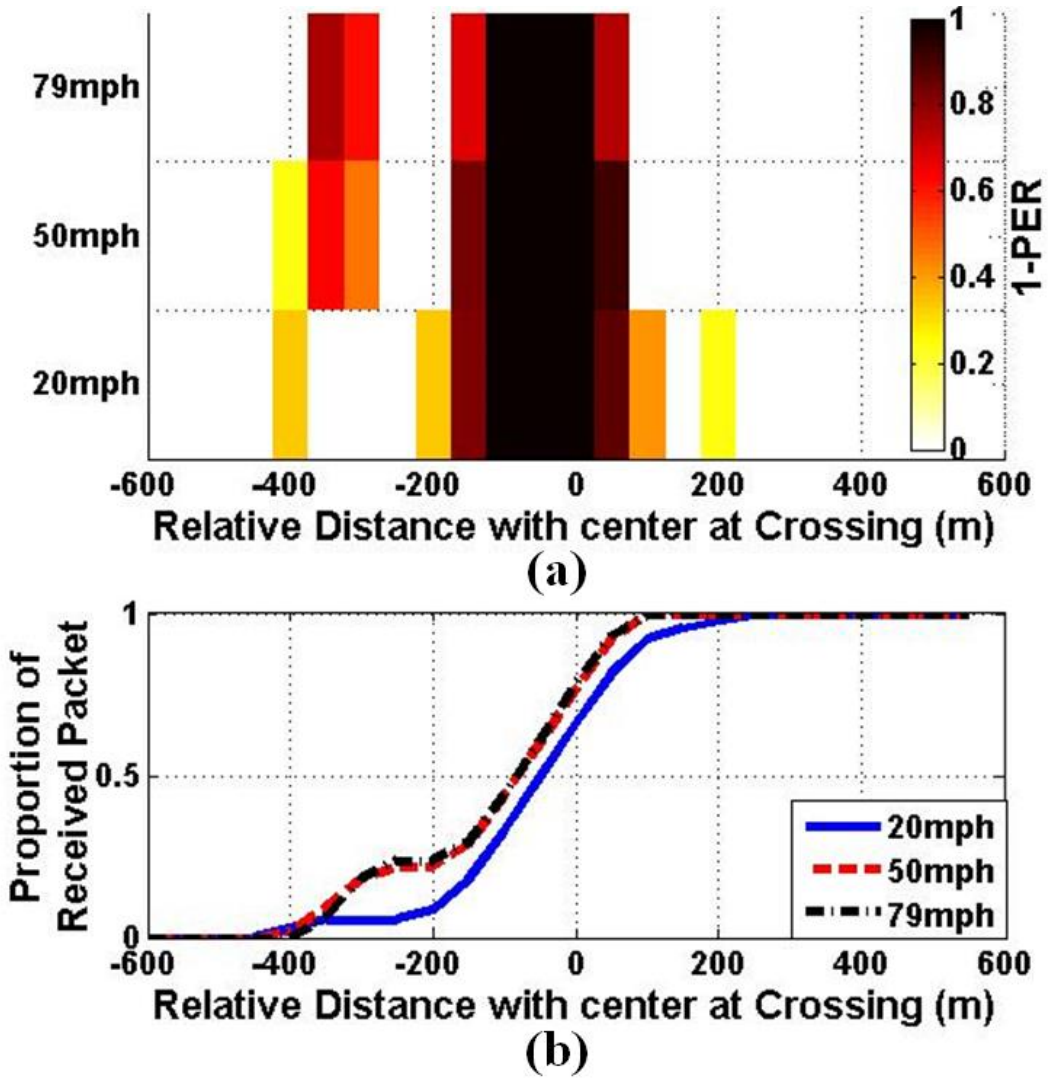

Figure 13 DSRC performance with different speeds for the artificial shadowing (a) distribution of the DSRC performance (1-PER), (b) proportion of received packets

3.6.4 Conclusions of TTCI Measurements

From the DSRC performance and the propagation channel measurements in the wide-open space and artificial shadowing setups, we observe that the DSRC performance could be identified as *satisfactory* for both the wide-open space and artificial shadowing environments, regardless of the train speed. At the same time, we observe that DSRC could receive a BSM, even if the signal is weak; whenever shadowing appears, no packet is captured by the DSRC

radio. In addition, with the assumption of operating in a rural environment, a V2T communication propagation environment will be similar to the vehicle communication-propagation environment, with a lesser effect of multipath components. From the TTCI track experiments, we identify DSRC as a feasible V2T early warning communication environment for operation in both the best- and worst-case propagation environments—a wide-open space and shadowing, respectively—a train can face.

3.7 SVRR Results/Evaluations

The SVRR tracks were used to evaluate the DSRC performance in a real environment with the desired V2T communication setup and to confirm the communication environment through propagation channel characteristic measurements. We took measurements at six different crossings, as shown in Figure 14 and Figure 15. The SVRR tracks are placed in a small town, Staunton, Virginia; therefore, the environment near the crossings has real vehicle traffic, buildings, woods, and parking lots, as shown in Figure 14. Three crossings, shown in Figure 14(a), were considered a rural environment, and three crossings, shown in Figure 14(b), were considered a suburban environment (Sheriffs-Skyview Circle in Figure 15).

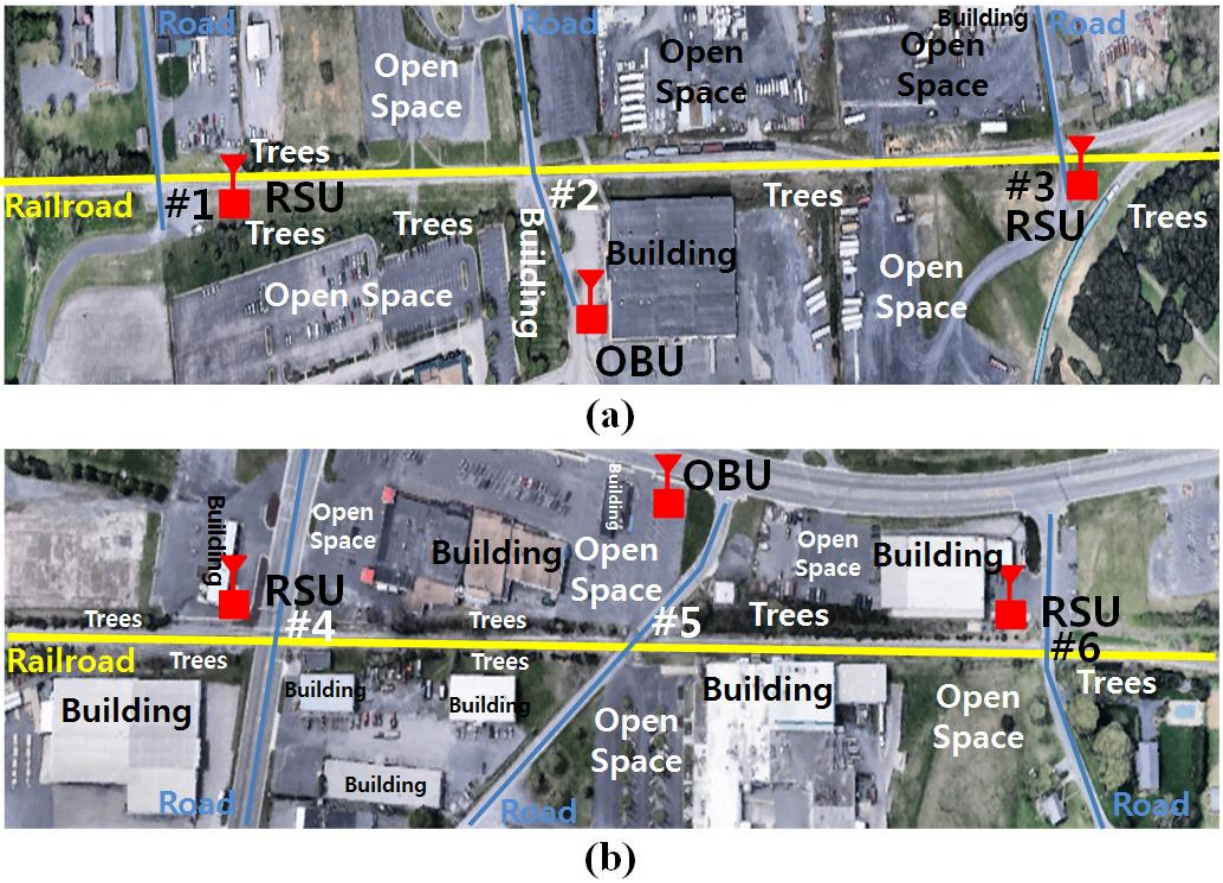

Figure 14 SVRR tracks: (a) Crossings #1, #2, and #3; (b) crossings #4, #5, and #6

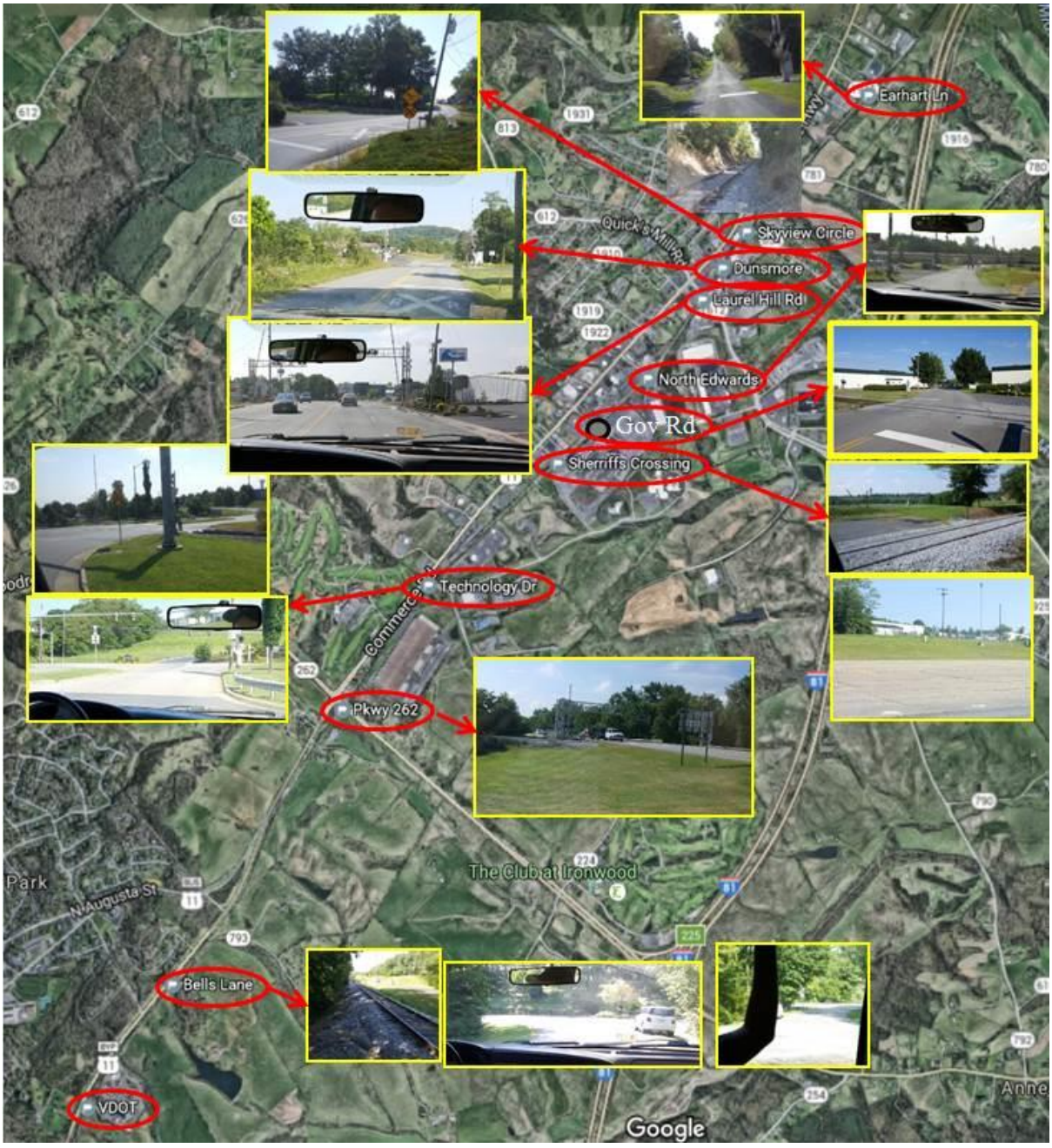

Figure 15 Crossing locations and crossing sites

3.7.1 SVRR Sites

We used six different crossings along the SVRR tracks, as shown in Figure 14. Figure 14(a) shows the environments near crossings #1, #2, and #3, while Figure 14(b) shows the

environments near crossings #4, #5, and #6. We placed the DSRC RSU at crossings #1, #3, #4, and #6, and we placed the DSRC OBU at crossings #2 and #5 for the measurements.

As shown in Figure 14(a), the environments of crossings #1, #2, and #3 feature a small number of buildings near the crossings and many open spaces between the locomotive and DSRC radios, and the potential fading sources are woods. Buildings with too low a height exist near the DSRC radio position at crossing #2.

As shown in Figure 14(b), the environments of crossings #4, #5, and #6 are somewhat more likely suburban environments than those of crossings #1 to #3. There are more buildings near crossings #4, #5, and #6 than near crossings #1–#3. Crossing #4 is located right beside a four-lane vehicle road, while crossing #5 suddenly opens from wood walls, and there are additional buildings nearby.

From the performance evaluations of the SVRR track, we may make detailed parametric decisions about V2T communications in a real environment with both a *direct* and an *indirect warning* case. The crossings using the DSRC RSU—#1, #3, #4, and #6—represent the *indirect warning*, and the crossings using the DSRC OBU—#2 and #5—represent the *direct warning* case.

On the SVRR tracks, the speed limit for vehicles is 25 mph. For this speed limit, the stopping distance is 51.3 m and the stopping time is 4.62 s, as shown in Table II. As with the TTCI scenarios, the minimum notification time of 10 s is enough for the SVRR track scenarios. Due to track regulations, the locomotive is only able to operate at 10 mph on the SVRR tracks. Therefore, the regions of interest for the SVRR tracks are 44.4 m before and after the crossings.

3.7.2 Electromagnetic Interference (EMI)

The scenarios for electromagnetic interference (EMI) measurements are 1) a **10-mph** run with the throttle notch in **idle, 2, 5, 8** and 2) a **25-mph** run with the throttle notch in **idle, 2, 5, 8**.

For each locomotive scenario, the measurement was taken using two SA-2500 spectrum analyzers; one measured EMI inside the crew cabin and the other measured EMI outside the locomotive. The SA-2500 settings were: span of 10 MHz, resolution bandwidth of 50 kHz, and reference level of -50 dBm. Each scanning process searches for 10 MHz starting from 5.85 GHz until 5.93 GHz, which covers all DSRC channels.

Sample result plots in Figure 16, Figure 17, and Figure 18 show essentially noise.

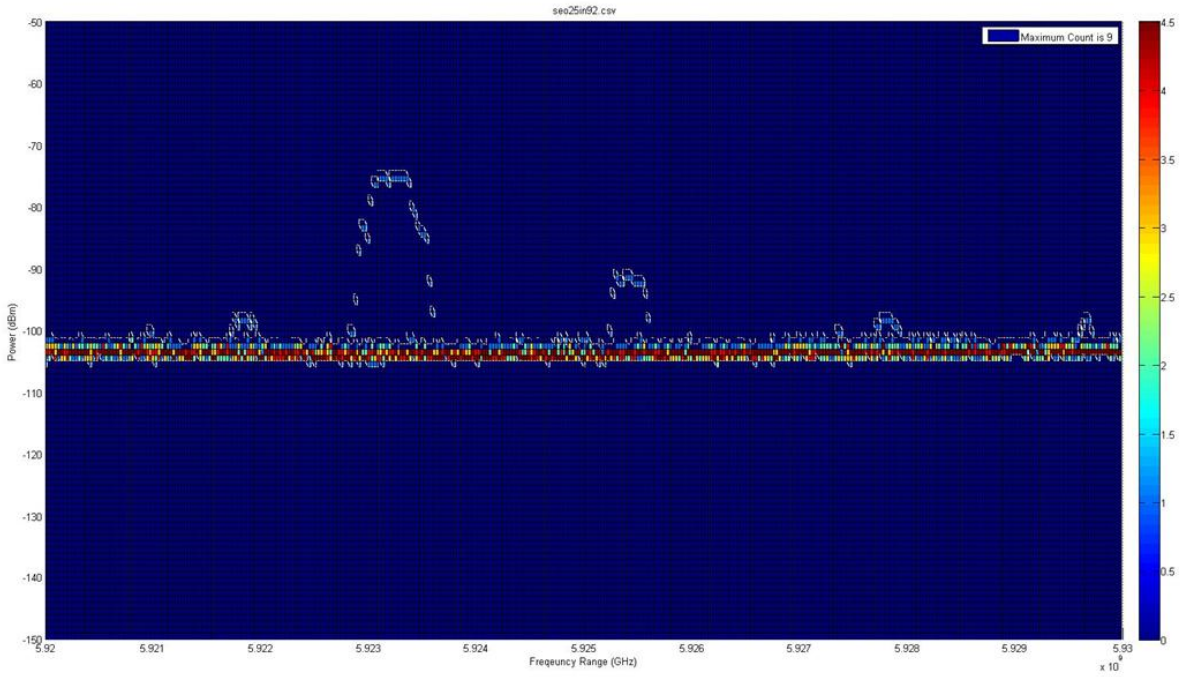

Figure 16 EMI measurement result (outside antenna, 25 mph, idle notch, no brakes, 5.92–5.93 GHz).

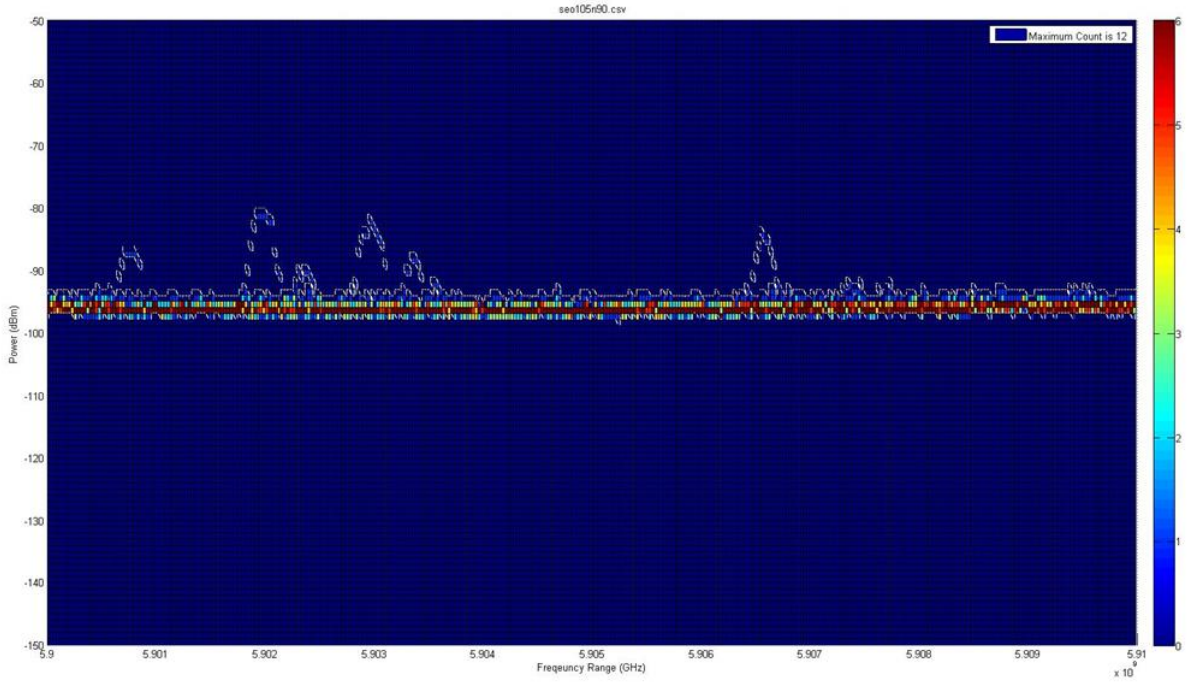

Figure 17 EMI measurement result (outside antenna, 10 mph, notch #5, no brakes, 5.9–5.91 GHz).

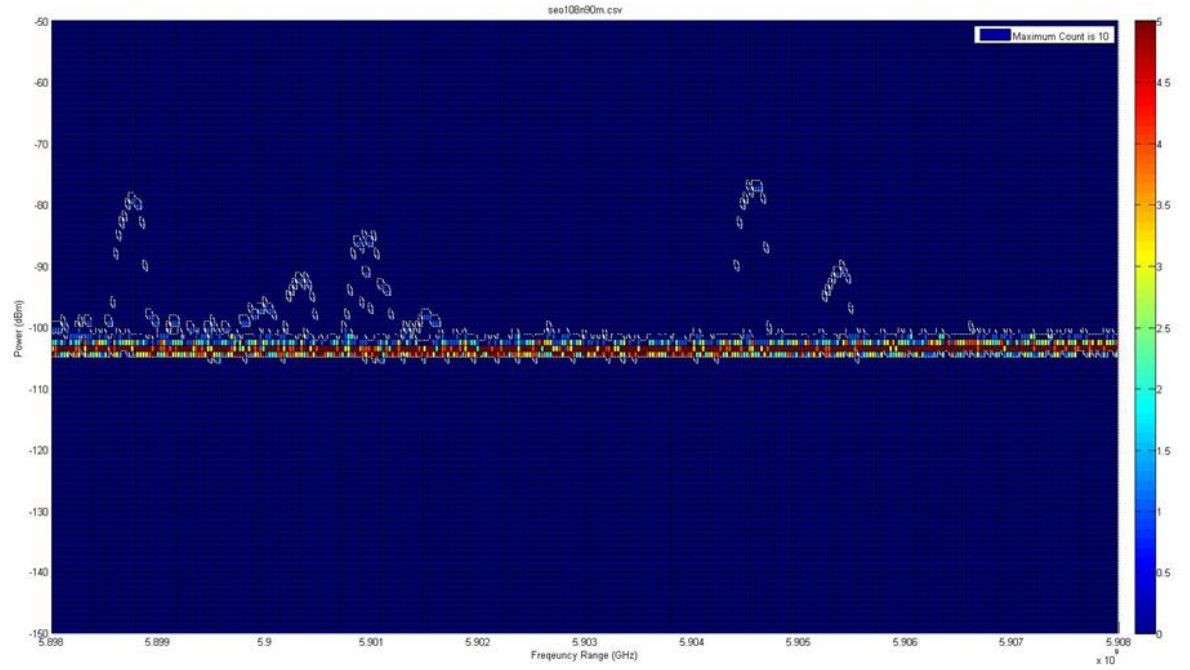

Figure 18 EMI measurement result (outside antenna, 10 mph, notch #8, no brakes, 5.898–5.908 GHz).

Occasionally, RF signals were captured, but only for one swipe, which means the signal is not generated by the locomotive. Rather, there is a possibility that when the locomotive passed a certain point at a certain time, other wireless sources were captured by our spectrum analyzers. Other than these three figures, all other plots showed consistent RF power levels corresponding to noise.

From these results, we can conclude there is no EMI from the locomotive. Some cases showed a few excursions into higher power; however, the peaks were instant and the power level was only 20–30 dBm above the baseline and lower than -70 dBm. Hence, we conclude that these signals did not come from the locomotive.

3.7.3 Propagation Channel Measurements

The propagation channel parameters for six crossings are shown in Table VI. Unfortunately, we were unable to record proper data for crossing #1 with an omnidirectional antenna. The Ricean K factor values over time and PDP values of approaching, at the crossing of, and departing from crossings #3, #4, #5 are shown in Figure 19–23 and Figures 25–30

Table VI Propagation Channel Parameters for SVRR Tracks

Crossing #	Considerable Environment	Antenna	Propagation Channel			
			K_{avg} (dB)	τ_{rms} (ns)	n (dB)	σ (dB)
1	Rural	Omni	N/A	N/A	N/A	N/A
		Bi	8.01	152	2.27	7.74
2	Rural	Omni	3.81	204	2.62	4.11

		Bi	6.3	136	1.97	5.65
3	Rural	Omni	3.96	205	2.5	3.48
		Bi	7.7	125	2.07	8.41
4	Suburban	Omni	3.16	227	3.04	5.35
		Bi	5.08	140	2.52	5.87
5	Suburban/ Urban	Omni	4.25	840	3.6	4.81
		Bi	6.83	632	3.34	6.28
6	Rural	Omni	4.56	184	2.79	4.64
		Bi	6.54	96	2.16	6.73

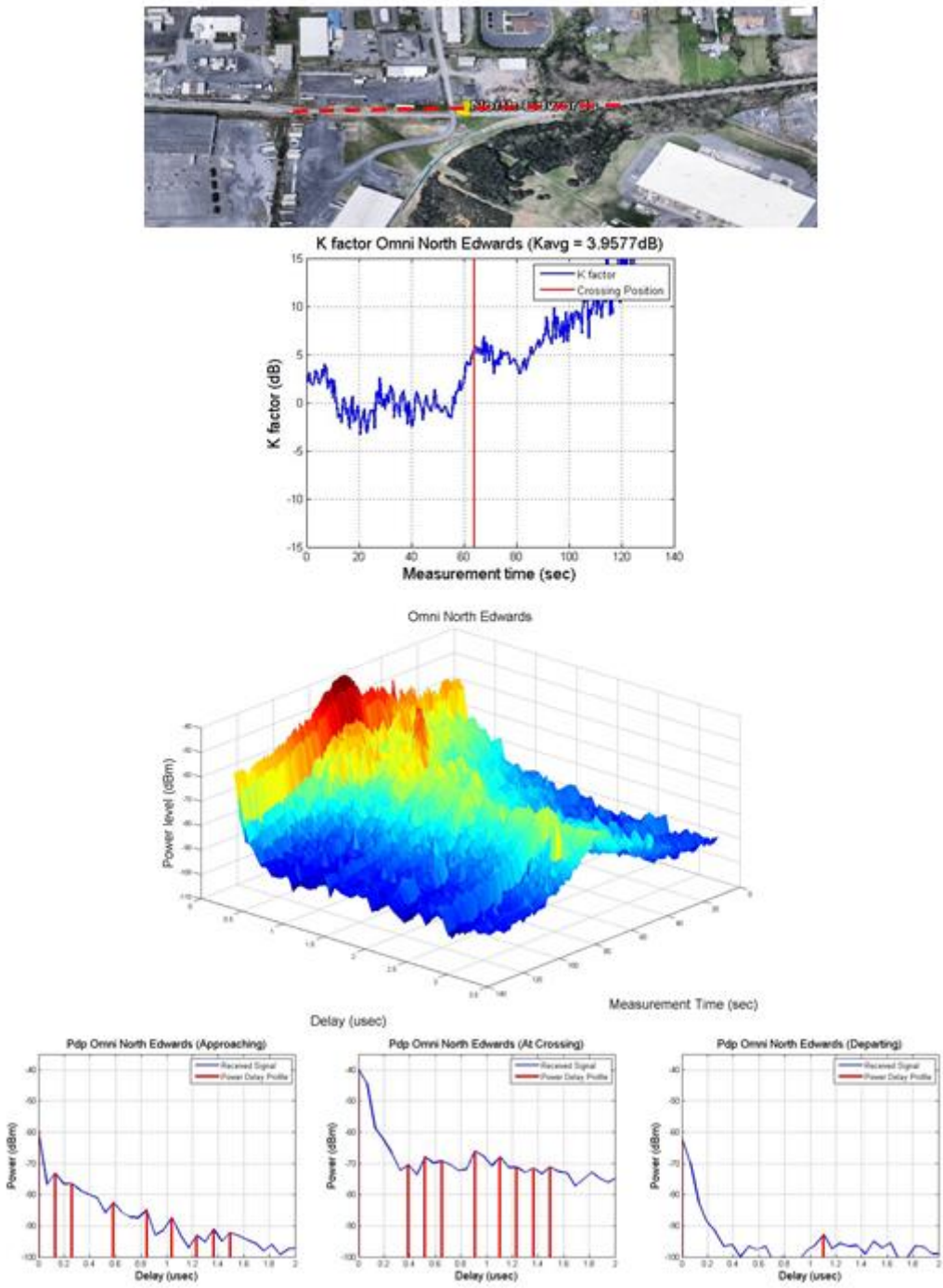

Figure 19 Ch sounder result (omnidirectional crossing #3)

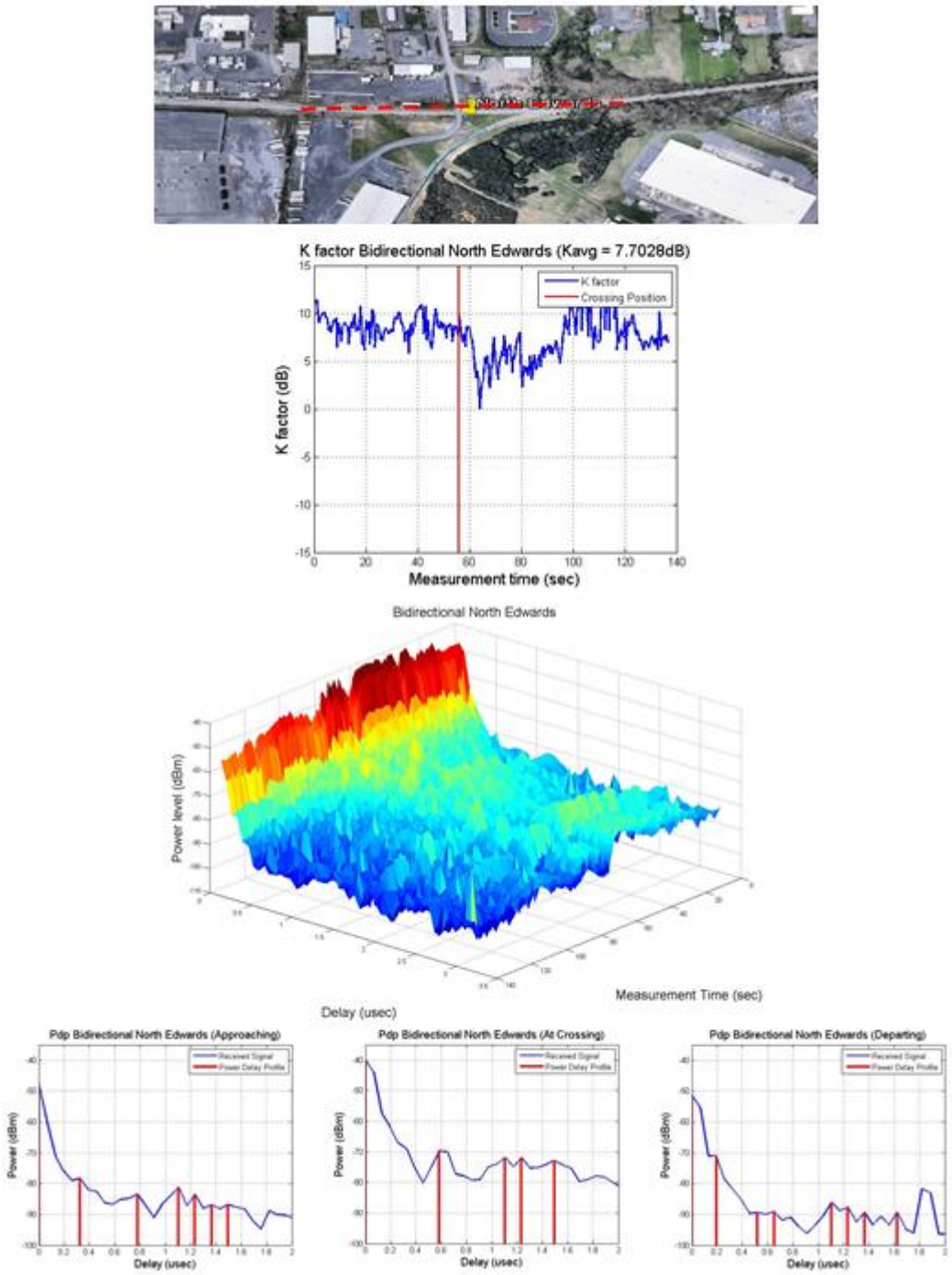

Figure 20 Ch sounder result (bi-directional crossing #3)

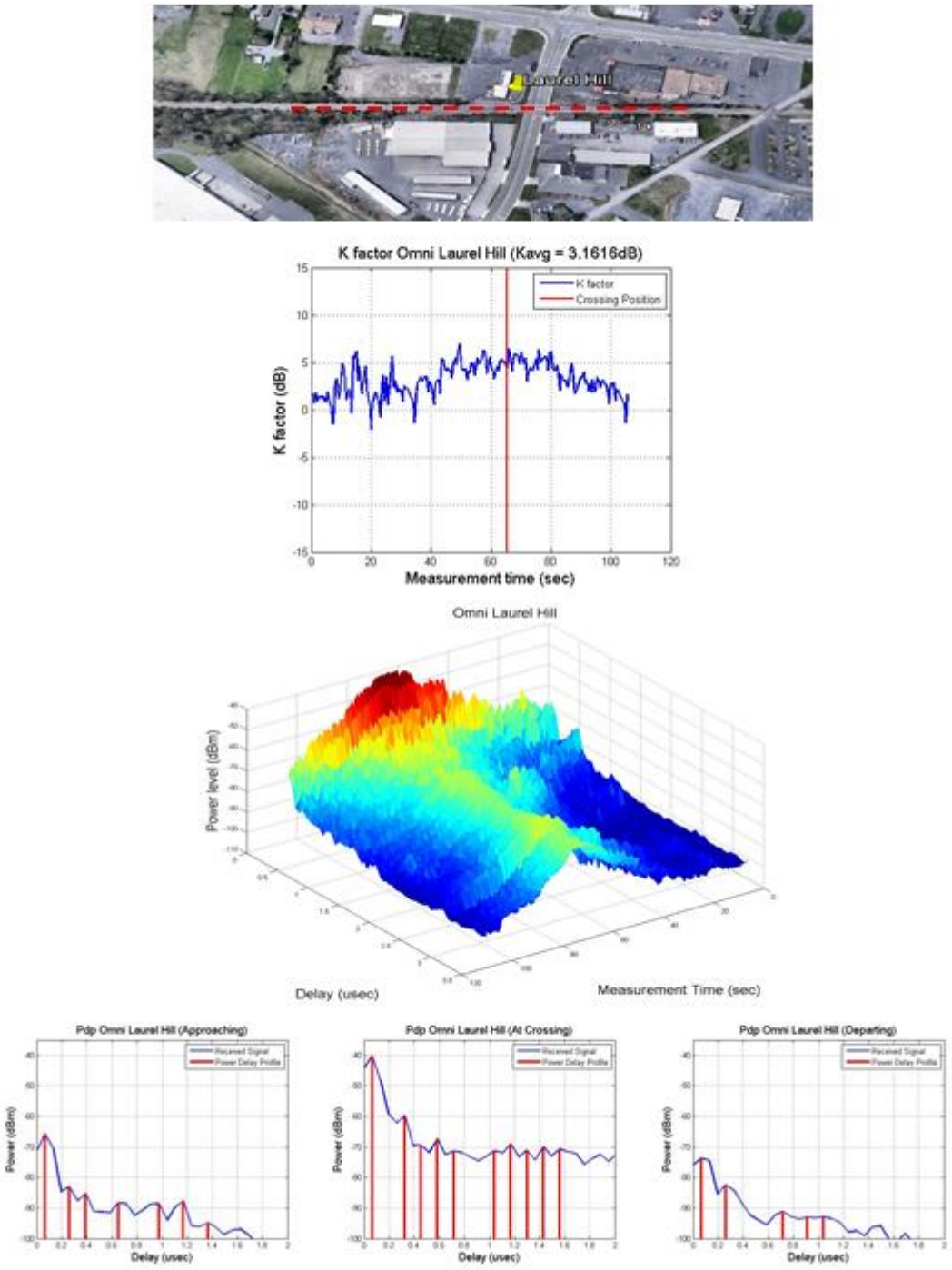

Figure 21 Ch sounder result (omnidirectional crossing #4)

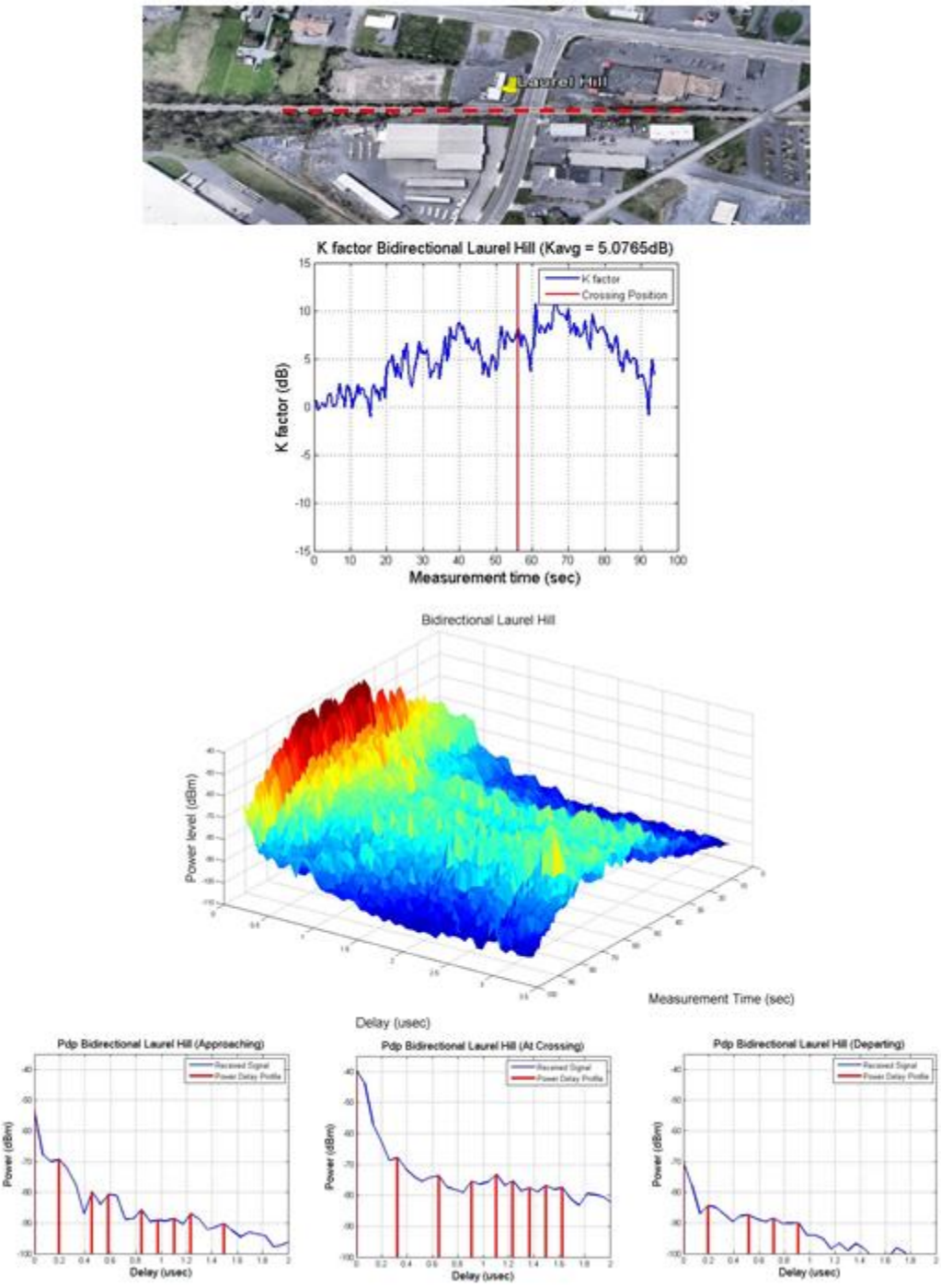

Figure 22 Ch sounder result (bi-directional crossing #4)

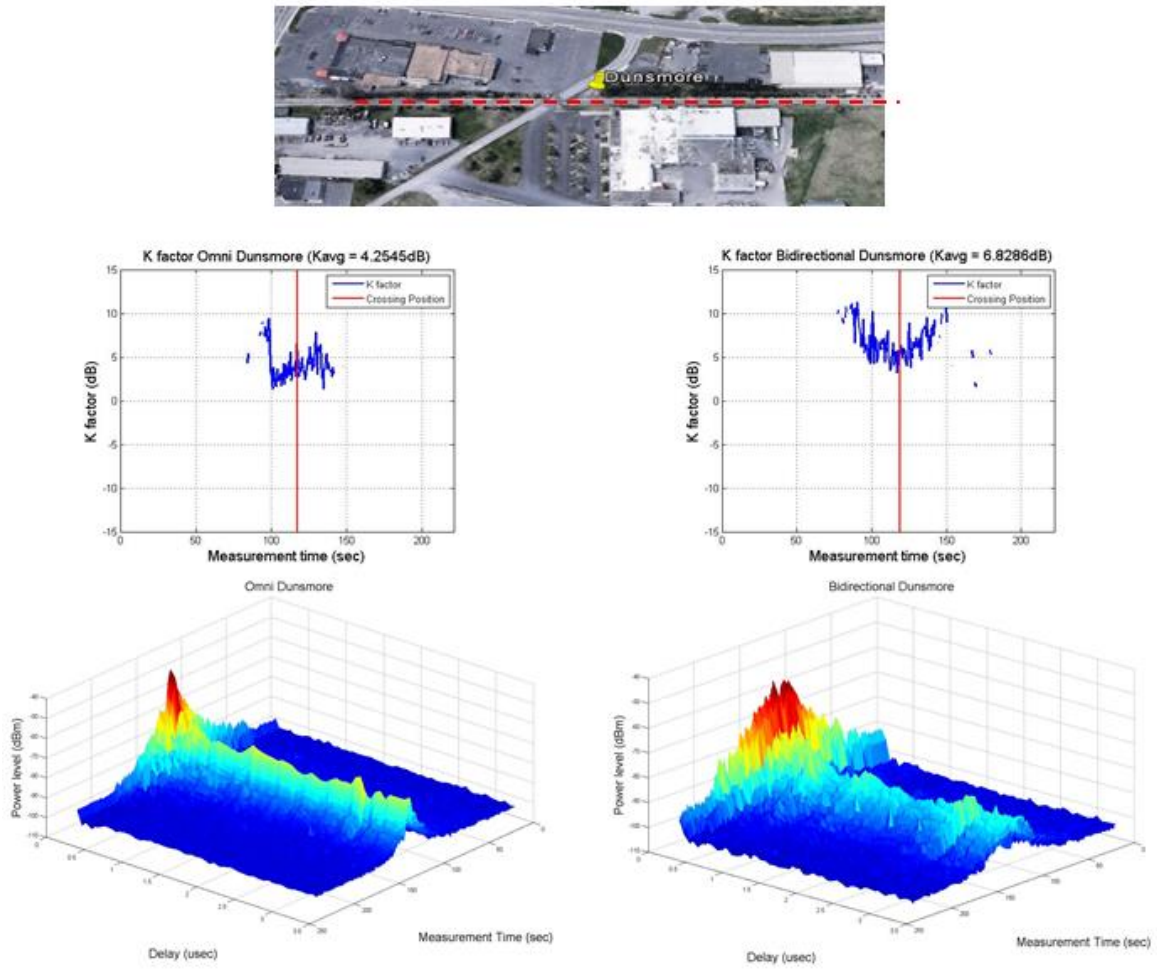

Figure 23 Ch sounder result (crossing #5)

To confirm the communication environment for each crossing, we compare each crossing's path loss with the omnidirectional antenna from the PDP and path loss model from the 3rd Generation Partnership Project (3GPP) [31]. We consider certain models to compare: Rural Macro LoS (RMa LoS), Suburban Macro LoS (SMa LoS), Suburban Macro NLoS (SMa NLoS), Urban Macro LoS (UMa LoS), and Urban Macro NLoS (UMa NLoS).

RMa LoS is given by:

$$PL_{RMa\ LoS} = 20log_{10}\left(\frac{40\pi d f_c}{3}\right) + 0.48log_{10}d - 0.7 + 0.0014d \quad (8)$$

SMa LoS is given by:

$$PL_{SMa\ LoS} = 20log_{10}\left(\frac{40\pi d f_c}{3}\right) + 1.57log_{10}d - 2.31 + 0.002d \quad (9)$$

SMa NLoS is given by:

$$PL_{SMa\ NLoS} = 122.14 + 38.63(log_{10}d - 3) + 20log_{10}f_c \quad (10)$$

UMa LoS is given by:

$$PL_{UMa\ LOS} = 22log_{10}d + 28 + 20log_{10}f_c \quad (11)$$

UMa NLoS is given by:

$$PL_{UMa\ NLoS} = 130.8 + 39.1(log_{10}d - 3) + 20log_{10}f_c \quad (12)$$

Figure 24 shows the measured path loss and 3GPP path loss model for crossings #2–#6. We confirm the communication environment of each crossing by comparing the path loss with the 3GPP model, as shown in Figure 24, and other propagation channel parameters. Because the 3GPP path loss model is applicable for longer than 10 m, each figure was plotted with a boundary at -10 and 10 m.

For crossing #5, we determine that the calculated value for the Ricean K-factor was inaccurate due to the low power of the LoS path signal. The Ricean K-factor is calculated using the ratio between the LoS path signal power and the reflected signal power. Because the LoS path signal power is as low as the reflected signal power, the calculated Ricean K-factor is reasonably higher. Therefore, even though the calculated value is 4.25 dB, the actual Ricean K-factor is supposed to be lower.

Ricean K-factor. From [22], the author categorized road crossing-suburban environments as having a K-factor of 3.7 with traffic and 4.5 without traffic, and our measured results show values of 3.81–4.56 for rural and 3.16 for suburban environments. Even though our assumption was that crossings #1, #2, #3, and #6 were rural and crossings #4 and #5 were suburban, all crossings fall into the road crossing-suburban category given in [22].

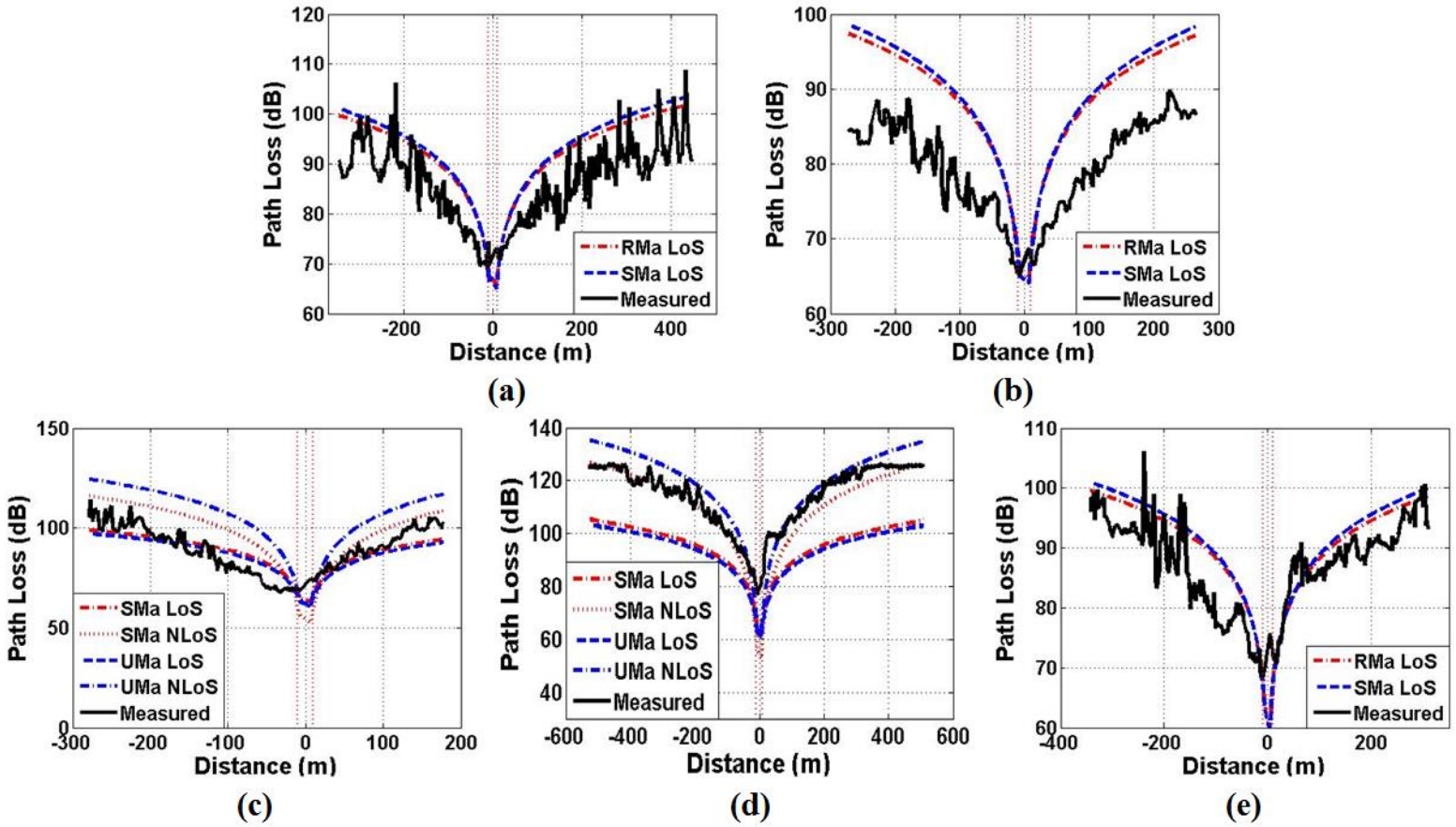

Figure 24 Comparison of measured path loss values and 3GPP path loss models for (a) crossing #2, (b) crossing #3, (c) crossing #4, (d) crossing #5, and (e) crossing #6

The Ricean K-factor results from the omnidirectional antenna are 3.16–4.56, while they are 5.08–8.01 for the bi-directional antenna. We can definitively conclude that the bi-directional antenna will face lesser fading than the omnidirectional antenna. In addition, the Ricean K-factor from [22] shows 7.6 for a general LoS highway environment, and the results for the bi-directional antenna can be considered within this category.

Furthermore, by comparing the results from the TTCI tracks, where there are no obstructions near the crossings, we measure the Ricean K-factor as 9.76–11.31, while we measure it as 3.16–4.56 for the SVRR tracks. Within our measurements, we can conclude that the Ricean K-factor for rural environments can be considered representative of a no-obstruction environment for a V2T communication propagation environment and that a suburban environment can be considered representative rural and suburban regions.

Path Loss. By looking at the measured path loss and 3GPP path loss model, reasonably, crossings #1, #2, #3, and #6 can be considered in a rural environment. Even though crossing #1, with an omnidirectional antenna, does not have values, the values for a bi-directional antenna are relatively similar for crossings #2, #3, and #6. Therefore, we considered crossing #1 to be rural, as well. As shown in Figure 24(a) and (e), crossings #2 and #6 almost match the RMa LoS path loss values. As shown in Figure 24(b), crossing #3 has a somewhat lesser path loss shown than the 3GPP model. With Figure 24, we could assume crossings #1, #2, #3, and #6 fall into the rural environment category.

Crossings #4 and #5 can be considered to be in a suburban environment. As shown in Figure 24(c), shorter distances, such as in the range of -100–0 m, are considerable for the rural environment; however, most distances are between SMa LoS and NLoS. Therefore, we assumed crossing #4 to be in a suburban environment. In addition, as shown in Figure 8(d), interestingly, the measured path loss is almost identical to SMa NLoS before the crossing and

UMa NLoS after the crossing. With this result, we are able to assume crossing #5 to be somewhat between a suburban and an urban environment.

The interesting aspect relating to path loss is that the path loss is much lower at +/- 100 m than the 3GPP path loss model. As shown in Figure 24(a), (c), and (e), which show considerably classic rural and suburban environments, we are able to see that both the measured and 3GPP models match at distances farther away from the crossing; however, in a near region, within +/- 100 m, the path loss is much lower than the 3GPP model. We assume this behavior is due to the special environment of crossings; the environment around the crossing is reasonably wide open, with possibly a strong LoS environment and a lack of interference sources nearby.

RMS Delay Spread. We observe the RMS delay spread to be in the range of 184–227 for the omnidirectional antenna and 96–152 for the bi-directional antenna, and these values are much higher than those that were observed at the TTCI tracks. We assume the difference appeared due to the existence of a few obstructions, such as trees, buildings, or parked cars, near the crossings.

The omnidirectional antenna results are much higher than any values from [23] and [24], but the urban LoS with a 600-m distance result from [25] is somewhat similar. The bi-directional antenna results are similar to the street crossing-suburban category from [23] and highway LoS from [25].

Through the propagation channel characteristic measurements and analyzed values, we are able to confirm the communication environment of the crossings, where we also measured the DSRC performance. When comparing our outcomes with the results from [22]–[25], we observe a V2T communication propagation environment similar to the suburban environment

using an omnidirectional antenna and to the highway environment using a bi-directional antenna. Interestingly, the 3GPP model matches our assumed environment.

3.7.4 DSRC Performance Measurements

The DSRC performance measurement results for the SVRR tracks are shown in Figures 25–30. Even though we took the measurements in combinations of three modulations and two power levels, here, we present BPSK, QPSK, and 16 QAM with the high transmission power of 23 dBm and QPSK and with the low power of 11 dBm. All of the intersecting roads at the six crossings have a speed limit of 25 mph, and the train speed was limited to 10 mph due to track regulations. With these speed limits, we considered 10 s as a minimum notification time to be enough; the stopping time for 25 mph is 4.62 s, as shown in Table I, with a notification distance of 44.4 m, as shown in Table II. Therefore, the region of interest is +/- 44.4 m. Even though we know the region of interest, we compare the DSRC performance with the +/- 400-m range because of the potential of our contribution to other applications that require a longer range than our defined region of interest.

he DSRC performance measurements on the SVRR tracks can be combined into the rural/suburban environment and *direct warning*/*indirect warning* scenarios. Crossings #1, #3, and #6 can be considered as being in a rural environment with an *indirect warning* scenario. Crossing #2 can be considered as being in a rural environment with a *direct warning* scenario. Crossing #4 can be considered as being in a suburban environment with an *indirect warning* scenario, and crossing #5 can be considered as being in a suburban/urban environment with a *direct warning* scenario. With these combinations of scenarios, we can properly evaluate the feasibility of DSRC for V2T safety.

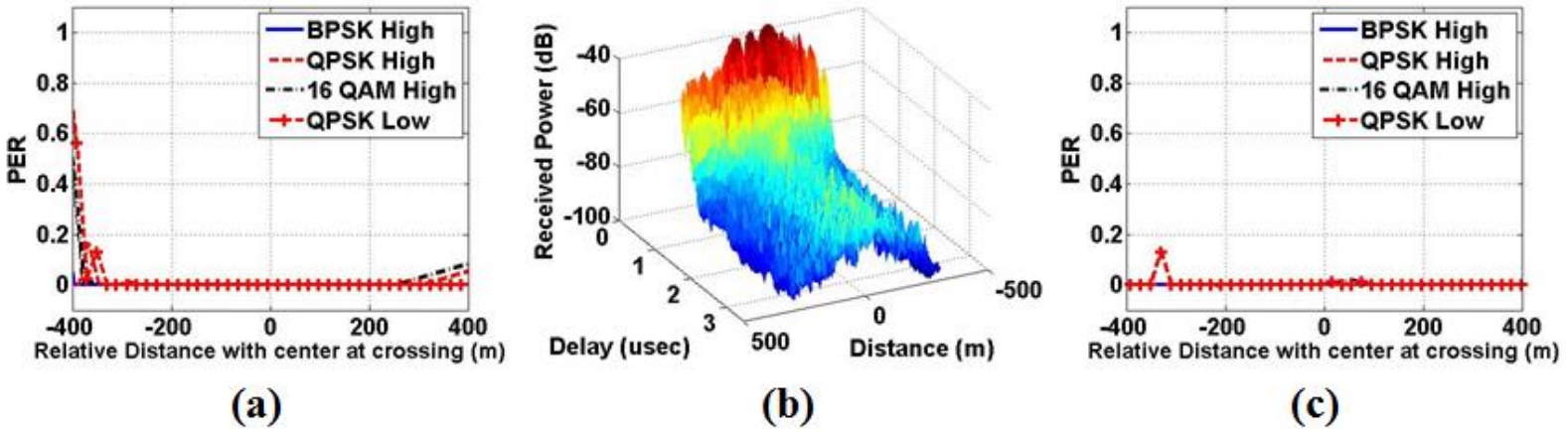

Figure 25 Crossing #1: (a) PER with omnidirectional antenna, (b) PDP with bi-directional antenna, (c) PER with bi-directional antenna

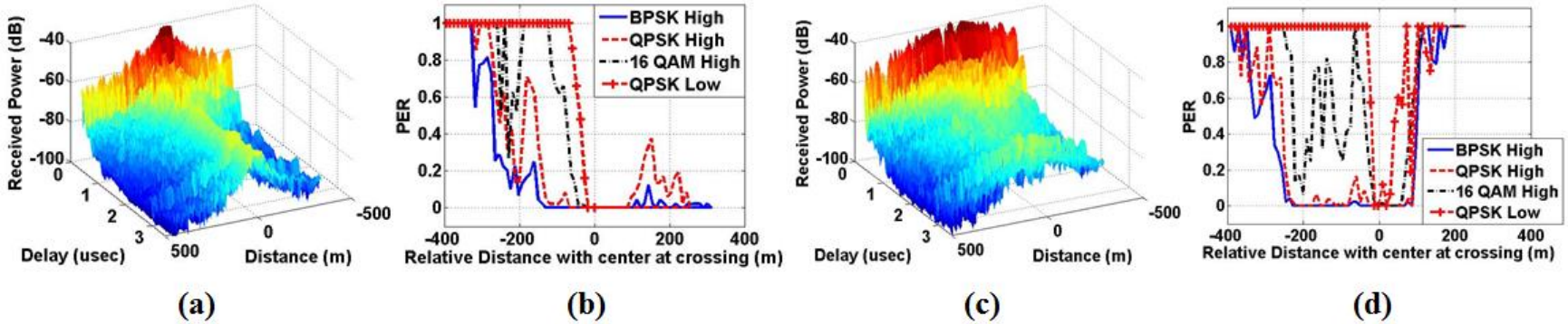

Figure 26 Crossing #2: (a) PDP with omnidirectional antenna, (b) PER with omnidirectional antenna, (c) PDP with bi-directional antenna, (d) PER with bi-directional antenna

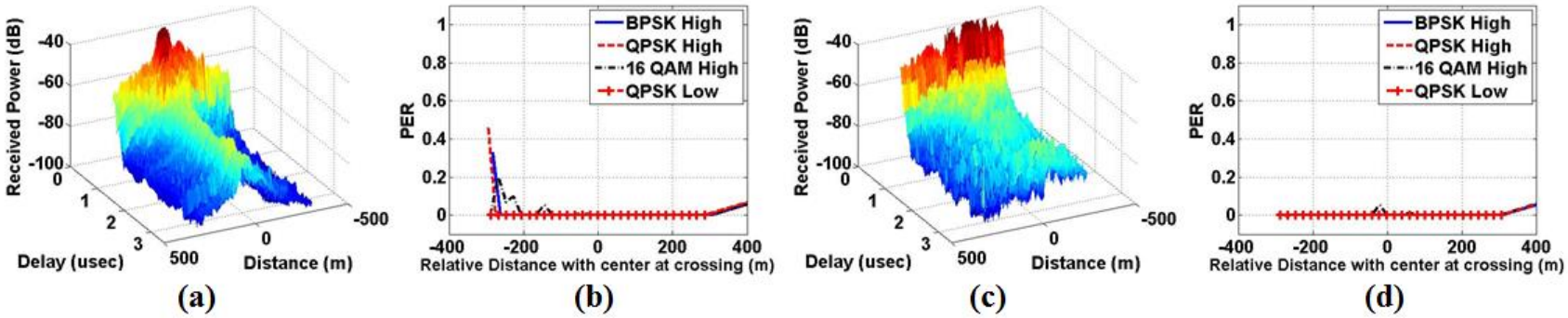

Figure 27 Crossing #3: (a) PDP with omnidirectional antenna, (b) PER with omnidirectional antenna, (c) PDP with bi-directional antenna, (d) PER with bi-directional antenna

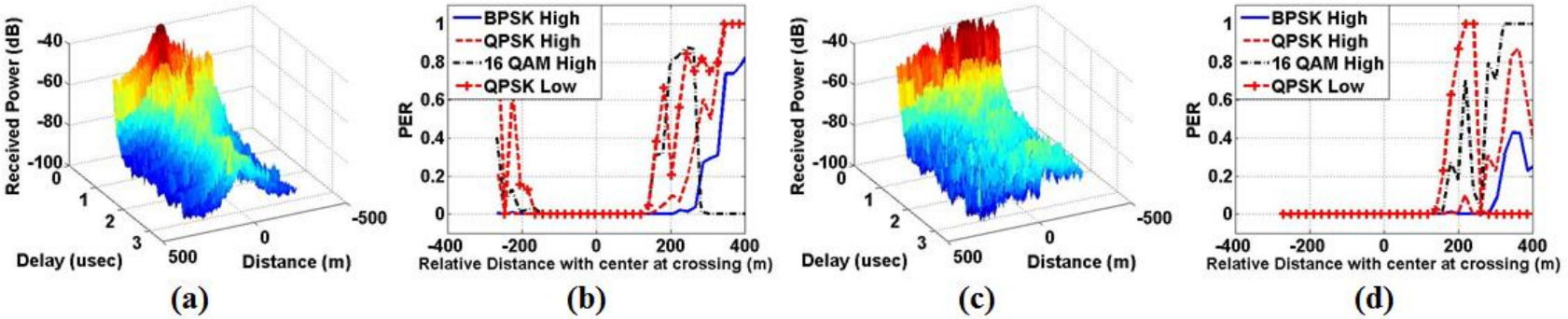

Figure 28 Crossing #4: (a) PDP with omnidirectional antenna, (b) PER with omnidirectional antenna, (c) PDP with bi-directional antenna, (d) PER with bi-directional antenna

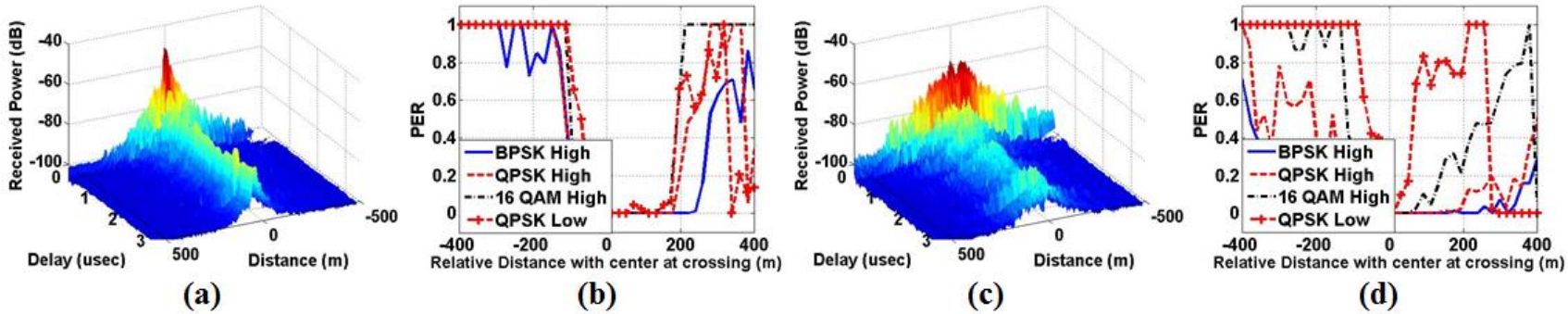

Figure 29 Crossing #5: (a) PDP with omnidirectional antenna, (b) PER with omnidirectional antenna, (c) PDP with bi-directional antenna, (d) PER with bi-directional antenna

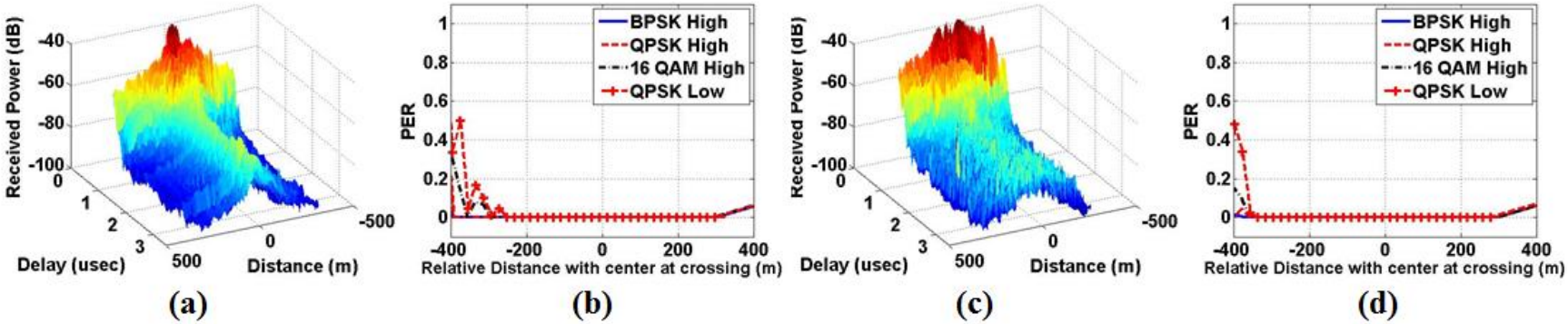

Figure 30 Crossing #6: (a) PDP with omnidirectional antenna, (b) PER with omnidirectional antenna, (c) PDP with bi-directional antenna, (d) PER with bi-directional antenna

Figures 25, 27, and 30 show the results for a rural environment with an *indirect warning* scenario. From all three figures, the DSRC performance in a rural environment with an *indirect warning* scenario can be said to *satisfy* the minimum requirement for safety. The range that satisfies the requirement, PER <0.9, is more than +/-400 m for all three crossings. The performances with a bi-directional antenna are also similar to those with an omnidirectional antenna. However, as clearly shown for crossings #1 and #6, the performance with an omnidirectional and 16 QAM high power/QPSK low power shows an increase in the PER at 400 m before the crossing, and it is expected to not *satisfy* around the 500-m range. Meanwhile, the performance with a bi-directional antenna is steady for the whole range. From these comparisons, we can expect DSRC with an omnidirectional or bi-directional antenna to provide a similar performance, but using a bi-directional antenna can provide a slightly longer range. In addition, with these results, we can identify that a DSRC radio is adaptable for a V2T communication system in a rural environment with an *indirect warning* scenario.

Figure 26 presents the results for a rural environment with a *direct warning* scenario. The DSRC performance with an omnidirectional antenna can be considered to *satisfy* the minimum requirement for safety, but QPSK with low power is near the minimum notification distance. However, if the minimum notification time is 15 s, QPSK with low power may not *satisfy*. Interestingly, the performances between the omnidirectional and bi-directional antennas for this scenario are similar; the coverage range is similar for each combination of modulation schemes and power levels. Moreover, the performance of the bi-directional antenna after the crossing is worse due to a blockage from a building placed after the crossing, which is the reason for creating the NLoS environment. With the comparison, we are able to identify that a bi-directional antenna performs worse than an omnidirectional antenna for the

NLoS environment. From the evaluations, we confirm the DSRC radio is adaptable for a V2T communication system in a rural environment with a *direct warning* scenario. In addition, different from the evaluation of a rural environment with an *indirect warning* scenario, omnidirectional and bi-directional antennas can provide a similar performance, but bi-directional antennas can be worse when the communication environment changes to NLoS from LoS.

For a suburban environment with an *indirect warning* scenario, we evaluated in Figure 28. The DSRC performance with an omnidirectional, as well as bidirectional antenna is able to considered to *satisfy* the minimum requirement for safety. The DSRC performance with a bi-directional antenna shows an advantage in terms of coverage range over an omnidirectional antenna for this scenario, and the performances after the crossing are similar for all modulation schemes and power levels. However, the performances before the crossing, which can be more important than after the crossing, show more variation than with an omnidirectional antenna. More interestingly, the performance difference is larger for a higher power level and lower modulation scheme; the difference in BPSK and QPSK is larger than the difference in 16 QAM high power and QPSK with lower power; the effect of antenna beamforming is higher for lower modulations From these evaluations, we confirm the DSRC radio is adaptable for a V2T communication system in a suburban environment with an *indirect warning* scenario. Moreover, we observe that using a bi-directional antenna can provide benefits in terms of coverage range over the omnidirectional antenna.

For a suburban environment with a *direct warning* scenario, we evaluated in Figure 29. The DSRC performance with an omnidirectional and with a bi-directional antenna is able to consider to *satisfy* the minimum notification range. The advantage of using the bi-directional antenna is able to observe in this scenario. The performance difference between the

omnidirectional and the bi-directional antennas is larger for higher power levels and lower modulation schemes, and this is observed in the suburban environment with an *indirect warning* scenario, as well. The difference is larger for a *direct warning* scenario than for an *indirect warning* scenario. Through the evaluation, we confirm a DSRC radio is adaptable for a V2T communication system in a suburban environment with a *direct warning* scenario. Furthermore, we can identify the advantages of using a bi-directional antenna in a suburban environment for both the *indirect* and *direct warning* scenarios.

3.7.5 Reliability Analysis

We choose crossing #4, one of the best performing crossings, and crossing #5, one of the worst performing crossings, to discuss the reliability of packet reception before the crossing using the CDF. We generate the CDF based on the number of correctly received packets at the granularity of 20 m as the train advances toward the crossing. Figure 31 and Figure 32 show the CDF for crossings #4 and #5.

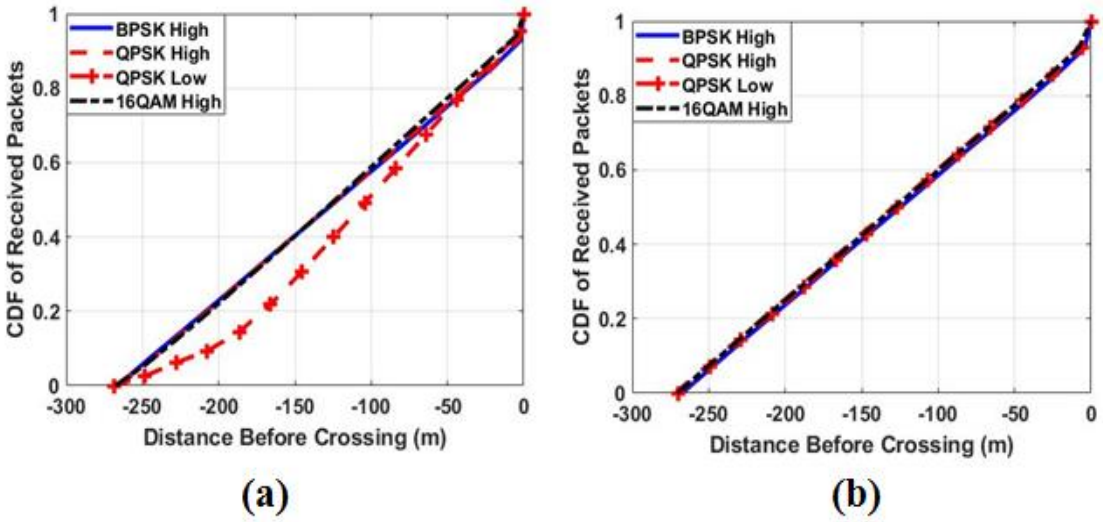

Figure 31 Crossing #4: CDF of successfully decoded packets before the crossing for (a) omnidirectional and (b) bi-directional

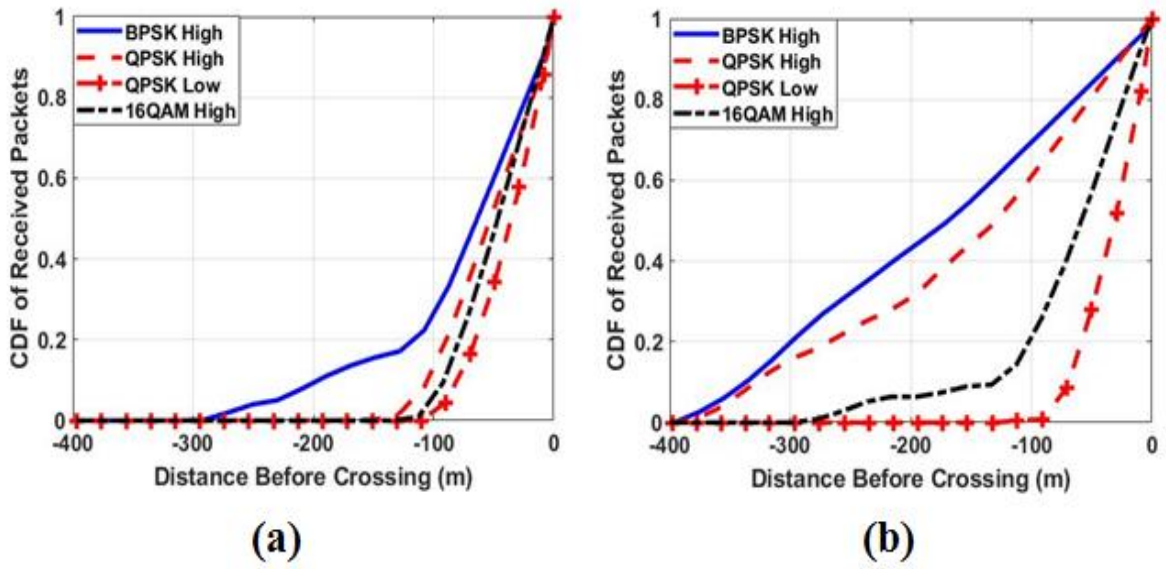

Figure 32 Crossing #5: CDF of successfully decoded packets before the crossing for (a) omnidirectional and (b) bi-directional

When the CDF curves are approximately linear with a slope of one over the distance where packets are being received, and if this distance is sufficiently long for an effective warning, the system can be considered reliable. This is the case for crossing #4, among others. For crossing #5, the reliability is high only for the bi-directional antenna system configuration and for a lower-order modulation and high power transmission.

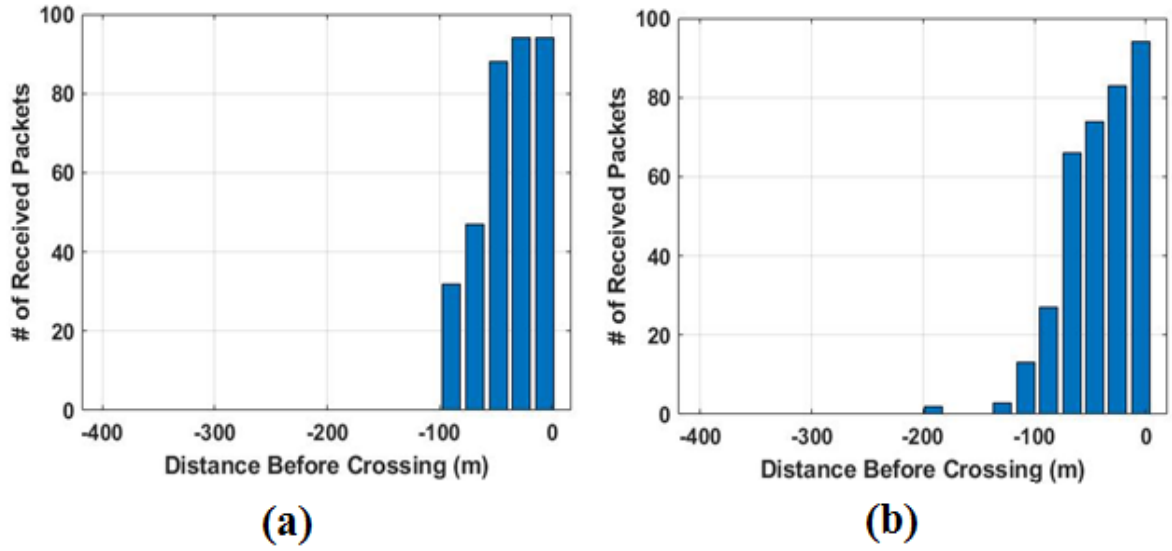

Figure 33 Number of correctly received packets for crossing #5 with QPSK and low power transmission for (a) omnidirectional and (b) bi-directional

Even though the system reliability of the omnidirectional antenna configuration for crossing #5 is low, a good amount of packets is actually being received before the minimum notification distance of 67 m. As shown in Figure 33, more than 60 packets are received before the critical distance of 67 m before the crossing. Therefore, we conclude the DSRC system is a good candidate for the proposed V2T safety-critical communications system, which warns cars well ahead of time of an approaching train.

3.7.6 Conclusions of SVRR Measurements

In Figure 25-30, we evaluate the DSRC performance in rural/suburban environments with *direct*/*indirect warning* scenarios. Through all combinations of scenarios, we conclude that DSRC is adaptable for use in a V2T communication for early warning application, as its performance can be considered to *satisfy* most of the scenarios with all modulation schemes and high/low transmit power levels within the minimum notification range with a minimum

notification time of 10 s. Unlike the TTCI track measurements, the interference sources were the real environment and random number of existence, and moving vehicles and objects existed during the measurement procedure. The measured results confirm that DSRC is adaptable for a V2T communication system in a real environment.

In Figure 24 and Table VI, we evaluate the propagation channel characteristics, path loss exponents, Ricean K-factors, and RMS delay spreads for the SVRR crossings. The measured path loss results have a fit similar to the 3GPP path loss models for urban, suburban, and rural environments with our assumed environment category. For fading-related parameters, Ricean K-factors, and RMS delay spreads, all crossings with the omnidirectional antenna are similar to suburban categories, as mentioned in [22]–[25]. In addition, the results with a bidirectional antenna show all crossings can be considered as within the highway category from [22] and [25], which is the major difference in performance between omnidirectional and bidirectional antennas.

3.8 Detailed Propagation Channel Characteristics

The interested propagation channel parameters are Ricean K-factor, path loss exponent and its standard deviation, and RMS delay spread. The channel parameters were calculated by PDP which generated by recorded waveform through channel sounder. An example of generate PDP plot is shown in Figure 34.

A generated PDP contains the strongest LoS signal and the signals that are delayed by interferences, which is able to capture up to 3.5 μsec. Each signal is captured where the locomotive started to move and where stopped move. The saved data contains GPS

information which can directly allocate propagation channel signal and the distance away from the crossing.

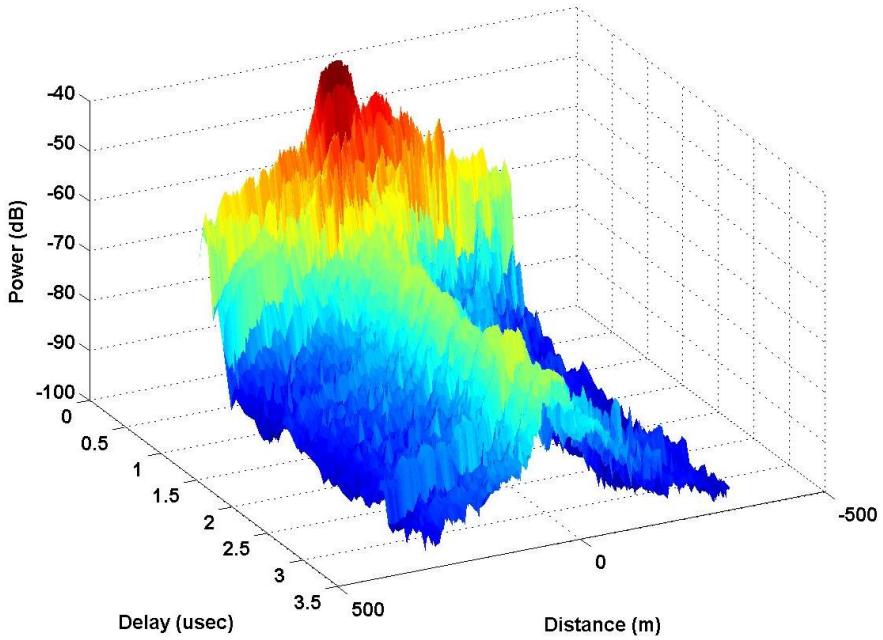

Figure 34 Example of Generated PDP

The calculation of propagation parameters is done with each recorded GPS location. One instantaneous signal is shown in Figure 35. In Figure 35, the continuous received signal is shown as blue line and each peak are represented as red lines. The power data at delay time 0 sec represents the strongest LoS signal and all others represents delayed signal. The calculation was done with using these signals.

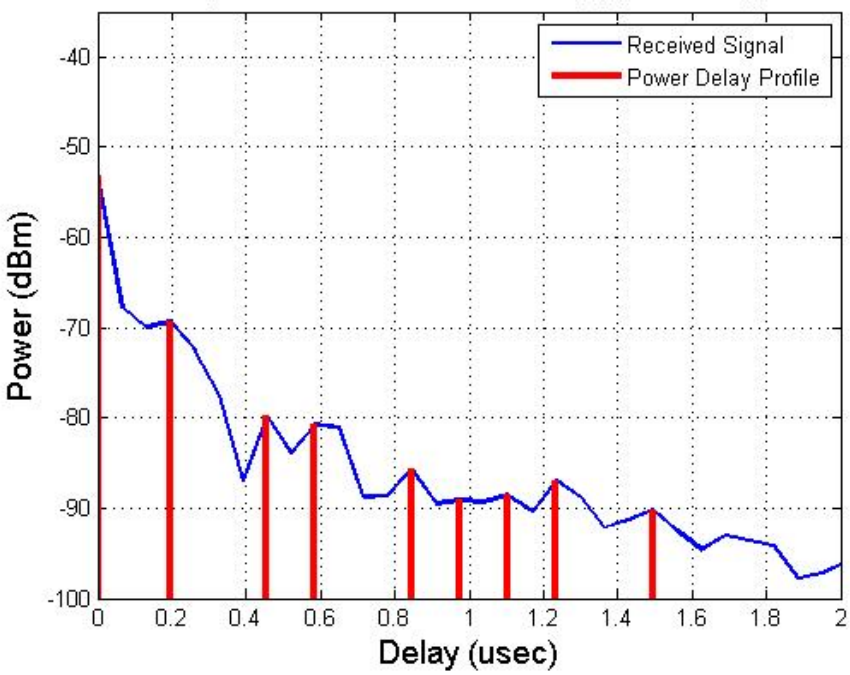

Figure 35 Example of Instantaneous PDP

3.9 Robust Estimation Methods

From PER and channel characteristics, the parameters are collected certain range window with sharing same distance parameter. With this information, we can estimate the channel characteristics values for V2T communication environment and find the linear form equations between PER and channel characteristics or distance and channel characteristics. For the estimation process, we will use the similar method used in [20]-[25]; 1) mean and variance, 2) linear regression and R^2, a coefficient of determination, to evaluate the goodness of fit.

For evaluate the channel characteristics, the measurements were done in a mixture of suburban and rural; therefore, we will use mean and variance with the assumption of Gaussian distribution to estimate. The estimation will not consider other potential affecting parameters. All of the calculated parameters are discrete results. The mean is defined by:

$$\mathrm{E}(\text{channel characteristics}) = \mu = \frac{\sum_{i=1}^{n} channel\ characteristics}{n} \quad (13)$$

The variance is defined by:

$$\mathrm{Var}(\text{channel characterisitcs}) = E[(channel\ characteristics - \mu)^2] \quad (14)$$

With (13) and (14), we can estimate the channel characteristics for mixed suburban and rural environment for V2T communication.

Since we're interested the relationship between PER and channel characteristics or distance and channel characteristics, the linear regression is applied to estimate. The linear regression representation is defined by:

$$\mathrm{z} = \mathrm{H} * \mathrm{x} + \mathrm{e} \quad (15)$$

where *z* is dependent variables, *H* is an estimator, *x* is an independent variable, and *e* is an error between the estimated value and measured value. Since the interesting parameters are one-to-one variables, the linear regression can be simplified into:

$$\mathrm{z} = \beta_0 + \beta_1 x + e \quad (16)$$

where β_0 is intercepted at *z* and β_1 is regression coefficient. This can be rewritten into vector form as:

$$\begin{bmatrix} z_1 \\ z_2 \\ \vdots \\ z_n \end{bmatrix} = \begin{bmatrix} 1 & x_1 \\ 1 & x_2 \\ & \vdots \\ 1 & x_n \end{bmatrix} \begin{bmatrix} \beta_0 \\ \beta_1 \end{bmatrix} \quad (17)$$

The coefficient of determination, R^2, is defined by:

$$R^2 = 1 - \frac{\sum_{i=1}^{n} (x_{meas.} - x_{est.})^2}{\sum_{i=1}^{n} (x_{meas.} - \mu)^2} \quad (18)$$

Also, R^2 can be rewritten with residuals:

$$R^2 = 1 - \frac{Sum\ of\ Squared\ Residuals}{Sum\ of\ Squared\ differences} \quad (19)$$

R^2 can be observed as the range of 0 to 1 and larger value considered as better to fit or better estimator.

With the linear regression process, we can generate estimated linear form equation for PER and channel characteristics or distance and channel characteristics. After observing the equations, R^2 can support whether the equation is good to use or more measurement is required to reduce randomness. The evaluations with measured and estimated results are shown in the next Section.

3.10 Analyses of Results

The mean and variance of Ricean K, path loss exponent, and RMS delay are shown in Table VII and their distributions are shown in Figure 36, Figure 37, and Figure 38. Due to units of variables, large or small value of variance is not good to compare. Interestingly, the distribution shape for Ricean K, RMS delay, and path loss exponent seems different. Only Ricean K distribution seems normal Gaussian distribution. RMS delay and path loss exponent seem exponential distribution or other than normal Gaussian. Therefore, finding the best fit distribution will make the mean and the variance to be useful to use for simulation or modeling for wireless communications.

Table VII Mean and variance of Ricean K, path loss exponent, RMS delay

	Ricean K (dB)	Path loss exponent (dB)	RMS Delay (μs)
Mean	3.9945	2.7738	0.1960
Variance	13.2669	0.1905	0.0029
Standard deviation	3.6424	0.4365	0.0539
Confidence interval	-1.5~13.5	2.34~4.00	0.13~0.33

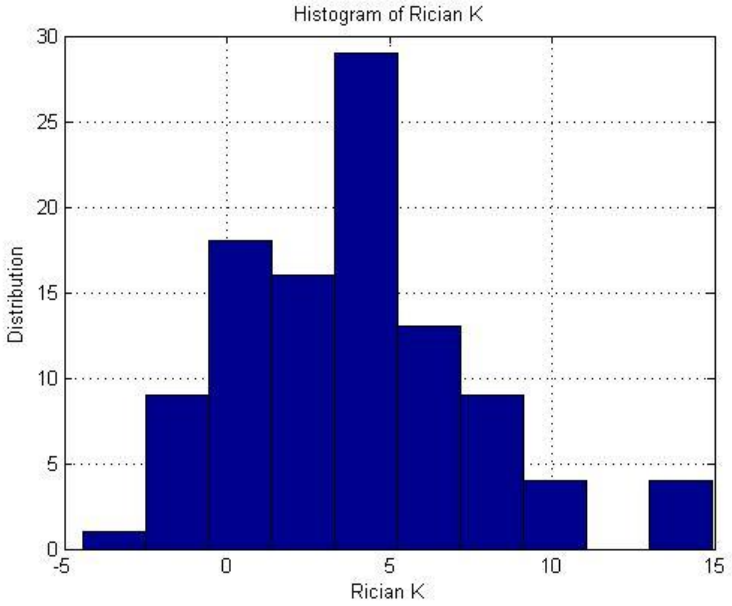

Figure 36 Distribution of Ricean K

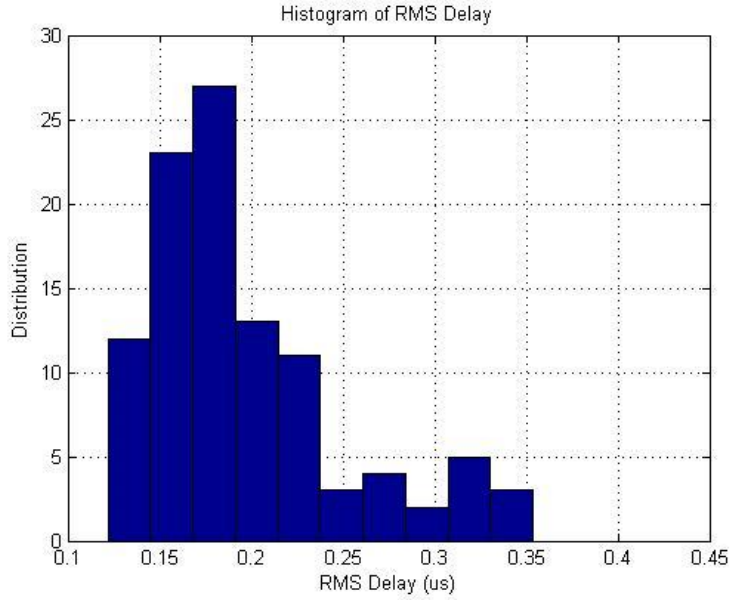

Figure 37 Distribution of RMS Delay

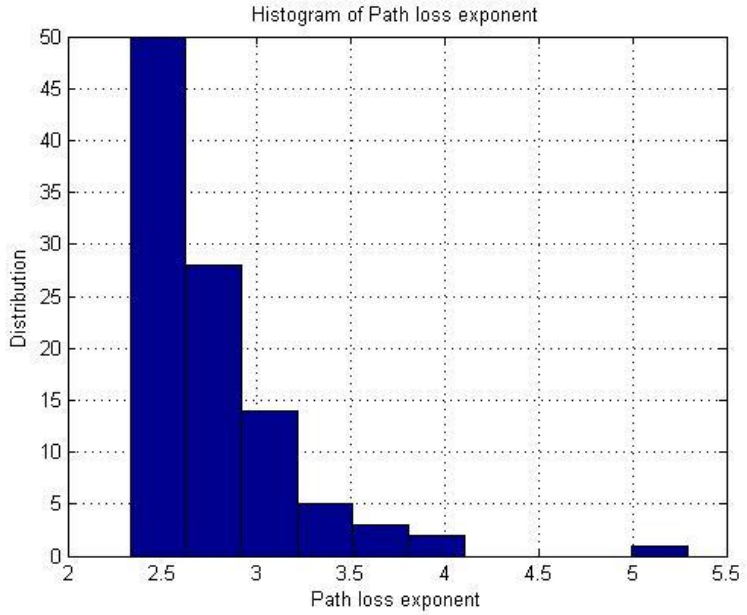

Figure 38 Distribution of path loss exponent

The linear regressions between PER and channel characteristics are shown in Figure 39, Figure 40, and Figure 41. Interestingly, all of them are flat lines with R^2 of around 0.002, which represent "poor" to fit. However, as shown in Figure 39, Figure 40, and Figure 41, the PER values are most likely 0s than well distributed; not much variance appears in PER values. Therefore, the evaluation of linear regression between PER and channel characteristics are useless until more vary PER values are collected. As the point of view to evaluate the performance of DSRC for V2T communications, the performance is really great due to properly working in different parameters of channel characteristics. However, as the point of view to evaluate the relationship, the data set is worse and the linear equation is useless due to less distributed PER values.

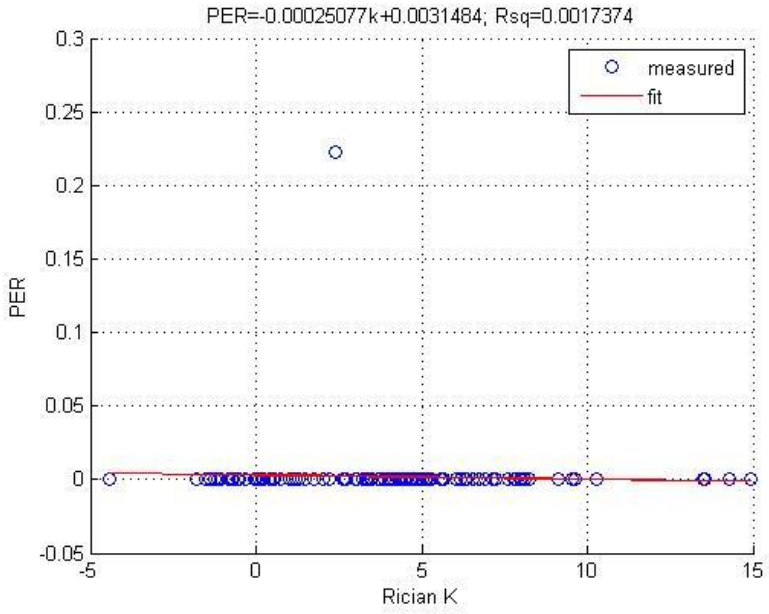

Figure 39 PER vs Ricean K

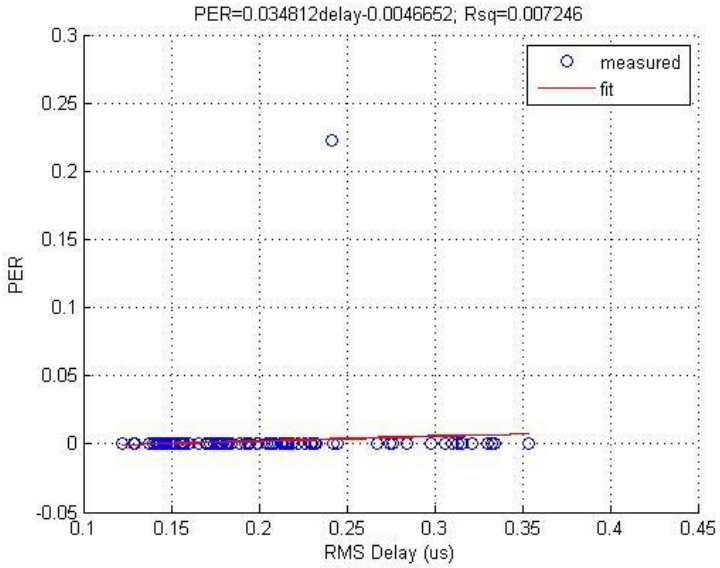

Figure 40 PER vs RMS Delay

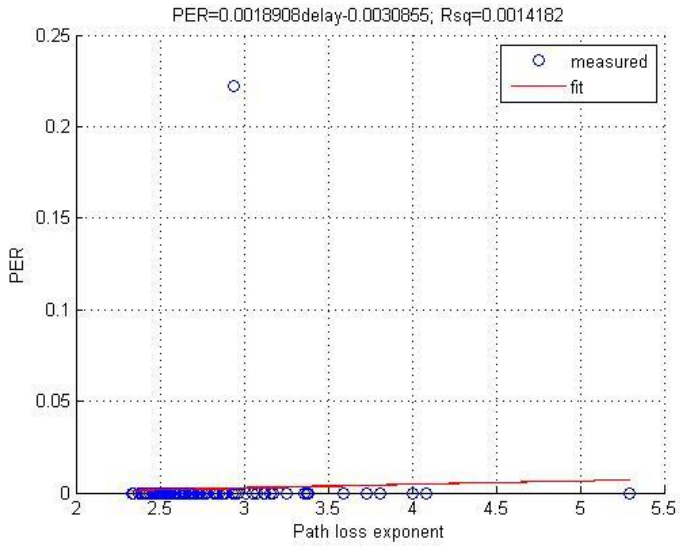

Figure 41 PER vs Path loss exponent

The linear regressions between the relative distance of train and crossing and channel characteristics are shown in Figure 42, Figure 43, and Figure 44. These are more interesting than the linear regressions between PER and channel characteristics. The linear regression of Ricean K is shown as:

$$K = 0.008d + 2.85 \quad (20)$$

with R^2 of 0.034. With this information, this model does not explain the relationship for Ricean K and relative distance, and more data are needed for solid relationship model. The linear regression of path loss exponent is shown as:

$$n = -0.002d + 3.04 \quad (21)$$

with R^2 of 0.144. With this information, we also can assume the model does not explain the relationship for path loss exponent and relative distance well. However, we expect using the exponent of distance or exponential relationship instead of linear can increase R^2, which represents a better model to estimate the model from the measured results. The linear regression of RMS delay is shown as:

$$\text{RMS delay} = 5.85e^{-6}d + 0.195 \quad (22)$$

with R2 of 9.24e-5. Based on this information, the data used in this analysis do not show a significant relationship between RMS delay and relative distance. From all three linear regression evaluation processes, none of the models provide a robust estimate of channel parameters based on relative distances. Other variables not considered in this model may explain more of the variation in channel parameters. However, more data collections may provide solid relationship model, also, the factor other than relative distance need to be considered.

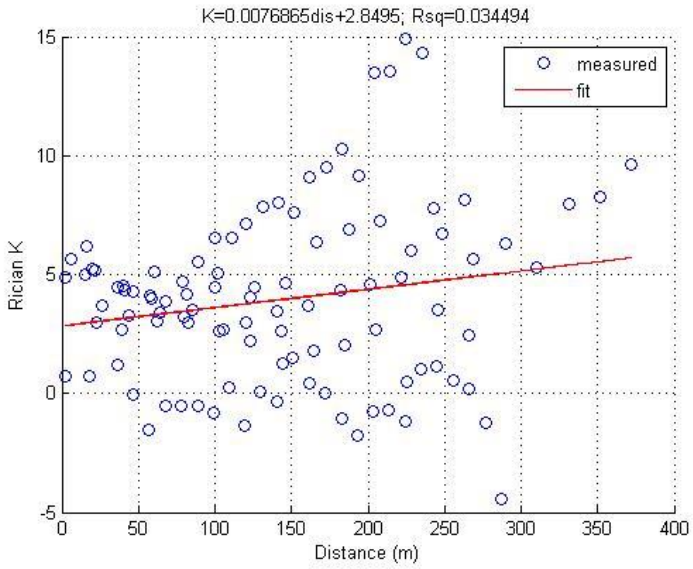

Figure 42 Ricean K vs Distance

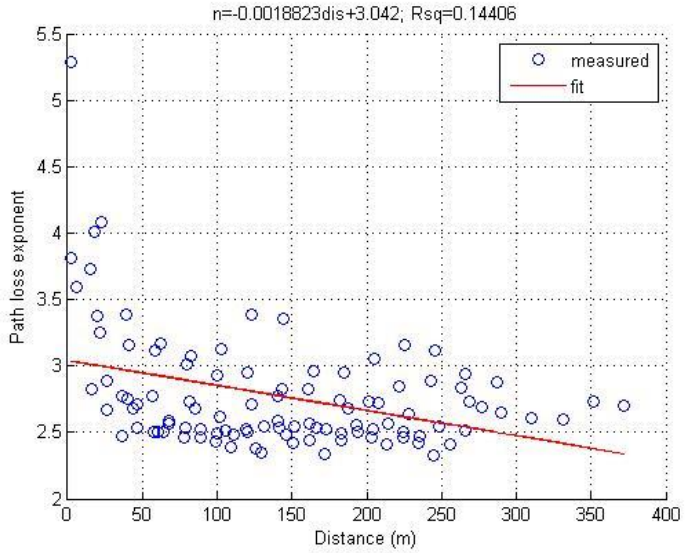

Figure 43 Path loss exponent vs Distance

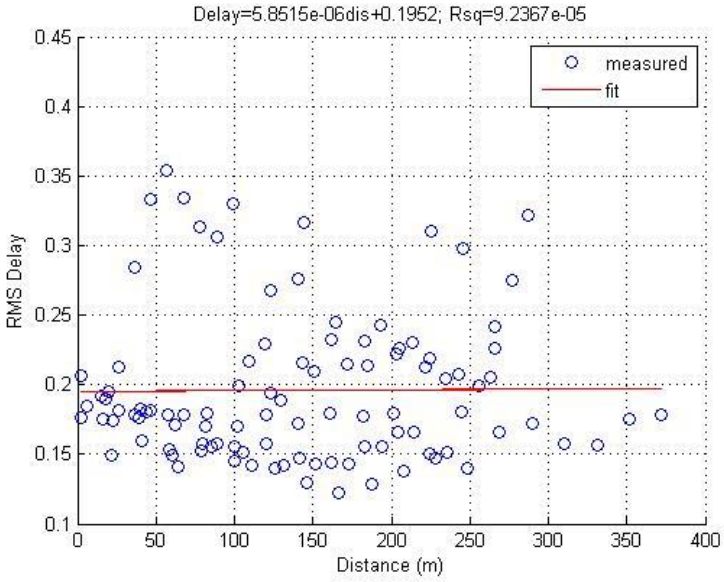

Figure 44 RMS Delay vs Distance

From the estimation process by finding mean and variance and linear regression, we were able to estimate the values of channel characteristics at V2T communication environment. For mean and variance, Ricean K is good to use since the distribution is normal Gaussian

distribution, which is usually used in simulation models. However, for RMS delay and path loss exponent, the distributions do not fit with the normal Gaussian distribution. Therefore, finding better-fitted distribution model is required and the new variance will be given after finding the new fitted distribution model. For linear regressions between PER and channel characteristics, we observe more vary PER values is required to identify the relationship between PER and channel characteristics. For linear regressions between relative distance and channel characteristics, the linear equation for Ricean K is not good due to low R-squared value. Also, the linear regression for path loss exponent is required to process with other than linear equational form. Also, we observe the no relationship between RSM delay and relative distance due to flat slope observed in the linear equation.

The authors of [20] presented a linear model of Ricean K-factor in relation to distance and given by:

$$K = 0.012d + 0.29 \tag{23}$$

Interestingly, our model from the measurement, (20), and the model presented in [20], (23), have a similar relationship between the distance and the Ricean K-factor, as 0.008 and 0.012, respectively. There are certain error observed; however, the similarity between V2T and V2V can be found.

More specific comparison between terrain parameters and crossings, we plotted propagation channel characteristics with related to distances in Appendix D. From each crossing figures, we observed similar behaviors in Ricean K factor and path loss exponent for rural crossing environments, Crossing #3 and #6; however, there are some outliers especially in Ricean K factor, which are due to in the transition between rural to suburban/urban like crossings.

Since Crossing #4 is only suburban crossing, we plotted rural like crossings for figures 45-47. From Figure 45, we observed similar results as shown in Figure 42 due to the outliers shown

in the ranges of 200 m. Based on Figure 97 and Figure 99, those points are observed after the crossings, and the region after Crossing #3 and #6 contains a large forests and buildings. The RMS delay stays as same conclusion as before. For the path loss exponent values, all of them are in the range of 2.5-3, except the values after the Crossing #6. Interestingly, the outliers of path loss exponents were not shown from Crossing #3, but from Crossing #6.

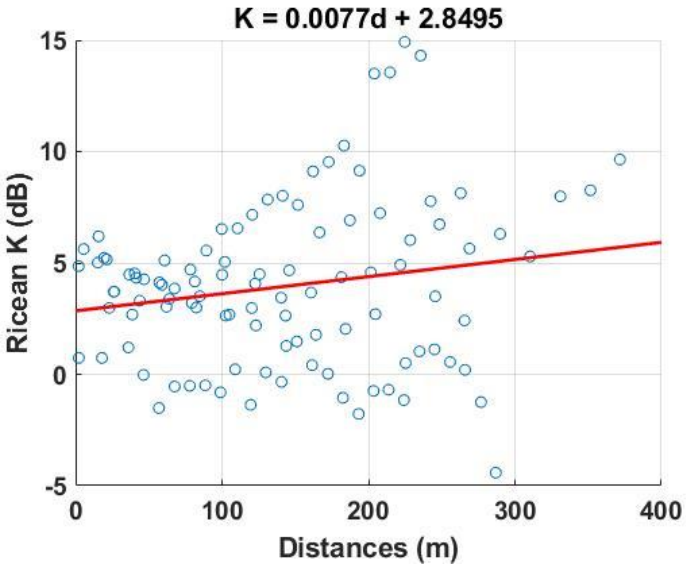

Figure 45 Ricean K for rural crossings

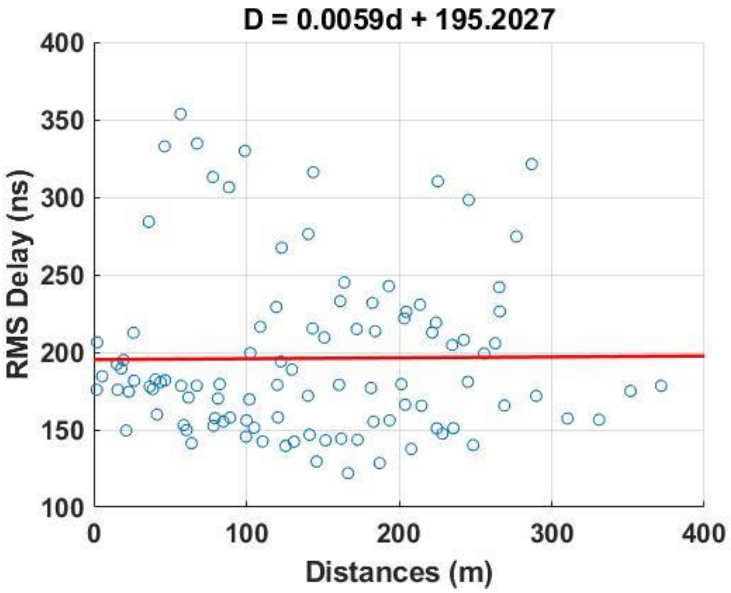

Figure 46 RMS delay for rural crossings

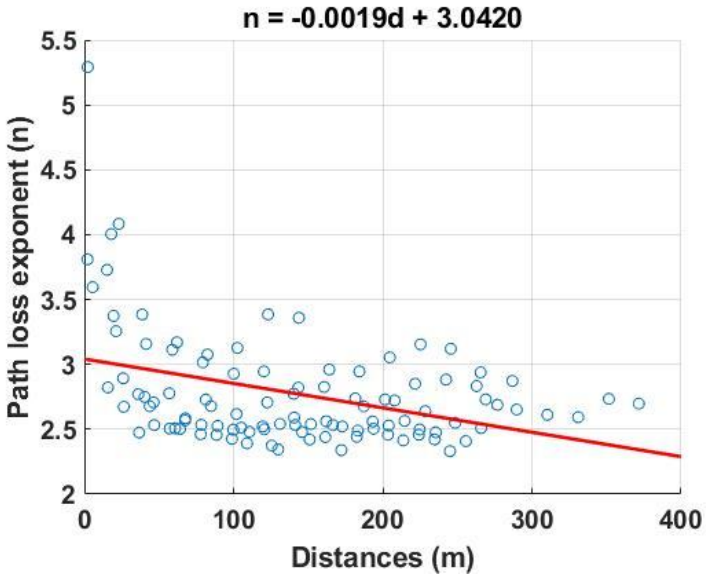

Figure 47 Path loss exponent for rural crossings

3.11 Conclusions for Estimation Methods Analysis

We faced a limitation in obtaining PER models due to PERs of zero for the range of propagation channel measurements. More measurements at different sites that will give non-

zero PERs are needed for a more accurate relationship model. From the measured results, we estimated the results by 1) mean and variance with the assumption of Gaussian distribution, 2) linear regressions between PER or distance and channel characteristics. From mean and variance, we observed only Ricean K is following Gaussian distribution while the other two does not. Therefore, the properly fitted distribution to find mean and variance is required. From linear regression of PER, we observed more varied PER is required to collect to estimate proper equation. From linear regression of distance, we won't find good fitted line, which give us the conclusion for more data collection is required. The suggested equations are not sufficient enough to use in the field yet due to low R^2 parameters for all fitted line, collected data in few crossings, which may not representative, and the parameter, especially path loss exponent, consider other equation than linear regression. Therefore, careful approaches to evaluate the equations for propagation characteristics with more field trial are required to suggest for design guidelines. Also, PER values are almost zero for all scenarios; therefore, another propagation channel measurement with worse performing DSRC environment is required for developed design guidelines.

Chapter 4

ITS Band Regulatory Survey

4.1 Introduction

A literature survey was performed to identify technical challenges and related prior research associated with possible future regulatory decisions related to the 5.9 GHz ITS band. These decisions relate to band sharing and mandatory use of a wireless communication standard or standards for vehicular safety communication. This study will help investigators to plan research that is highly relevant to the future regulatory environment of the 5.9 GHz band and to future ITS bands that may be subject to different combinations of regulations.

DSRC has been the dominant protocol recommended for vehicular communication such as V2V and V2I communications. In FCC Report and Order FCC-03-324 [32], the FCC allocated 75 MHz of the spectrum in the 5.9 GHz band for vehicular communications. DSRC has been using the 75 MHz of spectrum with seven different channels; each is 10 MHz bandwidth as per the recommendation of ITS.

However, more recently the FCC issued a NPRM regarding the potential use of the 5.9 GHz band for U-NII devices. Also, the FCC is considering sharing the spectrum of 5.85-5.925 GHz by both DSRC and U-NII devices, as mentioned in FCC Docket ET 13-49 [33]. The primary unlicensed devices that included in the FCC NPRM use a signal based on IEEE 802.11ac and operate at U-NII-4 band shown in Figure 1.

The channel allocations being considered for DSRC and U-NII-4 are shown in Figure 1. In the FCC NPRM, two interference mitigation approaches are presented: “Detect and Vacate (DAV)” and “Re-channelization”. DAV represents no changes to DSRC, but requires

unlicensed devices to avoid DSRC interference by detecting the DSRC signal up to Channel 178. “Re-channelization” is an allocation process where safety-related DSRC applications use the upper 30 MHz (Channels 180, 182, and 184) while non-safety-related DSRC and U-NII devices share the lower 45 MHz (Channels 172, 174, 176, and 178).

Furthermore, new developments of Vehicle-to-Everything (V2X), are expected over the next few years with releases 3GPP releases 16 and 17. One potential apporach is to provide services through LTE, which is refered to as C-V2X [34]. Recently, 3GPP presented the sidelink interface and the LTE cellular interface in Release 14 with fulfilling the requirements of V2X services [34]. Also, Society of Automotive Engineers (SAE) established five levels of vehicle automations, complete driver control (level 0) to complete autonomy (level 5), and the autonomous driving will highly rely on the communication functionality [35]. Although the technical details are still under development, C-V2X will brings additional complexity to the discussion on how to allocate spectrum bands in the 5.9 GHz band due to involvement of traditional vehiclular communication in the architecture.

As Wi-Fi, LTE, and DSRC are competeing for the 5.9 GHz spectrum, numerous technical challenges to research will arise. Since allocating the spectrum is organized by FCC, and possibly the NHTSA may affect the regulation, there are some technical challenges that we further analysis in this paper. However, when a regulatory of 5.9 GHz spectrum band is fixed by both FCC and NHTSA, the technical challenges to research should somewhat align with expected regulations.

DSRC is the dominant protocol for 5.9 GHz band; however, deploying C-V2X, Wi-Fi, and other unlicensed devices at the band is considered. Within possible hypothesis about FCC and NHTSA’s decisions, we can generate possible combinations of regulations and associated technical challenges related to possible regulation scenarios. Moreover, we present a

comperhensive technical assessment that is related to the potential technical challenges for those regulations.

4.2 Possible FCC and NHTSA's Regulations

For adopting certain regulations for vehicular communication, FCC and NHTSA have the major role. Their decision may or may not conflict to each other; however, it is obvious to say that C-V2X or DSRC or both will be using the 5.9 GHz. Also, based on announced NPRM, FCC's position can be expected as using UNII-4 and DSRC with Re-channelization and under discussion about DAV while NHTSA is more focused on whether the technologies can satisfy their minimum safety requirements.

Possible FCC actions are following:

- Number of vehicular safety communication technologies in band: 1) one technology; or 2) two technologies
- If one safety technology in band: 1) DSRC Only; or 2) C-V2X Only
- If two or more safety technologies in band: 1) co-channel coexistence; or 2) adjacent channel coexistence
- Re-channelization: 1) Re-channelize, safety-related DSRC using upper 30 MHz and unlicensed devices using lower 45 MHz; or 2) Do not re-channelize
- Wi-Fi sharing: 1) Allowed through DAV; 2) Not allowed
- Other unlicensed technologies, most prominently LTE-U, LAA, and MuLTEfire: 1) Allowed; 2) Not allowed

Re-channelization and Wi-Fi sharing by DAV are considered as two different interference mitigation approaches. However, they can be used at the same time: using safety-related

DSRC to re-channelize at upper 30 MHz and allocate non-safety-related DSRC at 45 MHz with allowing Wi-Fi sharing through DAV. For the re-channelization scenario, Wi-Fi sharing is always allowed. For the do-not-re-channelization scenario, Wi-Fi sharing could either be allowed or not allowed.

With the interests of NHTSA, which technology using for vehicular communication, we can identify the possible NHTSA's regulations as:

- DSRC only
- C-V2X only
- Coexistence DSRC & C-V2X
  - Interoperable
  - Non-Interoperable
- No regulations

NHTSA is more interested about which technology is preferred for vehicular communication with fulfilling the safety requirements while FCC is interested about both the technology and how to efficiently using the 5.9 GHz band with the technologies. The scenario of coexistence can be considered as interoperable or non-interoperable. Interoperable represents as vehicles are using a device that allows DSRC and C-V2X to communicate each other. No regulation scenario represents the case when NHTSA does not impose a regulation for vehicular communication.

With the combinations of identified FCC and NHTSA's regulation scenarios, we have generated scenario regulation chart as shown in Figure 48.

For each combination of scenarios, certain technical challenges are inherent. The technical challenges are shown as alphabet code in Figure 48. The details of these technical challenges are listed in Table VIII.

Based on the expected scenarios, certain technical challenges can be faced:

- Effect of adjacent interference to DSRC or C-V2X, or vice versa
- Ability of Wi-Fi to detect DSRC or C-V2X signals
- Co-channel interference between Wi-Fi/DSRC/C-V2X
- Interoperability between DSRC and C-V2X
- Scheduling schemes to use the spectrum for DSRC and C-V2X

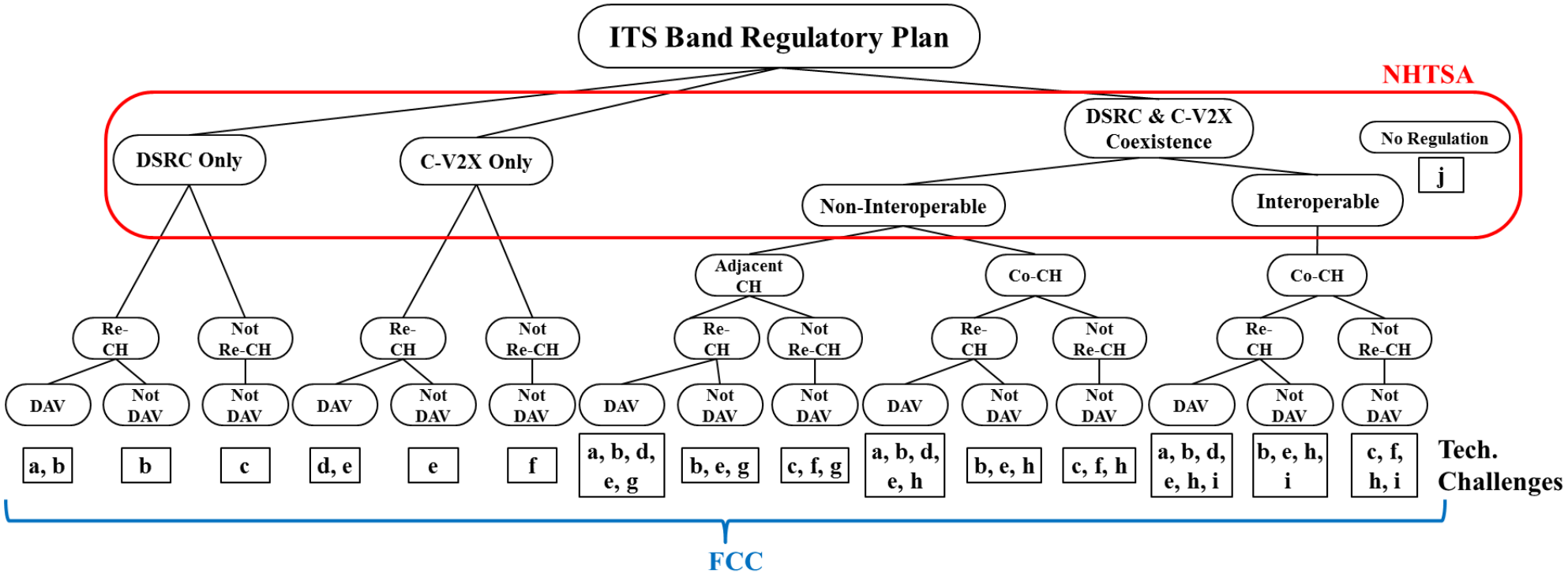

Figure 48 FCC and NHTSA's regulation plan

Table VIII List of technical challenges

Alphabet Code from Figure 48	Description	Alphabet Code from Figure 48	Description
a	Ability of Wi-Fi to detect DSRC signals to vacate	f	Co-channel interference between Wi-Fi and C-V2X
b	Adjacent interference to DSRC: out-of-band rejection of DSRC	g	Analyzing adjacent interference from DSRC to C-V2X and from C-V2X to DSRC. Depending on which system will use the lower frequency band, adjacent interference from Wi-Fi need to be analyzed
c	Co-channel interference between Wi-Fi and DSRC	h	How the co-channel coexistence between DSRC and C-V2X will affect the performance to each other

d	Ability of Wi-Fi to detect C-V2X signals to vacate	i	Interoperability between DSRC and C-V2X
e	Adjacent interference to C-V2X: out-of-band rejection of C-V2X	j	The “No Regulation” will inherit all technical issues in the column above it

4.3 Technical Surveys Related to Regulation Scenarios

By categorizing technical challenges as shown in Table VIII, we surveyed papers and categorized them into the related technical challenge topics. For the current FCC and NHTSA's plan is the scenario of DSRC only using for 5.9 GHz spectrum band, we found the greatest number of papers address this scenario. However, the least number of studies are related to the technical challenges for coexistence of DSRC and C-V2X scenario. Therefore, in this section, we identify the technology gaps that have not been addressed in the technical literature. Table IX summarizes addressed technical challenges that found in the literature and their key findings.

4.3.1 DSRC Only

Authors of [36] evaluated the effects of adjacent channel interference in multi-channel vehicular networks. In the model setup, a target node is observing in Service Channel (SCH) 4 and various numbers of nodes transmit on SCH3 to cause adjacent channel interference on the target node. Their study shows that a node tuning into a channel with a low transmission power, so to mitigate adjacent channel interference effects would preserve the communication quality at some extent. They also found that despite the blocking, channel access delay may be reduced and transmissions may be less prone to collisions.

The authors in [37] studied the effects of adjacent channel interference signal energy levels and channel access delay and packet loss in the multi-channel vehicular networks using an adjacent channel interference model through simulation that is able to control time, space, and frequency parameters for mobile nodes. They explored two scenarios: 1) vehicular nodes are arranged in a square and adjacent channel interference effects at the center are measured;

2) 60 cars are exponentially distributed over 3-lane highway. Through the simulations, they found that the effect of adjacent channel interference to be significant for transmission power settings of 20 dBm and when the involved nodes are at a distance lower than 7m. The results show that the increased packet losses is the more evident effect of adjacent channel interference in mixed co-channel and adjacent channel interference scenarios.

Impact of adjacent channel interference on DSRC Control Channel (CCH) communication due to communication in adjacent SCH channel is evaluated in [38]. They setup two devices communicating on CCH and two on SCH. Two nodes, one on each channel, are kept close together while the other two are farther away. 5, 10, 15, 20, and 33 dBm power levels used and 5-500 m separations used. Through the tests, the authors observed that 1) a transmit power of 33dBm is not applicable because the adjacent channel will be found busy by the nearby node; 2) it is not applicable to run both channels with a similar transmit power due to the reduction of the communication range to 100 m on both channels; 3) the best power difference seems to be 10 dB where the best communication range on the CCH and SCH can be achieved.

The impact of on-board 802.11a Wi-Fi device communication with an electronic toll collector on the vehicle's DSRC communication is evaluated in [39]. The tests were done with 3 lanes and 100 cars in each lane. Two traffic cases were considered: 1) normal traffic case, in which cars move at 54 km/h and the average inter-car distance is 10 m; 2) traffic jam case, which assumes that cars are moving at 3.6 km/h and the average inter-car distance is 3 m. Also, sensitivity to power was considered by: 1) vary percentage of cars using 802.11a; 2) vary transmit power of 802.11a with percentage cars held constant; 3) vary transmit power of 802.11p RSU. Through the tests, authors of [39] found that the effect of 802.11a interference

can’t be eliminated just by increasing the 802.11p transmit power and need further mechanisms to make DSRC more reliable and rugged.

Authors of [40] tested the interference to DSRC communication when the interferer is another DSRC radio on the same vehicle as well as on another vehicle. They tested with two scenarios: 1) V2V communications with equipped 6 dBi antenna; 2) V2I communications with RSU equipped 16 dBi and OBU equipped 6 dBi antenna and 33 dBm transmit power. For V2V scenario, they observed the receiver can only receive other adjacent signals within 14.19 m and non-adjacent signals within 71.13 m with full transmission rate, 27 Mbps. For V2I scenario, they observed the receiver can only receive other adjacent signals within 174.6 m and non-adjacent signals within 875.1 m with full transmission rate, 27 Mbps.

Reference [41] analyzed the coexistence between Wi-Fi and DSRC by analyzing the physical layer challenges and the MAC layer challenges for the two systems to coexist. At short distances between DSRC transmitter and receiver from there is no significant coexistence issues. For long range DSRC communications, there is high DSRC packet loss due to interference from Wi-Fi, but long distances are not critical for safety related DSRC applications. At medium distances, outdoor Wi-Fi can coexist better than indoor Wi-Fi, the latter creating non-negligible packet loss, which can be problematic for DSRC safety applications. Their results show that even with DAV, indoor Wi-Fi can cause interference to DSRC, and it was recommended to reduce the Wi-Fi transmit power in this case to avoid creating an interference to the DSRC. Also, the results shows the DAV provides better coexistence mechanism for the DSRC, and it was recommended in the paper to adopt this technique if Wi-Fi and DSRC share the same band.

From the surveys, we expect following additional technical analysis is needed for DSRC Only regulatory scenario:

- Evaluation of adjacent channel or co-channel Wi-Fi interference effects
- Technical improvement of Wi-Fi to detect DSRC signal for advanced DAV algorithm

4.3.2 C-V2X Only

Reference [42] analyzed the effect of the aggregate adjacent channel interference generated from LTE small-cells to a user in macro-cells. The authors propose an interference approximation model for the interference generated from small-cell to a device connected to the macro-cell as a weighed-sum of lognormal-based distributions. They found that if small-cell intensity increases, the outage probability of victim user increases and under same small-cell intensity, as the distance between victim user and macro-cell BS increases, outage probability increases.

The authors of [43] proposed a modified OFDM-based scheme for V2X communication to improve performance and robustness of the vehicular communications against fast fading, which will happen when vehicles travelling at high speed. The authors analyzed the effect of subcarriers numbers on the date rate under different relative speeds. They concluded that when the data rate increases from 1 Mbps to 10 Mbps under a relative speed of 200 km/h, the larger number of subcarriers is preferred to satisfy the link performance requirements, especially to prevent frequency selective fading.

The authors of [44] evaluate the performance of V2I communications based on a freeway scenario in which the coverage is provided by LTE-A. The authors used an LTE system simulation platform for which the system throughput performance and signal-to-interference-plus-noise ratio (SINR) have been rigorously assessed. For the case in which the network is dense and the reliability requirement is high, the results indicate there is a need for novel

resource allocation and interference mitigation techniques to meet the performance requirements. For the case in which the minimum and maximum distances between vehicles are 200 m and 300m, respectively (which corresponds to around 40 vehicles connected to each RSU), the result shows that about 50% of vehicles can achieve an SINR of 15 dB and cell edge vehicles (5% from CDFs) can achieve SINR of 2 dB.

The authors of [45, 46] studied about performances of LTE-V mode 4 for C-V2X and presented LTE-V mode 4 with using sidelink. From [44], the authors compared the performances of DSRC and LTE-V under highway fast and slow environments and evaluated LTE-V performances with different modulation schemes. From the studies, the authors observed LTE-V outperforms DSRC when DSRC is using low data rate and alternative DSRC due to its improved link budget, the support for redundant transmissions per packet, and different sub-channelization schemes. However, the careful configuration parameters are required for more efficient usage. The authors of [45] analyzed the performance with different Semi-Persistent Scheduling (SPS) parameters of C-V2X. The authors of [45] observed Packet Delivery Ratio (PDR) improved as the number of available sub-channels and increasing of resource reservation interval can obtain increasing of PDR in dense networks.

From the surveys related to C-V2X Only regulatory scenarios, we expect following technical challenges are needed:

- Observation of the configuration of C-V2X that can outperforms DSRC
- Evaluations of adjacent or co-channel Wi-Fi interference effect to C-V2X
- Signal scheduling schemes for C-V2X networks

4.3.3 Coexistence between DSRC and C-V2X

In [47], the 5GAA proposes splitting the lower 30 MHz of the band between DSRC and C-V2X, where each technology is allocated 10 MHz (5875-5885 MHz, 5895-5905 MHz), and there is 10 MHz in between (5885-5895 MHz), which can be used by either technology through a Detect and Vacate mechanism. According to 5GAA, the upper 45 MHz allocation can be addressed in the future.

Since we won't able to search many surveys related to Coexistence between DSRC and C-V2X regulatory scenario, the additional technical challenges covers all challenges that mentioned previous regulatory scenarios:

- Evaluations of adjacent or co-channel interference effect between DSRC and C-V2X; both can be main signal and interference source
- Signal scheduling schemes of DSRC and C-V2X in the spectrum bands
- Interoperability between DSRC and C-V2X
- DSRC/C-V2X detection and identification methodology
- Wi-Fi to detect DSRC/C-V2X for advanced DAV algorithm
- Advanced channelization, avoidance, and interference mitigation techniques

Table IX Summary of technical surveys

Regulatory Scenarios	Contributions
DSRC Only	• A node tunes into a channel with a low transmission power to mitigate adjacent channel interference effects would preserve the communication quality at some extent [36] • Interference to nearby nodes gets weaker [36]

	• Effect of adjacent channel interference should not be neglected for transmission power of 20 dBm at a distance lower than 7 m [37] • Increase of channel access delay due to adjacent channel interference is largely negligible when co-channel interference is also experienced [37] • The best power difference is around 10 dB where the best communication range on the CCH and SCH can be achieved [38] • Effect of 802.11a interference can't be eliminated by increasing 802.11p transmit power [39] • Receiver can receive other adjacent signals within 174.6 m and non-adjacent signals within 875.1 m with 27 Mbps transmission rate [40] • Even with DAV, indoor Wi-Fi can cause interference to DSRC and recommended to reduce Wi-Fi transmit power to avoid creating an interference to DSRC [41]
C-V2X Only	• If small-cell intensity increases, the outage probability of victim user increase [42] • As the distance between victim user and macro-cell BS increases, outage probability increase [43] • When the data rate is increasing from 1 Mbps to 10 Mbps under a relative speed of 200 km/h, the larger number of subcarriers is preferred to satisfy maintain the link, especially to in the presence of frequency selective fading [43] • When the network is dense and reliability requirements are high,

	there is a need for novel resource allocation and interference mitigation techniques to meet the performance requirements [44] • LTE-V outperforms DSRC when DSRC is at 6 Mb/s, but DSRC can improve the performance with 18 Mb/s [45] • LTE-V can be an alternative of DSRC due to the improved link budget, the support for redundant transmissions per packet, and sub-channelization schemes; however, a careful configuration of the transmission parameters is required for transmitting more packets-per seconds (pps) [45] • PDR improves as the number of available sub-channels for sidelinks [46] • PDR increase from 10-25% to 60-85% when the resource reservation interval increased 100 to 1000 ms [46]
Coexistence between DSRC and C-V2X	• 5GAA proposed splitting lower 30 MHz of band between DSRC and C-V2X and upper 45 MHz allocation can be addressed in the future [47]

4.4 Conclusion of ITS band regulatory contingency and technical survey

We have analyzed the potential regulatory rules that can be made by FCC and NHTSA about 5.9 GHz spectrum band for vehicular communications and have created possible regulation scenarios. We have listed the technical challenges that can be brought up from the several

combinations of scenarios as shown in Table VIII. We have presented a complete survey for the vehicular communication related research work in the literature and have mapped this work into the different technical challenges we analyzed.

Through configuring possible regulation scenarios and technical surveys, we have identified that certain technical challenge topic had been researched more than the others. Even the frequent researches were done in related to DSRC only, C-V2X only, or coexistence of DSRC and C-V2X, we believe coexistence of DSRC and C-V2X will be the regulation in near future and C-V2X only will be the regulation for further future when the configurations of C-V2X that can outperform DSRC is confirmed. With the expected regulation, we believe interoperability technical issue should be investigated more due to the announcement of FCC, U-NII4 devices share with DSRC band, and rising of C-V2X. Beyond near-term regulatory decisions for the 5.9 GHz band, the survey will help researchers set appropriate agendas for investigations related to V2X communication in future bands that may be subjected to different combinations of regulations.

Chapter 5

Adjacent Channel Interference Evaluation

5.1 Introduction

From the technical survey for ITS band regulatory planning, we observed several technical challenges and distributions of studies related to possible 5.9 GHz band regulatory scenarios. Based on our observation, coexistence between DSRC and C-V2X scenario is not as thoroughly researched as other possible scenarios mentioned in the previous chapter. Therefore, we planned to conduct measurements to evaluate the feasibility of adjacent channel coexistence.

We conducted the measurements to evaluate the effect of adjacent channel interference, using interference sources such as IEEE 802.11ac and approximated C-V2X, to DSRC performance. With the results from the experiments, we can evaluate the possibility for DSRC Only & Re-channelization and DSRC and C-V2X adjacent channel coexistence & Re-channelization scenarios. We measured the performance of DSRC as metric of PER with adjacent channel interferences as IEEE 802.11ac, 20 and 40 MHz bandwidth, and approximated C-V2X signals and different path loss values.

5.2 Measurements Overview

The objective of our experiments is to empirically evaluate the performance of DSRC using PER as the performance metric, in the presence of interference from LTE and IEEE 802.11ac signal in adjacent channels. Because C-V2X equipment was not available at the time of writing, we used standard LTE/modified C-V2X signals to provide a rough approximation of

C-V2X. C-V2X includes provisions to reduce interference that are not included in the LTE waveform used in the experiments, so the interference from C-V2X to DSRC is likely to be less than observed in the experiments. With these evaluations, we can identify the effect of Wi-Fi, LTE, and C-V2X on DSRC to assess implications of the FCC's proposed plan for ITS band.

For C-V2X adjacent experiments, DSRC operates on Channel 172 and C-V2X on Channel (ch) 174. Since current Wi-Fi devices do not operate in the DSRC bands, we operate DSRC in ch 172 and record IEEE 802.11ac signals and upconvert them to ch 169 for a 20 MHz bandwidth Wi-Fi signal and to ch 167 for a 40 MHz wide signal. This allows us to conduct adjacent channel interference measurements and analyses.

We consider varying path loss between DSRC radios and Wi-Fi, LTE, and C-V2X radios. As shown in Figure 49 and Figure 50, our scenario contains a DSRC transmitter (Tx), receiver (Rx), and Wi-Fi, LTE, and C-V2X radio as the adjacent-channel interferer. We assume that both channels, DSRC Tx to Rx and interference source to DSRC Rx, are LOS. We consider DSRC Tx to DSRC Rx distances (D1) of 50, 75, 100, 150, 225, 300, and 415 m. The interference source to DSRC Rx distances (D2) are 25, 50, 75, and 100 m. Figure 49 and Figure 50 shows the desired setup for D1 and D2.

We used the Urban Micro LOS (UMi LOS) path loss model from 3GPP TR 36.814 [31]. The UMi LOS equations are

$$\mathrm{PL} = 22.0log_{10}(d) + 28.0 + 20log_{10}(f_c) \quad (23)$$

Where f_c is a center frequency in GHz, d the distances between two nodes in m. (23) applies to distances, d, below 1180 m, which are considered in these experiments.

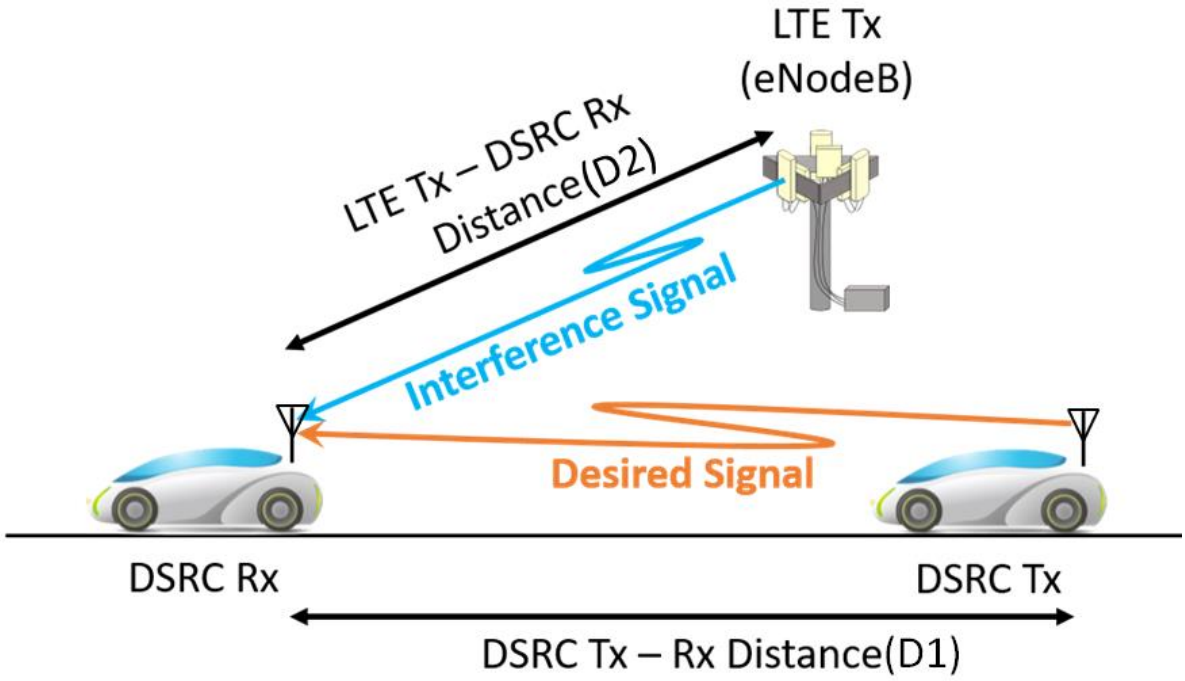

Figure 49 Scenario for DSRC Tx, Rx, and LTE coexistence

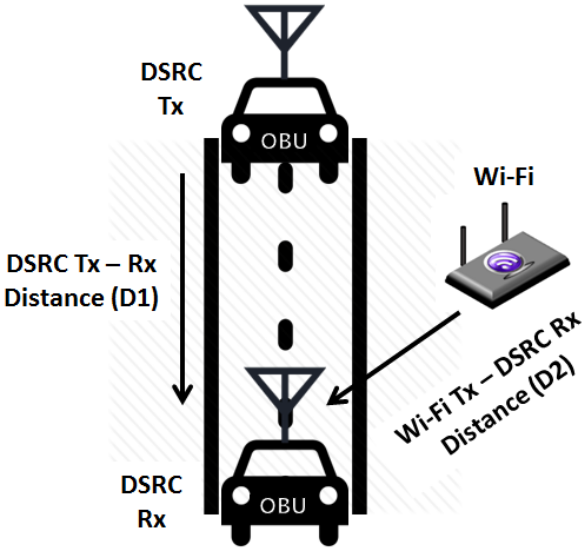

Figure 50 Scenario for DSRC Tx, Rx, and Wi-Fi coexistence

5.3 Hardware Setup

The hardware platform has three major components: (1) DSRC radios; (2) a recorded interference source; and (3) an emulated RF channel. All components are connected through short shielded cables to remove any external random effects.

5.3.1 DSRC

Savari MobiWAVE radios are used for the measurements. The DSRC signal has a transmit power level of 23 dBm, a bandwidth of 10 MHz, a packet length of 143 bytes, a packet interval of 100 ms, and transmits 6000 packets. We assume BSM types of applications. The BSM application contains these messages per each packet: transmit power, bit rate, channel, message length, message count (*msg_cnt*), id, section mark (*secMark*), latitude (*lat*), longitude (*long*), elevation, speed, heading, angle, acceleration in latitude, acceleration in longitude, acceleration in vertical, acceleration in yaw, brake status, width, and length. We post-process the transmitted and received packet by comparing '*msg_cnt*', '*secMark*', '*lat*', and '*long*' parameters to determine the number of correctly received and dropped packets to calculate the PER as

$$\text{PER} = 1 - \frac{Number\ of\ Received\ Packets}{Number\ of\ Transmitted\ Packets} \tag{24}$$

5.3.2 Interference Sources

The recorded LTE signal consists of Time Division Duplex (TDD) LTE Uplink (UL) and Downlink (DL) signals which were generated by a Rhode & Schwarz CMW 500 Wideband Radio Communication Tester with center frequency at 2.4 GHz and bandwidth of 10 MHz. We used USRP B210 to playback the recorded LTE signal by adjusting transmit power level

to 23 dBm and center frequency at Channel 174 to provide a rough approximated C-V2X signals with nearly 100% channel capacity.

The recorded Wi-Fi signal is generated using a TP-LinkAC1900 IEEE 802.11ac Wi-Fi AP. The 20 MHz signal uses ch 161 and the 40 MHz signals uses ch 159 with a transmit power of 36 dBm. Wi-Fi AP is connected to a Microsoft Surface Pro 3 notebook to record both uplink and downlink signals. The channel capacity is nearly 100 %, as controlled by *iperf*. The recording is done using GNU Radio with a USRP B210. The recorded signal is played back at a desired center frequency using the same software-defined radio setup. Since a large amount of memory is required for recording the wideband signal and the out-of-band signal leakage, we only record the 15 MHz of the Wi-Fi signal/leakage portion that overlaps with the DSRC signal. This is illustrated in Figure 51.

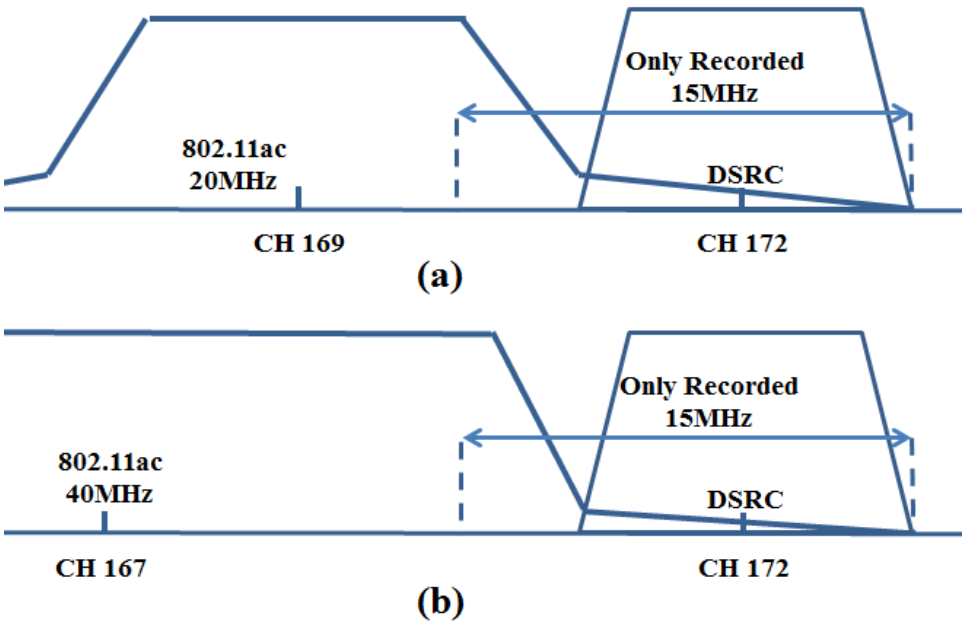

Figure 51 (a) Region of recorded 20 MHz Wi-Fi signal, (b) region of recorded 40 MHz Wi-Fi signal

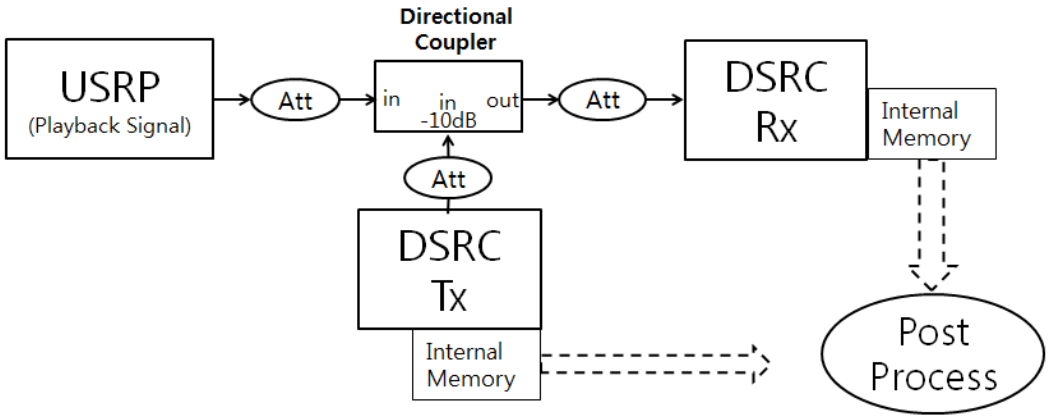

Figure 52 RF channel emulator implemented as variable attenuators

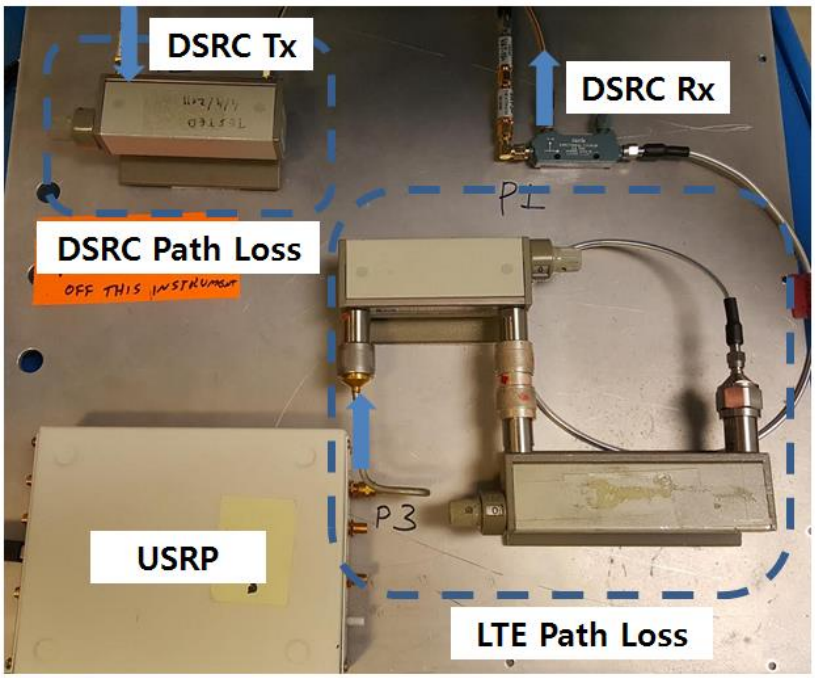

Figure 53 Photo of attenuators

5.3.3 Emulated RF Channel

To emulate large-scale path loss (PL), we physically connect attenuators to the junction between DSRC Tx to Rx and Wi-Fi interference to DSRC Rx separately as shown in Figure 52. The attenuated signals are combined at the input of the DSRC Rx. The actual connections

of attenuators are shown in Figure 53. The attenuation values are obtained based on (23). Since the center frequencies for DSRC and 20 and 40 MHz Wi-Fi signals are different, the calculated PL values differ; however, the difference is less than 1 dB, which is the minimum step size of the controllable attenuators that we have. Therefore, attenuator values for 50, 75, and 100 m LOS distances for the Wi-Fi and DSRC paths are set to the same values of 81, 84, and 87 dB, respectively. The selected distances for Wi-Fi to DSRC Rx path are 25, 50, 75, and 100 m with path loss of 74, 81, 84, and 87 dB. The selected distances for DSRC Tx to Rx path are 50, 75, 100, 150, 225, 300, and 415 m with path loss of 81, 84, 87, 91, 95, 98, and 101 dB. Table X captures the experimental paraemters, including path loss values between DSRC Tx and Rx and adjacent interference source to DSRC Rx, as well as the emulated distance values. The signal validations are shown in Appendix C.

Table X Measurements Configurations

Configurations	Parameters
DSRC transmit power	23 dBm
LTE/C-V2X transmit power	40/23 dBm
Wi-Fi transmit power	36 dBm
DSRC channel	172
C-V2X channel	174
Distance between DSRC Tx and Rx (D1)	50, 75, 100, 150, 225, 300, 400 m
Path loss on DSRC link	81, 84.6, 87.4, 91, 95, 97.9, 100.7 dB
Adjacent Channel Tx and DSRC Rx distance D2	25, 50, 75, 100 m
Path loss along D2	74, 81, 84.6, 87.4 dB

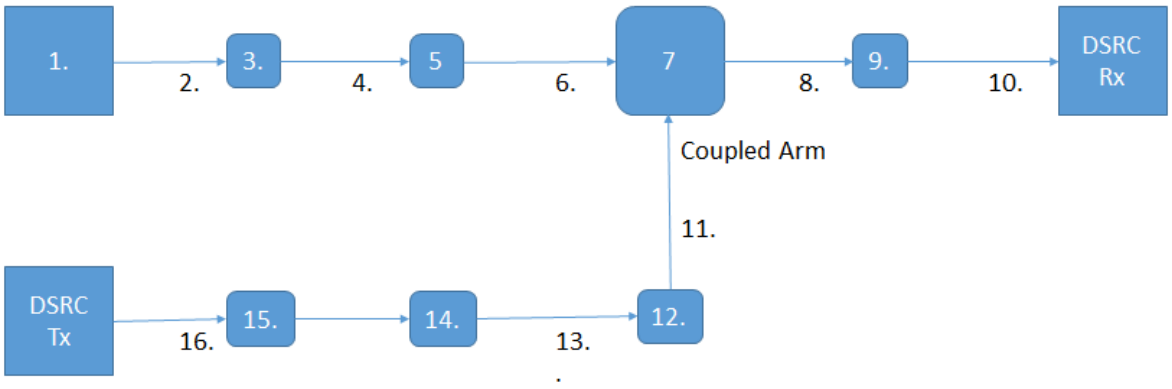

Figure 54 Parts labels for USRP and DSRC Tx/Rx connections for LTE measurements

Table XI Part names from Figure 54

Part Label Number	Part Name
1	USRP B210 Software Defined Radio Transmitter
2	Custom .141 Semi-Rigid Coaxial Cable (SMA-M to N-M approx. length 0.1m)
3	HP 8495B 10 dB Step Attenuator (N-F)
4	N-M to N-M Coaxial Adapter
5	HP 8494B 1 dB Step Attenuator (N-F)
6	United Microwave Microflex 150 Coaxial Cable, 18 inches.
7	Narda 424410 Directional Coupler (4-8 GHz)
8	Right Angle Adapter (SMA-M-F)
9	MC VAT-3+ Coaxial Fixed Attenuator
10	United Microwave Products Microflex 150 Coaxial Cable to DSRC , 24

	inches.
11	United Microwave Products Microflex 150 Coaxial Cable, 12 inches
12	HP 8495B 10 dB Step Attenuator (sma-f)
13	United Microwave Microflex 150 Coaxial Cable , 24 inches.
14	MC VAM-3W2 Coaxial Fixed Attenuator (substitute as required)
15	MC VAT-6+ Coaxial Fixed Attenuator (substitute as required)
16	United Microwave Microflex 150 CoaxialCable from DSRC, 72 inches

Note: Components tested as an assembly using R&S ZVL-13 Vector Network Analyzer calibrated with ZV-Z132 calibration kit.

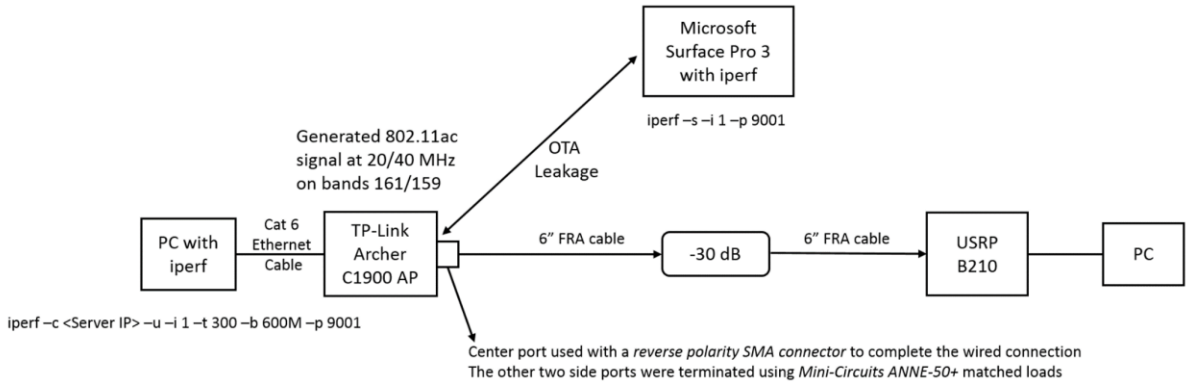

Figure 55 Wi-Fi interference signal recording diagram for 20 & 40 MHz

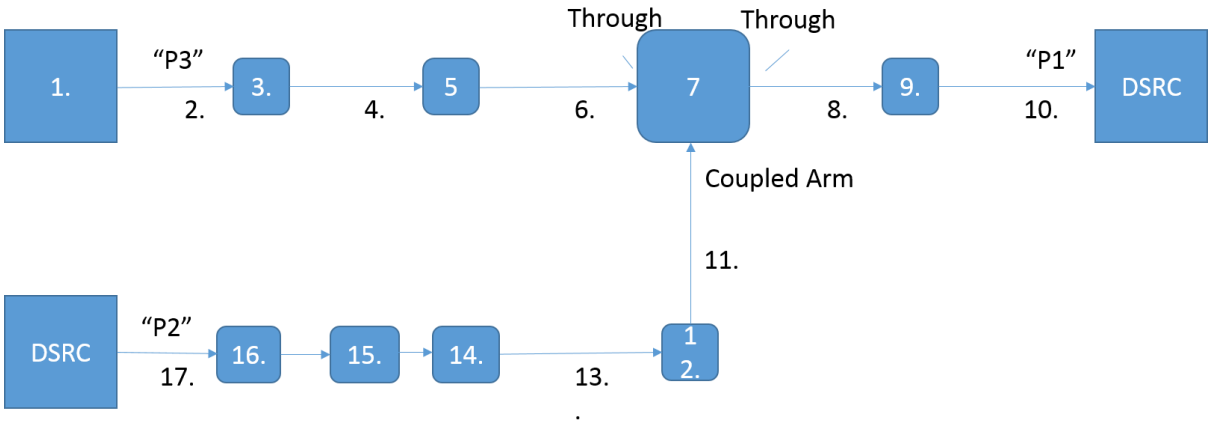

Figure 56 Parts labels for USRP and DSRC Tx/Rx connections for Wi-Fi measurements

Table XII Part names from Figure 56

Part Label Number	Part Name
1	USRP B210 Software Defined Radio Transmitter
2	United Microwave Microflex 165 Coaxial Cable, 24 inches
3	HP 8495B 10 dB Step Attenuator (N-F)
4	N-M to N-M Coaxial Adapter
5	HP 8494B 1 dB Step Attenuator (N-F)
6	United Microwave Microflex 150 Coaxial Cable, 18 inches
7	Narda 424410 Directional Coupler (4-8 GHz)
8	Right Angle Adapter (SMA-M-F)
9	MC VAT-3+ Coaxial Fixed Attenuator
10	United Microwave Products Microflex 150 Coaxial Cable to DSRC, 72 inches
11	United Microwave Products Microflex 150 Coaxial Cable, 12 inches
12	HP 8495B 10 dB Step Attenuator (SMA-F)
13	United Microwave Microflex 150 Coaxial Cable, 24 inches.
14	MC VAM-3W2 Coaxial Fixed Attenuator (substitute as required)
15	MC VAT-6+ Coaxial Fixed Attenuator (substitute as required)
16	MC VAM-3W2 Coaxial Fixed Attenuator (substitute as required)
17	Times Microwave LMR-200 Coaxial Cable from DSRC Tx to fixed attenuators, 24 inches

Note: Components tested as an assembly using R&S ZVL-13 Vector Network Analyzer calibrated with ZV-Z132 calibration kit.

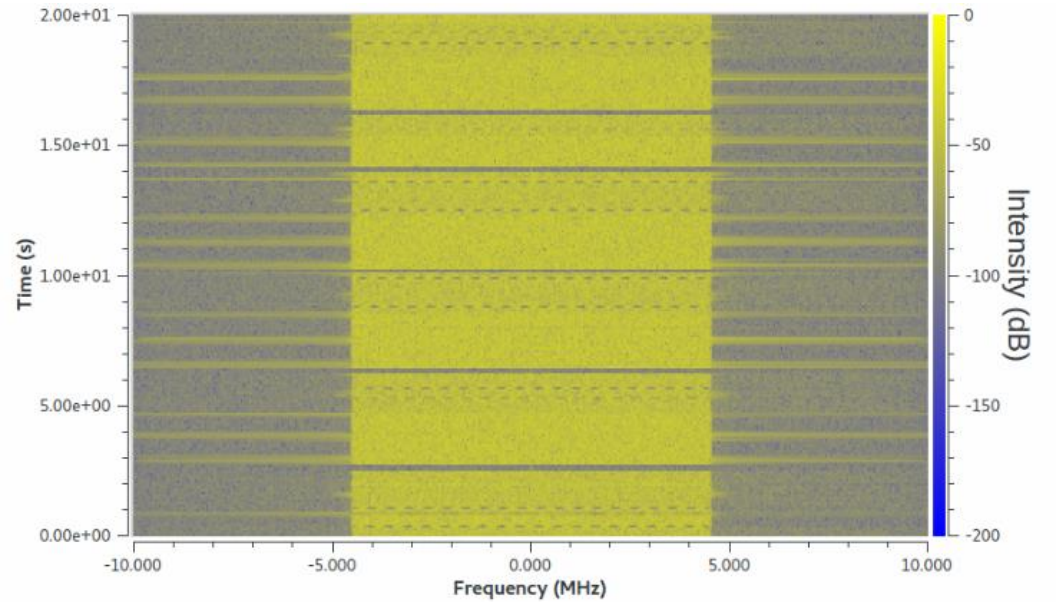

Figure 57 Waterfall plot of recorded LTE signal

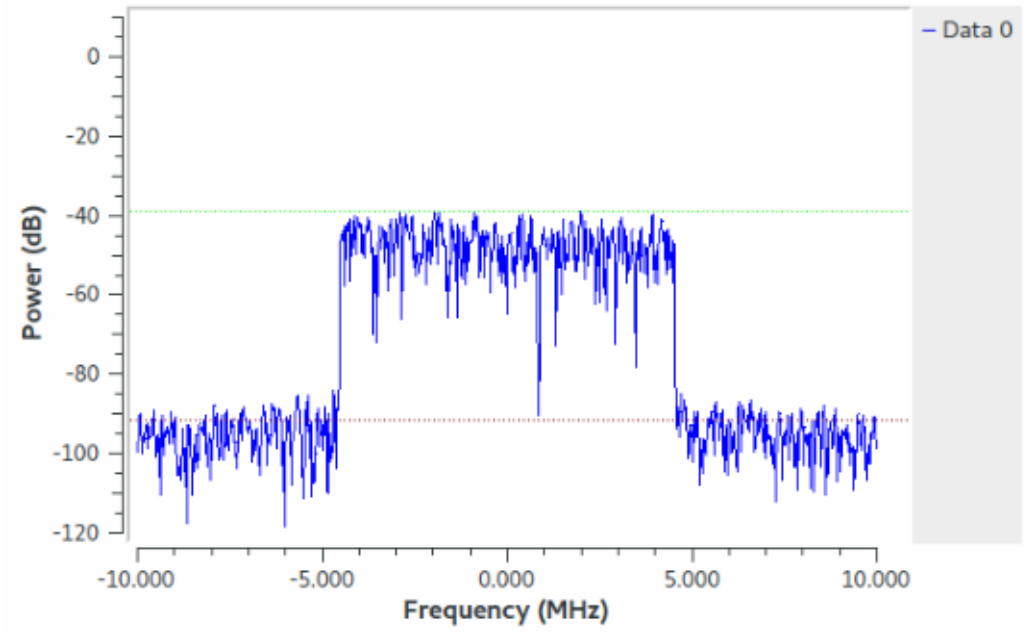

Figure 58 Instantaneous recorded LTE signal

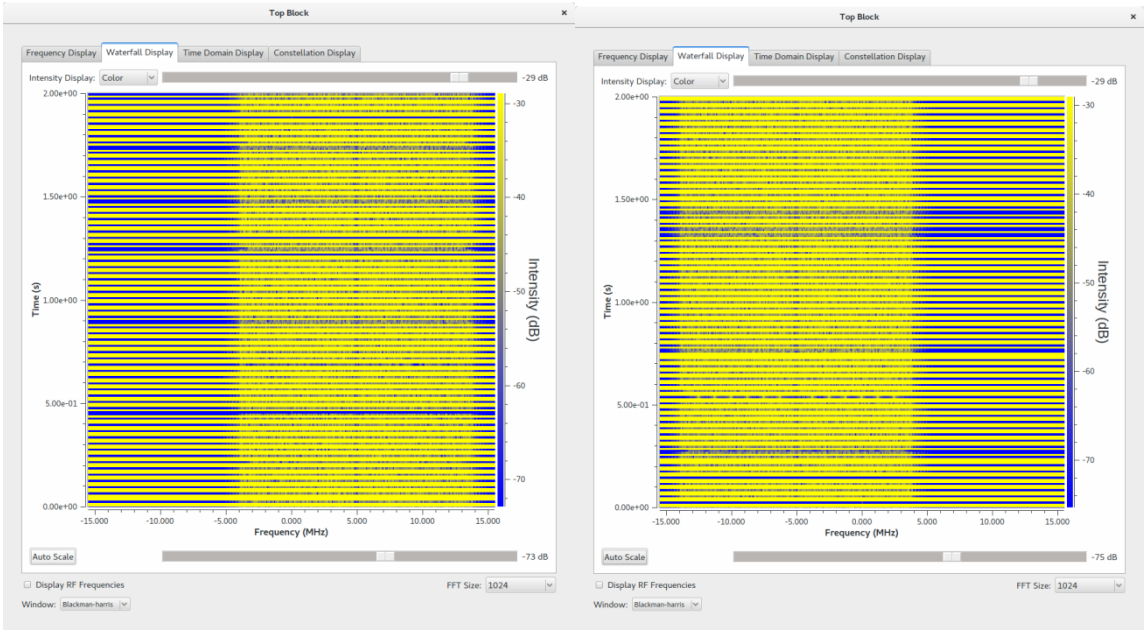

Figure 59 Waterfall plot of 20 MHz Wi-Fi signal (lower and upper end)

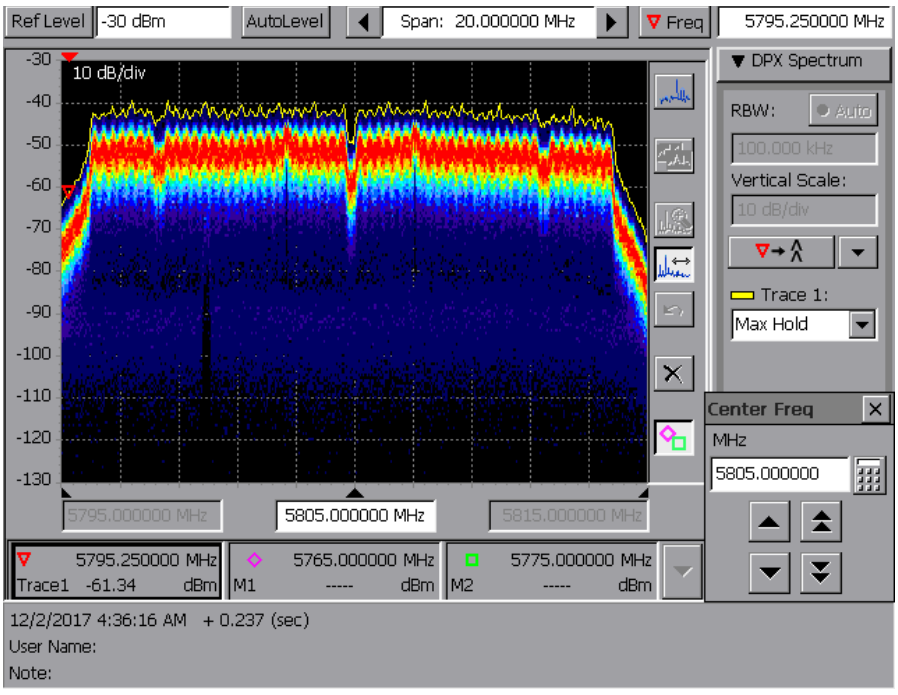

Figure 60 Instantaneous 20 MHz Wi-Fi signal

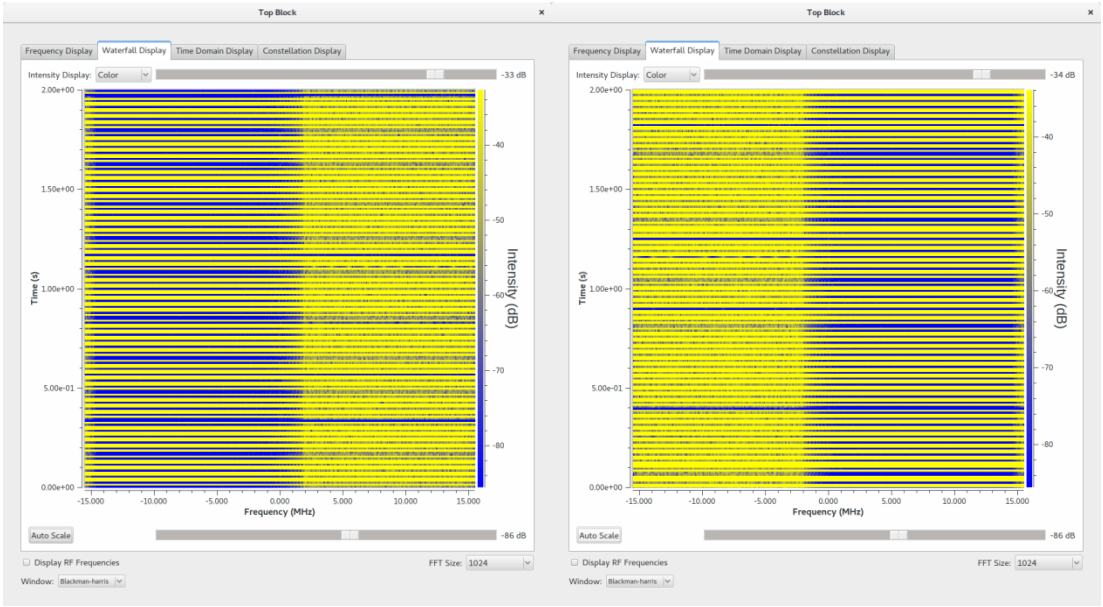

Figure 61 Waterfall plot of 40 MHz Wi-Fi signal (lower and upper end)

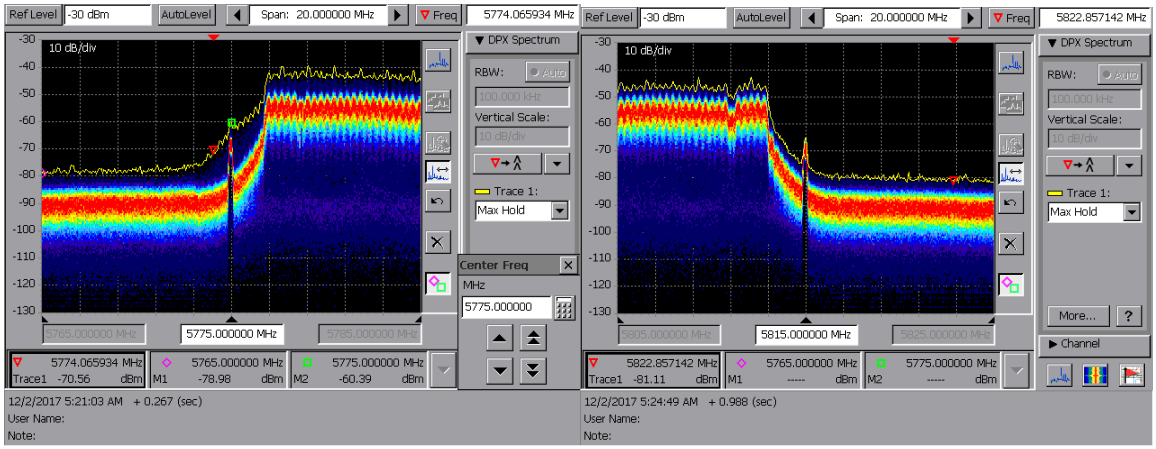

Figure 62 Instantaneous 40 MHz Wi-Fi signal (lower and upper end)

5.4 Results

Since the number of transmitted packet is 6000, we plot the PER value as $<10^{-4}$ when no packets are dropped at the receiver. We conduct each scenario one time, 6000 packet transmissions; therefore, there is a possibility of capturing higher PER than our results if more packets transmitted.

5.4.1 LTE/C-V2X Interference Scenario Results

We analyze LTE and C-V2X coexisting in adjacent channel with DSRC. The PER is around 0.5 for D2 of 25 m; however, the PER is around 0.1 for all other D2 distances. The PER is almost zero for all scenarios except for the D1 of 50 m and D2 of 25 m. This scenario has the strongest effect of the interference, which is reflected by the results. The PER value of 1.5*10^-3 is low and has little effect on the service. Therefore, we conclude that LTE adjacent channel signal has significant impact on DSRC for short distances and less for further distances, and C-V2X adjacent channel signal has almost no effect on the DSRC performance and both can coexist in adjacent channels.

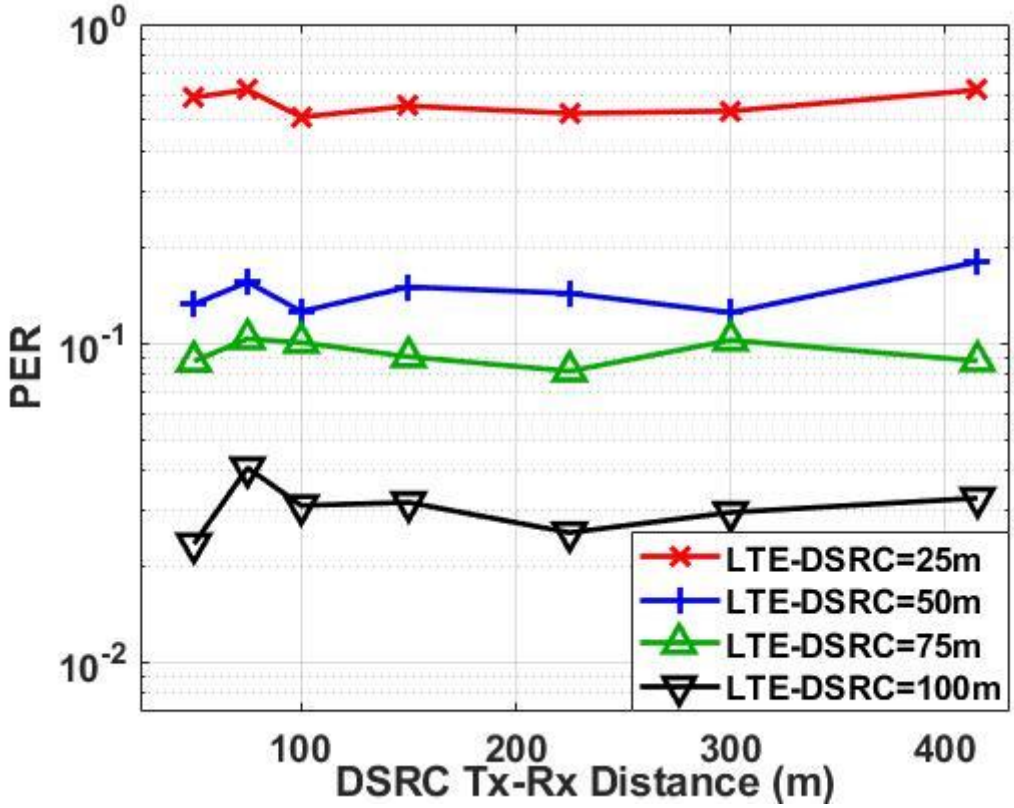

Figure 63 PER of DSRC for different LTE BS-DSRC Distances

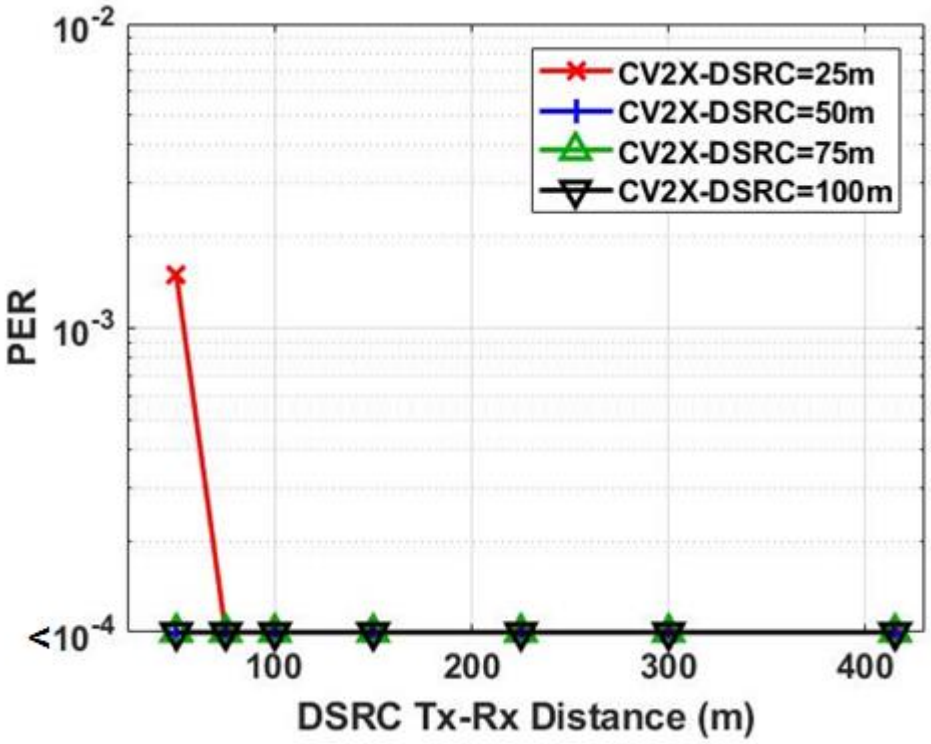

Figure 64 PER of DSRC with C-V2X

5.4.2 20 MHz Wi-Fi Interference Scenario Results

When Wi-Fi is operating in channels of DSRC transmissions, the PER of Figure 65 is obtained. We observe low PERs for all scenarios except for Wi-Fi distances of 25 m. For Wi-Fi distances between 50 and 100 m, we observe PER in the range between $1.65e^{-4}$ and $6.57e^{-4}$, which represents packet losses of 1-4 packets out of 6000 transmission. When comparing this with the C-V2X results, we conclude that Wi-Fi is a worse channel neighbor than C-V2X. However, even though the Wi-Fi distance of 25 m leads to non-negligible PER, the performance of DSRC will not be critically affected. Therefore, we conclude that 20 MHz Wi-Fi adjacent channel signals will affect DSRC performance only when the Wi-Fi AP is within 25 m of the DSRC receiver. Also, interestingly, we observe that the PER is less affected by the path loss changes on the D1 link than on D2. From this observation we

conclude that the effect of changes in the out-of-band emission of Wi-Fi is more harmful than the effect of path loss changes of DSRC.

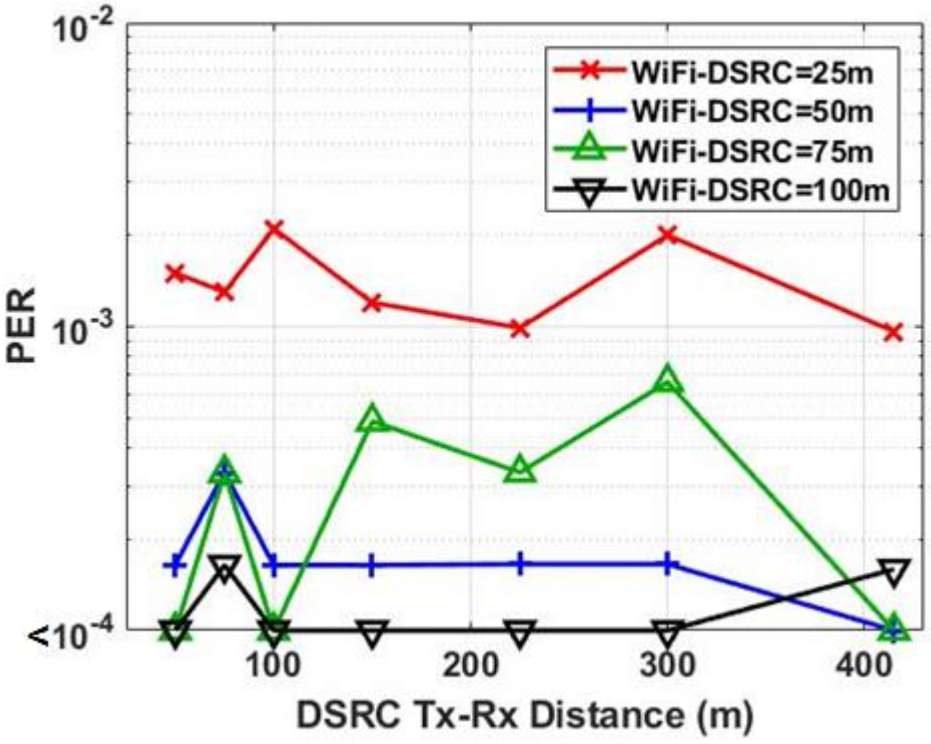

Figure 65 PER of DSRC with 20 MHz Wi-Fi adjacent channel transmissions

5.4.3 40 MHz Wi-Fi Interference Scenario Results

Figure 66 illustrates the PER of DSRC with a 40 MHz adjacent channel Wi-Fi system. Interestingly, we find a lower PER for all scenarios when compared to the 20 MHz Wi-Fi case. The highest PER occurs at D1 of 50 m and D2 of 25 m; however, the two lost packets out of 6000 transmitted can be considered a negligible performance degradation of DSRC. Therefore, we conclude that 40 MHz Wi-Fi adjacent channel signal will not affect DSRC performance. Also, we find as before that the effect of DSRC path loss changes is less severe than changes in the Wi-Fi out-of-band emission.

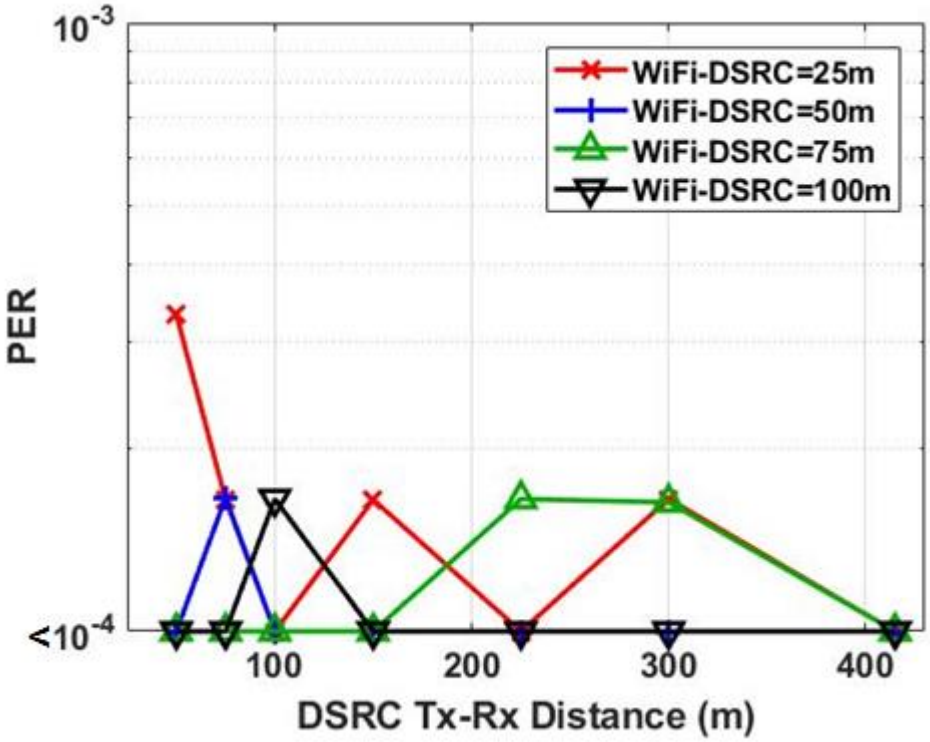

Figure 66 PER of DSRC with 40 MHz Wi-Fi adjacent channel transmissions

5.5 Conclusions for Adjacent channel interference measurements

We conducted the measurements to evaluate the effect of adjacent channel interference, the sources as Wi-Fi, roughly adjusted C-V2X, and LTE, to the performance of DSRC. The setup was DSRC at Channel 172, Wi-Fi at Channel 169 for 20 MHz bandwidth and at Channel 167 for 40 MHz, and LTE/C-V2X at Channel 174 with almost 100% spectrum capacity. From the measurements, we observed higher PER values for D1 of 50 m and D2, Wi-Fi scenario, of 25 m; however, we concluded as not much critically affect the DSRC performance. Also, we concluded C-V2X adjacent interference does not critically affect the DSRC performance as well as 20 and 40 MHz Wi-Fi adjacent interferences. However, LTE adjacent interference has significant effect to DSRC performance with shorter distances and decreases as the distance increases.

From the measurements, we conclude adjacent channel coexistence between DSRC, C-V2X, and Wi-Fi can be deployable for 5.9 GHz spectrum band. However, the real environment testing is required to make a solid conclusion for adjacent channel coexistence.

Chapter 6:

Summary

6.1 Summary of V2T Communications

We presented a V2T early warning application architecture with requirements. For the feasibility study, we conducted propagation channel measurements and DSRC performance measurements at railroad crossings in open spaces, artificial shadowed environments, rural, and suburban environments. From the analysis of the results, we concluded that DSRC protocol can be adapted to the early warning application architecture and feasibility analyses provide guidance for implementation of V2T warning systems. Contribution 1 also benefits researchers by presenting methodologies for measurements of V2T radio channels and V2T warning system radio link performance. The higher level of architecture of V2T is combinations of V2V and V2I, but in more detail, we presented numeric regions, distances, and the notification time based on the speed of vehicles or trains. From the conducted propagation channel and DSRC performance measurements, we used estimation methods to generate linear regression models. From the models and comparison between existing works, we observed more physical experiments are required, but collected Ricean K factor under V2T communications are similar to V2V model. Estimation methods evaluation benefits researchers by presenting mathematical approaches and methodology for vehicular communication modelling and will benefit system designers and operators by presenting measured and calculated models for use in simulation and field trials.

6.2 Summary of ITS Band Regulatory Study

The 5.9 GHz band has been sought after by several stakeholders, including traditional mobile operators, DSRC proponents, and C-V2X proponents. FCC and NHTSA are responsible for regulations related to vehicular communications, and have not finalized the rules regarding this band. We provided possible regulatory scenarios that could result from rule-making by these agencies, and identified relevant technical challenges for these scenarios. We identified interoperability between DSRC and C-V2X as the most challenging of the potential new technical requirements. The study provides information that can support regulatory decision-making and spectrum-sharing system deployments by presenting the issues and possible solutions.

6.3 Summary of Adjacent Channel Interference Measurements

Based on the technical survey and technical challenges, we observed that more study related to coexistence between DSRC and C-V2X is needed. Therefore, we conducted adjacent channel interference measurements with Wi-Fi, LTE, and modified C-V2X as the interference sources. From the results, we concluded DSRC can coexist with adjacent channels of Wi-Fi, LTE, and C-V2X, although additional measurements that include fading will help to confirm this. The study supports regulatory decision-making by a summary and analysis of relevant research, and by providing an assessment of interference between wireless technologies that are candidates for co-existing deployments in ITS bands.

6.4 List of All Publications

Table XIII List of papers related to contributions

Contributions	Title of Papers	Status
V2T Communications	Measurement and Configuration of DSRC Radios for Vehicle-to-Train (V2T) Safety-Critical Communications	IEEE Wireless Communications Letters (Published)
	7 conference papers	Published

6.4.1 Published Journal Papers

1. **J. Choi** et al., "Measurement and Configuration of DSRC Radios for Vehicle-to-Railroad (V2R) Safety-Critical Communications," *IEEE Wireless Communications Letters*, vol. 7, no. 3, pp. 428-431.
2. S. Kim, **J. Choi**, and C. Dietrich, "PSUN: An OFDM-pulsed radar coexistence technique with application to 3.5 GHz LTE," *Mobile Information Systems*, 2016.

6.4.2 Published Conference Papers

3. **J. Choi** et al., "*Measurements and Analysis of DSRC for V2TSafety-Critical Communications,*" 2018 IEEE Connected and Automated Vehicles Symposium (IEEE CAVS 2018)
4. **J. Choi** et al., "*Measurement and Configuration of DSRC Radios for Vehicle-to-Railroad (V2R) Safety-Critical Communications,*" 2018 IEEE International Conference on Communications (ICC), Kansas City, MO, 2018.

5. X. Ma, S. Guha, **J. Choi**, C. R. Anderson, R. Nealy, J. Withers, J. H. Reed, C. Dietrich, *"Analysis of directional antenna for railroad crossing safety applications,"* 2017 14th IEEE Annual Consumer Communications & Networking Conference (CCNC), Las Vegas, NV, 2017, pp. 1-6.
6. X. Ma, S. Guha, **J. Choi**, C. R. Anderson, R. Nealy, J. Withers, J. H. Reed, C. Dietrich, *"Prototypes of using directional antenna for railroad crossing safety applications,"* 2017 14th IEEE Annual Consumer Communications & Networking Conference (CCNC), Las Vegas, NV, 2017, pp. 594-596.
7. S. Kim, **J. Choi** and C. B. Dietrich, *"Coexistence between OFDM and pulsed radars in the 3.5 GHz Band with imperfect sensing,"* 2016 IEEE Wireless Communications and Networking Conference Workshops (WCNCW), Doha, 2016, pp. 437-442.
8. **J. Choi**, S. Guha, X. Ma, C.B. Dietrich, *"PHY and MAC Layer Simulator for Dedicated Short Range Communication (DSRC) Vehicular Communications,"* 25th Anniversary Wireless Symposium (Wireless@VT), May 2015.
9. X. Ma, **J. Choi**, S. Guha, C. Anderson, C.B. Dietrich, *"DSRC Feasibility Study for Railroad Grade Crossing Safety Improvement - A Measurement Plan,"* 25th Anniversary Wireless Symposium (Wireless@VT), May 2015.
10. **J. Choi**, S. Guha, C.B. Dietrich, "*A Simulink-Based Model and Analysis of the PHY Layer in Vehicular Communications,"* SDR / WInnComm 2015, San Diego, CA, March 24-26, 2015.
11. **J. Choi**, S. Guha, F. M. Romano, R. Galeshi, T. Smith-Jackson and C. B. Dietrich, *"Exploration of efficient testing methodology for effective spectrum sharing,"* 2014

USNC-URSI Radio Science Meeting (Joint with AP-S Symposium), Memphis, TN, 2014, pp. 297-297.

12. **J. Choi**, S. Guha, F.M. Romano, T.L. Smith-Jackson, C.B. Dietrich, "*A flexible and extensible cognitive radio test system (CRTS),"* SDR / WInnComm 2014, Schaumburg, IL, March 11-13, 2014.

References

[1] P. Levin, Thomas, Mitchell, Echsner & Proctor, Attorneys at Law. (2012). *Railroad Accident Questions*. Available: http://train-accident-law.com/faq.html

[2] Federal Railroad Administration, "FRA Office of Safety Analysis," Feb. 2018. [Online]. Available: http://safetydata.fra.dot.gov/OfficeofSafety/Default.aspx

[3] Federal Communications Commission, "In the Matter of Revision of Part 15 of the Commission's Rules to Permit Unlicensed National Information Infrastructure (U-NII) Devices in the 5 GHz Band," ET Docket No. 13-49, February 20, 2013.

[4] A. Rostami *et al*., "Stability challenges and enhancements for vehicular channel congestion control approaches," *IEEE Trans. Intell. Transp. Syst.*, vol. 17, no. 10, pp. 2935-2948, 2016.

[5] X. Xiang, W. Qin, and B. Xiang, "Research on a DSRC-based rear-end collision warning model," *IEEE Trans. Intell. Transp. Syst.*, vol. 15, no. 3, pp. 1054-1065, 2014.

[6] S. Ucar, S. C. Ergen, and O. Ozkasap, "Multihop-cluster-based IEEE 802.11p and LTE hybrid architecture for VANET safety message dissemination," *IEEE Trans. Veh. Technol.*, vol. 65, no. 4, pp. 2621-2636, 2016.

[7] K. Dhondge *et al.*, "WiFiHonk: smartphone-based beacon stuffed WiFi Car2X-communication system for vulnerable road user safety," In Proc. IEEE Vehicular Technology Conference, 2014, pp. 1-5.

[8] M. Shi *et al.*, "DSRC and LTE-V communication performance evaluation and improvement based on typical V2X application at intersection," In Proc. Chinese Automation Congr., 2017, pp. 556-561.

[9] R. He *et al.*, "Measurement-based analysis of relaying performance for Vehicle-to-Vehicle communications with large vehicle obstructions," In Proc. IEEE Vehicular Technology Conference, 2016, pp. 1-6.

[10] J. J. Anaya *et al.*, "Vehicle to pedestrian communications for protection of vulnerable road users," In Proc. IEEE Intelligent Vehicles Symposium, 2014 pp. 1037-1042.

[11] Y. Song *et al*., "Long term evolution for wireless railway communications: testbed deployment and performance evaluation," *IEEE Commun. Mag.*, vol. 54, no. 2, pp. 138-145, 2016.

[12] J. Kim *et al*. "Automatic train control over LTE: Design and performance evaluation," *IEEE Commun. Mag.*, vol. 53, no. 10, pp. 102-109, 2015.

[13] F. Balouchi, A. Bevan, and R. Formston, "Detecting railway under-track voids using multi-train in-service vehicle accelerometer," In Proc. IET Conf. on Railway Condition Monitoring, 2016, pp. 1-6.

[14] S. Banerjee, M. Hempel, and H. Sharif, "A survey of wireless communication technologies & their performance for high speed railways," *Journal of Transportation Technologies*, vol. 6, pp. 15-29.

[15] J. Singh *et al.*, "Cooperative intelligent transport systems to improve safety at level crossing," In Proc. 19th ITS World Congr., 2012.

[16] X. Ma *et al.*, "Analysis of directional antenna for railroad crossing safety applications," in Proc. Consum. Commun. Netw. Conf., 2017, pp. 1-6.

[17] X. Ma *et al*, "Prototypes of using directional antenna for railroad crossing safety applications," in Proc. Consum. Commun. Netw. Conf., 2017, pp. 594-596.

[18] T. W. Tedesso *et al*., "Propagation Measurements at 5.8 GHz for Railroad Intelligent Transportation Systems," in Proc. *2017 IEEE Wireless Commun. and Net. Conf., 2017, pp. 1-6.*

[19] J. Choi *et al.*, "Measurement and configuration of DSRC radios for Vehicle-to-Train (V2T) safety-critical communications," *IEEE Commun. Lett.*, vol. 7, no. 3, pp. 428-431.

[20] R. He *et al*., "Measurements and analysis of propagation channels in high-speed railway viaducts," *IEEE Trans. Wireless Commun.*, vol. 12, no. 2, pp.794-805, 2013.

[21] M. Yang *et al.*, "Path loss characteristics for vehicle-to-infrastructure channel in urban and suburban scenarios at 5.9 GHz," In Proc. General Assembly and Scientific Symp. of the Int. Union of Radio Science, 2017, pp. 1-4.

[22] L. Bernado *et al.*, "Time- and frequency- varying K-factor of non-stationary vehicular channels for safety-relevant scenarios," *IEEE Trans. Intell. Trans. Syst.*, vol. 16, no. 2, pp. 1007-1017, 2015.

[23] L. Bernado *et al.*, "Delay and Doppler spreads of nonstationary vehicular channels for safety-relevant scenarios," *IEEE Trans. Veh. Technol.*, vol. 63, no. 1, pp. 82-93, 2014.

[24] P. Alexander, D. Haley, A. Grant, "Cooperative intelligent transport systems: 5.9-GHz field trials," *Proc. of the IEEE*, vol. 99, no. 7, pp. 1213-1235, 2011.

[25] I. Tan *et al*., "Measurement and analysis of wireless channel impairments in DSRC vehicular communications," In Proc. IEEE Int. Conf. on Comm., 2008, pp. 4882-4888.

[26] Virginia Department of Motor Vehicles. "Virginia driver's Manual," Feb. 2018. [Online]. Available: http://www.dmv.state.va.us/webdoc/pdf/dmv39.pdf

[27] C. R. Anderson, “Design and implementation of an ultrabroadband milli meter-wavelength vector sliding correlator channel sounder and in-building multipath measurements at 2.5 & 60 GHz,” M. S. thesis, Dept. Elect. Eng., Virginia Tech, Blacksburg, VA, USA, 2002.

[28] Cohda Wireless. “MK5 OBU,” Feb. 2018. [Online]. Available: http://www.cohdawireless.com/soltions/hardware/mk5-obu/

[29] Mobile Mark. “Broadband, Omni-Directional DSRC 5.9 GHz,” Feb. 2018. [Online]. Available: https://www.mobilemark.com/wp-content/uploads/2015/04/antenna-spec-144-eco-5900.pdf

[30] Ventev. “4.9-6.1 GHz, 20.5-23 dBi Dual Polarized Outdoor Panel Antenna With N Connectors”, 2017. [Online]. Available: http://www.ventevinfra.com/

[31] 3rd Generation Partnership Project, “Technical Specification Group Radio Access Network; Evolved Universal Terrestrial Radio Access (E-UTRA); Further advancements for E-UTRA physical layer aspects; 3GPP TR 36.814 (Release 9),” 3GPP, Valbonne, France, Mar. 2010.

[32] Federal Communications Commission, “*Amendment of the Commission’s Rules Regarding Dedicated Short-Range Communication Services in the 5.850-5.925 GHz Band (5.9 GHz Band); Amendment of Parts 2 and 90 of the Commission’s Rules to Allocate the 5.850-5.925 GHz Band to the Mobile Service for Dedicated Short Range Communications of Intelligent Transportation Systems*, ET Docket No. 98-95, WT Docket No. 01-90, FCC 03-324,” FCC, Feb. 2004.

[33] Federal Communications Commission, “Unlicensed national information infrastructure (U-NII) devices in the 5 GHz band, ET Docket No. 13-49, FCC 16-68,” FCC, Jun. 2016.

[34] S. Sun, *et al*. "Support for vehicle-to-everything services based on LTE," *IEEE Wireless Commun.* vol. 2, no. 3, pp 4-8, Jun. 2016.

[35] A. Kousaridas, *et al*., "Recent advances in 3GPP Networks for vehicular communications," in *IEEE Conf. on Standards for Commun. and Networking*, Helsinki, Finland, 2017, pp. 91-97.

[36] C. Campolo, A. Molinaro and A. Vinel, "Understanding adjacent channel interference in multi-channel VANETs," in *IEEE Vehicular Networking Conf.*, Paderborn, Germany, 2014, pp. 101-104.

[37] C. Campolo, *et al.*, "On the impact of adjacent channel interference in multi-channel VANETs," in *IEEE Int. Conf. on Commun.*, Kuala Lumpur, Malaysia, 2016, pp. 1-7.

[38] R. Lasowski, *et al.*, "Evaluation of adjacent channel interference in single radio vehicular Ad-Hoc networks," in *IEEE Consumer Commun. and Networking Conf.*, Las Vegas, NV, 2011, pp. 267-271.

[39] K. Lan, C. Chou, and D. Jin, "The effect of 802.11a on DSRC for ETC communication," in *IEEE Wireless Commun. and Networking Conf.*, Shanghai, China, 2012, pp. 2483-2487.

[40] L. Zhao, *et al.*, "Feasibility analysis of mlti-radio in DSRC vehicular networks," in *Int. Symp. on Wireless Personal Multimedia Commun.*, Atlantic City, NJ, 2013, pp.1-6.

[41] I. Khan and J. Harri, "Can IEEE 802.11p and Wi-Fi coexist in the 5.9 GHz ITS band?," in *IEEE Int. Symp. on A World of Wireless, Mobile and Multimedia Networks*, Macau, China, 2017, pp. 1-6.

[42] M. Zhang, *et al.*, "Analysis of adjacent channel interference in heterogeneous cellular networks," in *Int. Conf. on Wireless Commun. & Signal Process.*, Nanjing, China, 2015, pp. 1-5.

[43] M. Hossen, *et al.*, "Performance analysis of an OFDM-based method for V2X communication," in *Int. Conf. on Ubiquitous and Future Networks*, Shanghai, China, 2014, pp. 238-242.

[44] P. Luoto, *et al.*, "System Level Performance Evaluation of LTE-V2X Network," in *European Wireless Conference*, Oulu, Finland, 2016, pp. 1-5.

[45] R. Molina-Masegosa and J. Gozalvez, "LTE-V for Sidelink 5G V2X," *IEEE Veh. Tec. Mag.*, vol. 12, no. 4, pp. 30-39, Dec. 2017.

[46] Nabil, Amr, *et al*. "Performance Analysis of Sensing-Based Semi-Persistent Scheduling in C-V2X Networks." *arXiv preprint arXiv:1804.10788* (2018).

[47] 5G Autonomous Association (Jun. 2017), *Coexistence of C-V2X and 802.11p at 5.9 GHz* [Online]. Apr. 2018, Available: http://5gaa.org/news/position-paper-coexistence-of-c-v2x-and-802-11p-at-5-9-ghz/

[48] Transportation Technology Center, Inc. (2017). Available: http://www.aar.com

[49] Shenandoah Valley Railroad, LLC. (2017). Available: http://www.svrr-llc.com

[50] Cohda Wireless. (2017). Available: http://www.cohdawireless.com

[51] J. Singh, A. Desai, F. Acker, S. Ding, S. Prakasamul, A. Rachide, et al., "Cooperative intelligent transport systems to improve safety at level crossing," in The 12th Global Level Crossing and Trespass Symp., London, 2012.

[52] Lansford, Jim, John B. Kenney, and Peter Ecclesine. "Coexistence of unlicensed devices with DSRC systems in the 5.9 GHz ITS band." In *Vehicular Networking Conference (VNC), 2013 IEEE*, pp. 9-16. IEEE, 2013.

[53] Moller, Andreas, Jorg Nuckelt, Dennis M. Rose, and Thomas Kurner. "Physical layer performance comparison of LTE and IEEE 802.11 p for vehicular communication in an

urban NLOS scenario." In *Vehicular Technology Conference (VTC Fall), 2014 IEEE 80th*, pp. 1-5. IEEE, 2014

[54] Matolak, David W., Qiong Wu, Juan J. Sanchez-Sanchez, David Morales-Jiménez, and M. Carmen Aguayo-Torres. "Performance of LTE in vehicle-to-vehicle channels." In *Vehicular Technology Conference (VTC Fall), 2011 IEEE*, pp. 1-4. IEEE, 2011.

[55] Liu, Jinshan, Gaurang Naik, and Jung-Min Jerry Park. "Coexistence of DSRC and Wi-Fi: Impact on the performance of vehicular safety applications." In *Communications (ICC), 2017 IEEE International Conference on*, pp. 1-6. IEEE, 2017.

[56] Molisch, Andreas F., Fredrik Tufvesson, Johan Karedal, and Christoph F. Mecklenbrauker. "A survey on vehicle-to-vehicle propagation channels." *IEEE Wireless Communications* 16, no. 6 (2009): 12-22.

[57] Zajić, Alenka. *Mobile-to-mobile wireless channels*. Artech House, 2012.

[58] A. P. Subramanian, V. Navda, P. Deshpande, and S. R. Das, "A measurement study of inter-vehicular communication using steerable beam directional antenna," presented at the Proceedings of the fifth ACM international workshop on VehiculAr Inter-NETworking, San Francisco, California, USA, 2008.

[59] F. R. A. Office of Safety Analysis. (2013). FRA Office of Safety Analysis Web Site. Available: http://safetydata.fra.dot.gov/OfficeofSafety/Default.aspx

[60] J. B. Kenney, "Dedicated Short-Range Communications (DSRC) Standards in the United States," Proceedings of the IEEE, vol. 99, pp. 1162-1182, 2011.

[61] C. Hsu, C. Liang, L. Ke, and F. Huang, “Verification of On-Line Vehicle Collision Avoidance Warning System using DSRC,” World Academy of Science, Engineering and Technology, vol. 55, pp. 377-383, 2009.

[62] Y. Xue, L. Jie, N. F. Vaidya, and Z. Feng, "A vehicle-to-vehicle communication protocol for cooperative collision warning," in The First Annual International Conference on Mobile and Ubiquitous Systems: Networking and Services, 2004, pp. 114-123.

[63] G. M. Jan Fischer-Wolfarth, Advanced Microsystems for Automotive Applications: Springer, 2013.

[64] "Railroad-Highway Grade Crossing Handbook," 2007.

[65] Z. Shaozhen, T. S. Ghazaany, S. M. R. Jones, R. A. Abd-Alhameed, J. M. Noras, T. Van Buren, et al., "Probability Distribution of Rician K-Factor in Urban, Suburban and Rural Areas Using Real-World Captured Data," IEEE Transactions on Antennas and Propagation, vol. 62, pp. 3835-3839, 2014.

[66] G. Acosta-Marum and M. A. Ingram, "Six Time- and Frequency Selective Empirical Channel Models for Vehicular Wireless LANs," IEEE Vehicular Technology Magazine, 2007.

[67] Recommendation, I. T. U. R. M. "1225, Guidelines for evaluation of radio transmission technologies for IMT-2000." International Telecommunication Union (1997).

[68] Doufexi, Angela, et al. “A comparison of the HIPERLAN/2 and IEEE 802.11 a wireless LAN standards.” *IEEE Communications magazine* 40.5 (2002): 172-180.

[69] Electro – Motive Division, General Motors Corporation, “SD40 Operators Manual,” 6th Edition, May 1971. Available at: http://rr-fallenflags.org/manual/manual.html

[70] G. I. P. P. Partnership, “5G Vision,” February, 2015.

[71] J. G. Andrews, S. Buzzi, W. Choi, S. V. Hanly, A. Lozano, A. C. Soong, *et al.*, “What will 5G be?,” *Selected Areas in Communications, IEEE Journal on*, vol. 32, pp. 1065-1082, 2014.

[72] H. Moiin, “Looking ahead to 5G – A symbiotic convergence of new and existing technologies,” presented at the EUCNC, 2014.

[73] J. Morrish. (June 2013). *The Connected Life*. Available: www.gsma.com

[74] B. C. Cheng *et al*., “Survey on networking for Internet of Vehicles,” *J. Internet Technol.*, vol. 14, no. 7, pp. 1007-1020, Dec. 2013.

[75] N. H. T. S. Administration, “Safety in Numbers,” vol. Volume 1 Issue 4, ed, August 2013.

[76] N. H. T. S. Administration, “Traffic Safety Facts, 2012 Data: Pedestrian,” *Annals of Emergency Medicine*, vol. 65, p. 452, 2015.

[77] A. Vinel, “3GPP LTE versus IEEE 802.11 p/WAVE: which technology is able to support cooperative vehicular safety applications?,” *Wireless Communications Letters, IEEE*, vol. 1, pp. 125-128, 2012.

[78] S. Kato, M. Hiltune, K. Joshi, and R. Schlichting, “Enabling vehicular safety applications over LTE networks,” in *Connected Vehicles and Expo (ICCVE), 2013 International Conference on*, 2013, pp. 747-752.

[79] L. Gallo and J. Harri, “Short paper: A LTE-direct broadcast mechanism for periodic vehicular safety communications,” in *Vehicular Networking Conference (VNC),2013 IEEE*, 2013, pp. 166-169.

[80] Z. H. Mir and F. Filali, “LTE and IEEE 802.11 p for vehicular networking: a performance evaluation,” *EURASIP Journal on Wireless Communications and Networking*, vol. 2014, pp. 1-15, 2014.

[81] K. Trichias, v. d. J. Berg, G. Heijenk, d. J. Jongh, and R. Litjens, “Modeling and evaluation of LTE in intelligent transportation systems,” 2012.

[82] G. Araniti, C. Campolo, M. Condoluci, A. Iera, and A. Molinaro, "LTE for vehicular networking: a survey," *Communications Magazine, IEEE*, vol. 51, pp. 148-157, 2013.

[83] H. Onishi and F. Mlinarsky, "Wireless technology assessment for automotive applications," in *Proc. ITS World Congress*, 2012.

[84] R. Atat, E. Yaacoub, M. S. Alouini, and F. Filali, "Delay efficient cooperation in public safety vehicular networks using LTE and IEEE 802.11 p," in *Consumer Communications and Networking Conference (CCNC), 2012 IEEE*, 2012, pp. 316-320.

[85] P. Caballero-Gil, C. Caballero-Gil, and J. Molina-Gil, "Design and implementation of an application for deploying vehicular networks with smartphones," *International Journal of Distributed Sensor Networks*, vol. 2013, 2013.

[86] S. Tornell, C. T. Calafate, J. C. Cano, P. Manzoni, M. Fogue, and F. J. Martinez, "Evaluating the feasibility of using smartphones for ITS safety applications," in *Vehicular Technology Conference (VTC Spring), 2013 IEEE 77th*, 2013, pp. 1-5.

[87] *Honda Demonstrates Advanced Vehicle-to-Pedestrian and Vehicle-to-Motorcycle Safety Technologies* Available: http://www.prnewswire.com/news-releases/honda-demonstrates-advanced-vehicle-to-pedestrian-and-vehicle-to-motorcycle-safety-technologies-221495031.html

[88] A. Mostafa, A. M. Vegni, R. Singoria, T. Oliveira, T. D. Little, and D. P. Agrawal, "A V2X-based approach for reduction of delay propagation in vehicular Ad-hoc networks," in *ITS Telecommunications (ITST), 2011 11th International Conference on 2011*, pp. 756-761.

[89] L. Reggiani, L. Dossi, L. G. Giordano, and R. Lambiase, *Small LTE Base Stations Deployment in Vehicle-to-Road-Infrastructure Communications:* INTECH Open Access Publisher, 2013.

[90] E. Abd-Elrahman, A. M. Said, T. Toukabri, H. Afifi, and M. Marot, "Assisting V2V failure recovery using Device-to-Device Communications," in *Wireless Days (WD), 2014 IFIP*, 2014, pp. 1-3.

[91] G. Hattori, C. Ono, S. Nishiyama, and H. Horiuchi, "Implementation and evaluation of message delegation middleware for its application," in *Applications and the Internet Workshops, 2004, SAINT 2004 Workshops. 2004 International Symposium on*, 2004, pp. 326-333.

[92] A. Elmurtada, Y. Awad, and M. Elnourani, "Adaptive Smart Antennas in 3G Networks and Beyond," in *Research and Development (SCORed) IEEE Student Conference 2012*, pp. 148-153.

[93] S. Pyun, H. Widiarti, and Y. Kwon, "Group-Based Channel Access Scheme for a V2I Communication System using Smart Antenna," *IEEE Communications Letters*, no. 8 (2011), pp. 804-806.

[94] H. Wu, C. Liu, and Y. Dai, "Adaptive Pattern Nulling Design of Linear Array Antenna by Phase Perturbations Using Invasive Weed Optimization Algorithm," in *2013 IEEE Third International Conference on Information Science and Technology (ICIST)*. 2013.

[95] X. Z. D. Qiao, "Quality, Reliability, Securit and Robustness in Heterogeneous Networks."

[96] W. Vandenberghs, I. Moerman, and P. Demeester, "Approximation of the IEEE 802.11 p standard using commercial off-the-shelf IEEE 802.11 a hardware," in *ITE Telecommunications (ITST), 2011 11th International Conference on*, 2011, pp. 21-26.

[97] L. M. s. Committee, "Part 11: Wireless lan medium access control (mac) and physical layer (phy) specifications," *IEEE-SA Standards Board*, 2003.

[98] *IEEE 802.11a WLAN Physical Layer, MathWorks,* Available: http://www.mathworks.com/help/releases/R2015b/comm/examples/ieee-802-11a-wlan-physical-layer.html

[99] J. Choi, S. Guha, C. B. Dietrich, "A Simulink-based Model and Analysis of the PHY Layer in Vehicular Communications," presented at the WInnComm 2015, San Diego, CA, 2015.

[100] Chen, Shanzhi, et al. "LTE-V: A TD-LTE-Based V2X Solution for Future Vehicular Network." *IEEE Internet of Things Journal* 3.6 (2016): 997-1005.

[101] Qualcomm Technologies, Inc. "Making 5G NR a reality: Leading the technology innovations for a unified, more capable 5G air interface." September, 2016.

[102] Borroni-Bird, Chris. "Enabling Connected and Electric Vehicles." *Qualcomm*. 2014.

[103] Zaki, Maged. "Accelerating C-V2X toward 5G for autonomous driving." *Qualcomm*. 2017. Available: https://www.qualcomm.com/news/onq/2017/02/24/accelerating-c-v2x-toward-5g-autonomous-driving

[104] Qualcomm. "Leading the world to 5G: Cellular Vehicle-to-Everything (C-V2X) technologies." June 2016.

[105] Lu, Ning, et al. "Connected vehicles: Solutions and challenges." *IEEE internet of things journal* 1.4 (2014): 289-299.

[106] Alleven, Monica. "Qualcomm: 'Steadfast' supporter of DSRC sees C-V2X providing clear path forward." *FierceWireless*. Available: http://www.fiercewireless.com/wireless/qualcomm-steadfast-supporter-dsrc-sees-c-v2x-providing-clear-path-forward

[107] Qualcomm Research. "Cooperative ITS for all: Enabling DSRC in mobile devices." Feb. 6, 2013.

Appendix A: TTCI Channel Sounder Results

A.1 RTT Channel Measurement Results

Table XIV Summary of Horn RTT Delay and Doppler Spread Measurements

	Delay Spread (ns)			Doppler Spread (Hz)		
Antenna Height	20 mph	50 mph	79 mph	20 mph	50 mph	79 mph
6 ft	64.76	257.873	199.095	790.861	1075.024	1032.217
25 ft	18.739	14.601	21.206	630.845	602.447	610.237
32 ft	91.738	145.678	22.934	706.524	900.282	839.518

Figure 67 Horn RTT Delay Spread Visualization in Google Earth

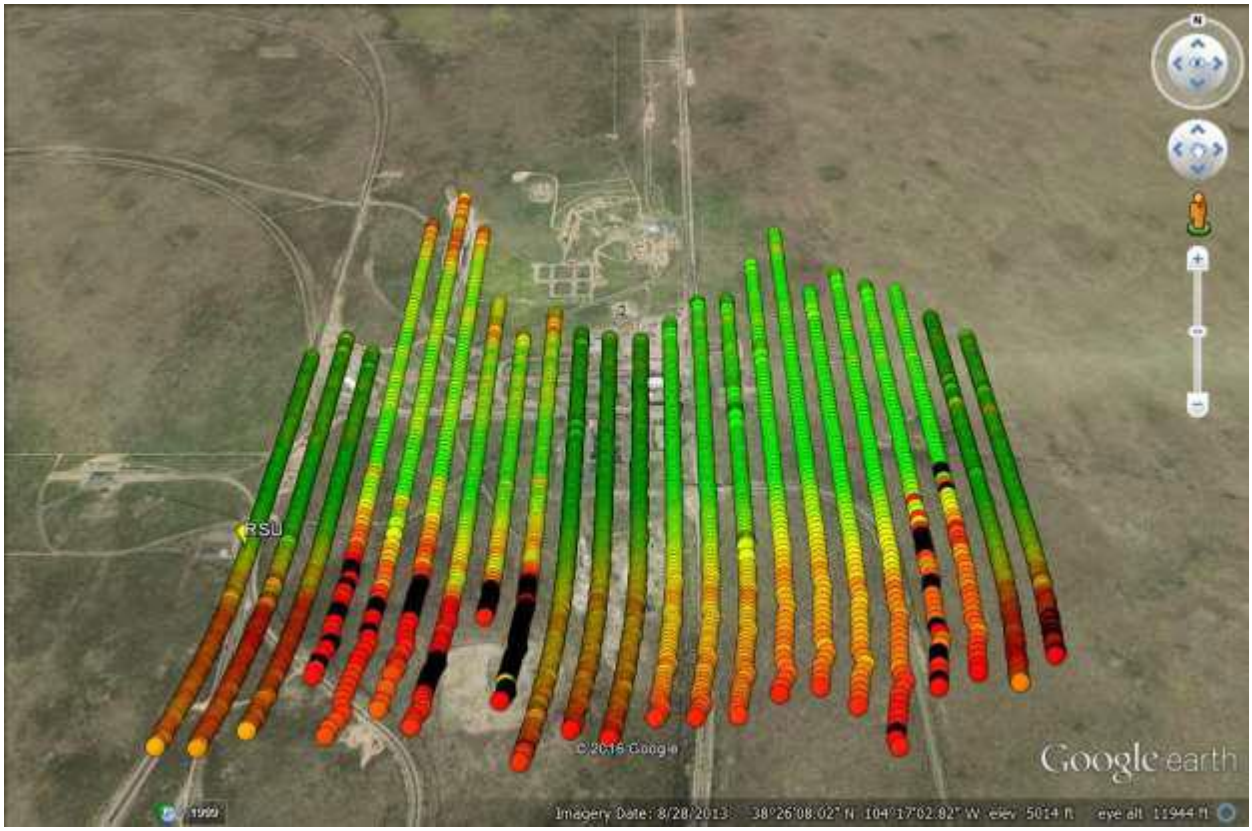

Figure 68 Horn RTT Doppler Spread Visualization in Google Earth

Table XV Summary of Discone RTT Delay and Doppler Spread Measurements

	Delay Spread (ns)			Doppler Spread (Hz)		
Antenna Height	20 mph	50 mph	79 mph	20 mph	50 mph	79 mph
6 ft	0.525	3.684	7.747	597.143	1084.990	788.858
25 ft	13.550	7.798	10.011	1011.176	1005.478	830.55
32 ft	0.119	4.598	13.710	866.912	625.537	1129.443

Figure 69 Discone RTT Delay Spread Visualization in Google Earth

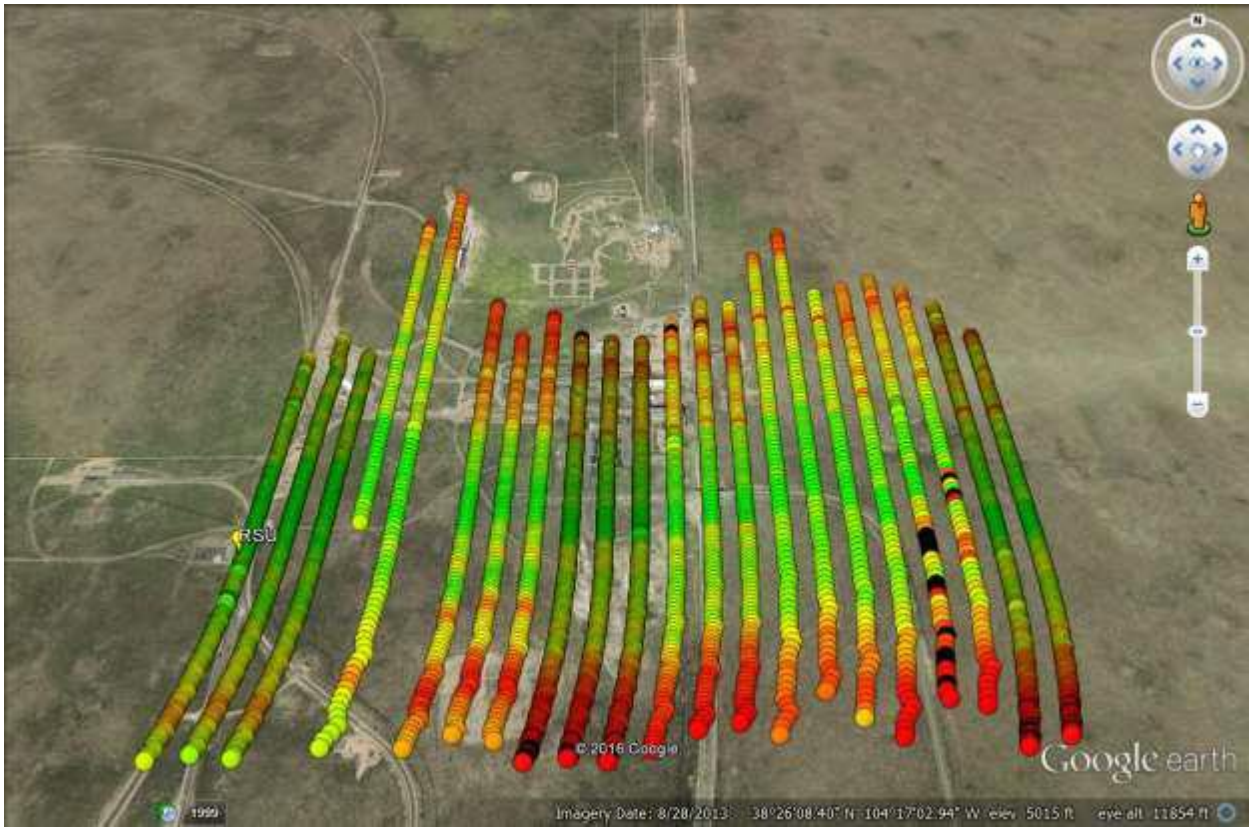

Figure 70 Discone RTT Doppler Spread Visualization in Google Earth

A.2 PTT Channel Measurement Results

Table XVI Summary of Horn PTT Delay and Doppler Spread Measurements

	Delay Spread (ns)			Doppler Spread (Hz)		
Antenna Height	20 mph	50 mph	79 mph	20 mph	50 mph	79 mph
6 ft	131.973	56.082	73.317	762.950	826.375	752.265
20 ft	20.575	55.007	7.533	684.558	711.836	527.887
40 ft	6.265	18.291	194.714	746.243	808.012	652.728

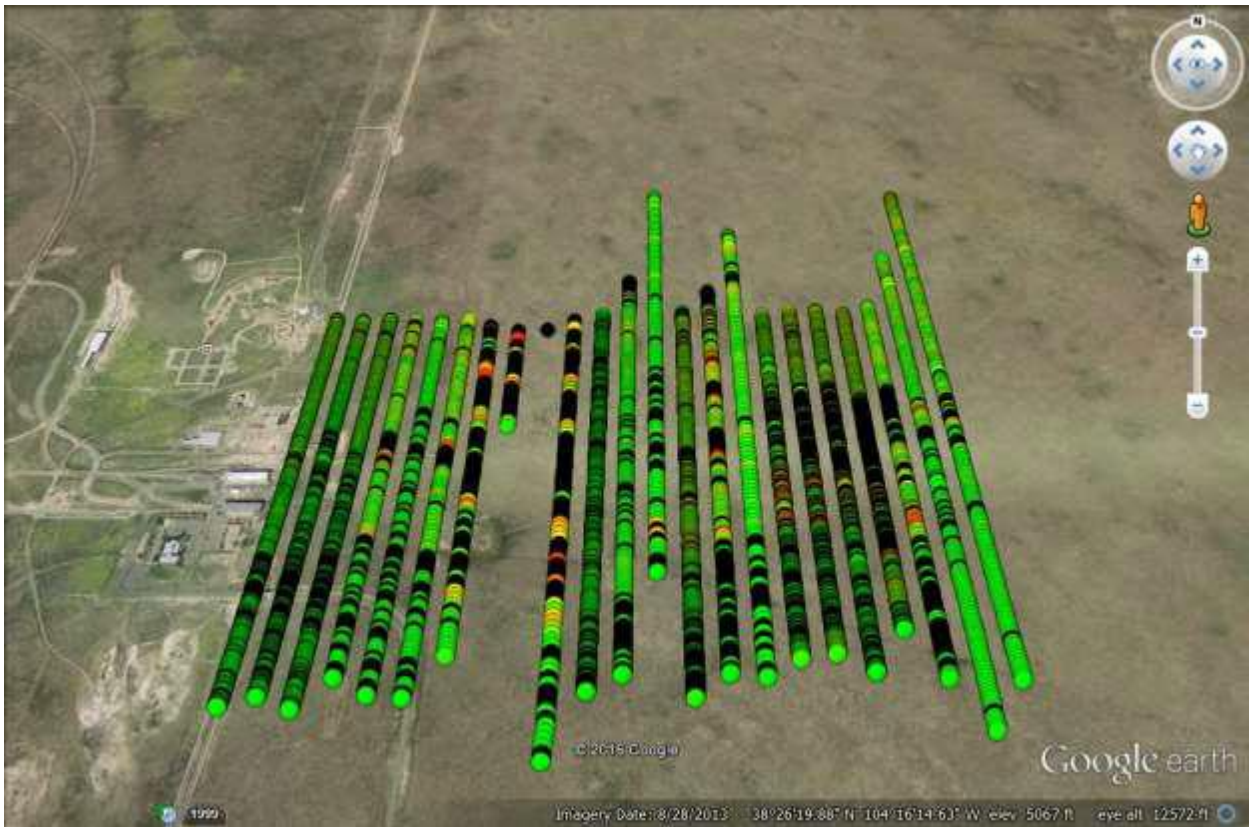

Figure 71 Horn PTT Delay Spread Visualization in Google Earth

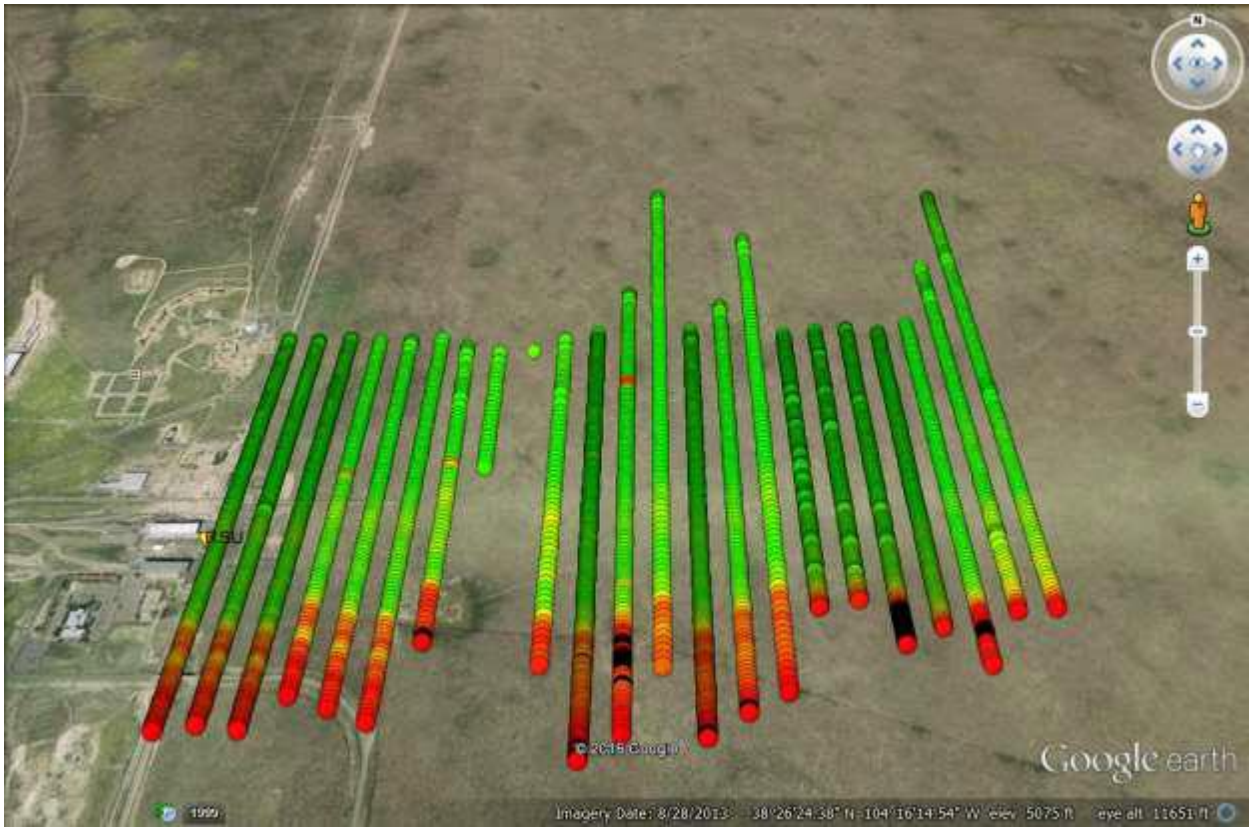

Figure 72 Horn PTT Doppler Spread Visualization in Google Earth

Table XVII Summary of Discone PTT Delay and Doppler Spread Measurements

	Delay Spread (ns)			Doppler Spread (Hz)		
Antenna Height	20 mph	50 mph	79 mph	20 mph	50 mph	79 mph
6 ft	1.359	5.640	14.336	666.965	672.816	643.17
20 ft	0.346	22.068	36.197	312.402	448.064	438.119
40 ft	2.941	9.164	3.825	405.394	437.655	469.813

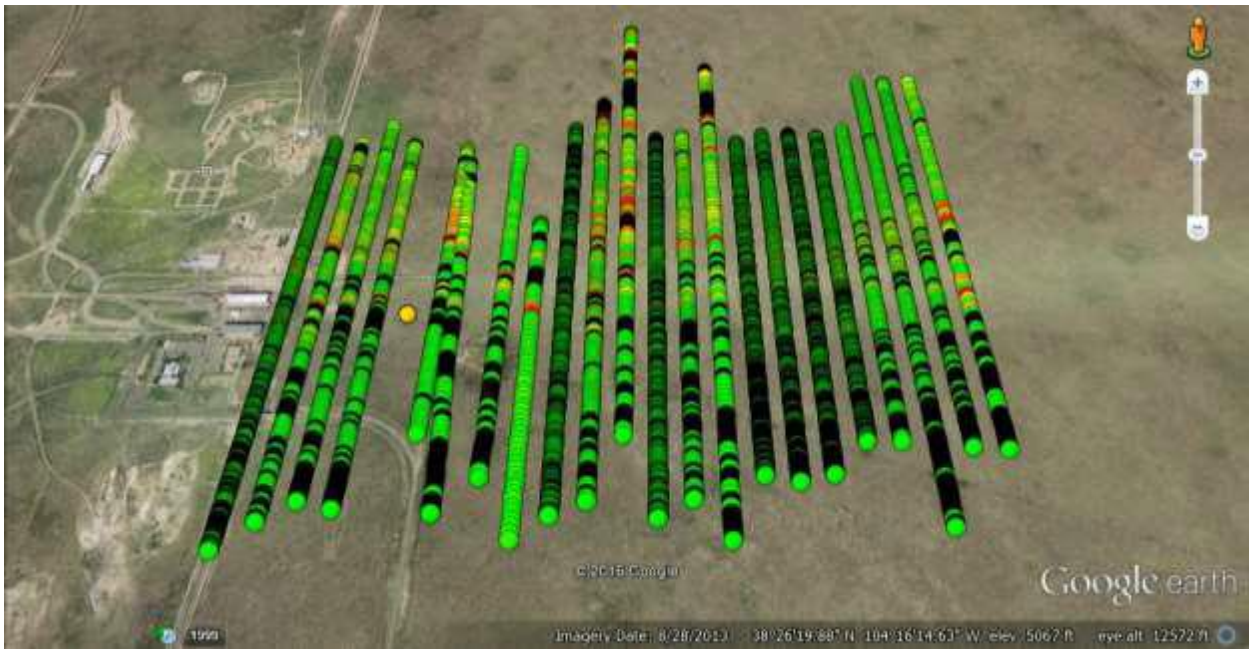

Figure 73 Discone PTT Delay Spread Visualization in Google Earth

Figure 74 Discone PTT Doppler Spread Visualization in Google Earth

A.3 RTT Channel Modelling Results

The calculated path loss exponents fall in the expected range between 2 and 3. These results are expected because the system was operating in an environment with few obstructions. The higher path loss exponents seen by the Discone antenna suggest that the system was operating in a more obstructed environment. The Discone antenna's path loss exponents do decrease as the antenna height is raised because the stronger line of sight component. These path loss models are also a based on an estimated receiver location since the GPS location of the receiver was not recorded. Consequently, the plots could show up to 164 ft of error due to the train speed and the estimated locations. While the error could some effect on path loss exponent, it does not affect Ricean channel model parameter, K.

Table XVIII RTT Path Loss Model Summary

Antenna Type	Antenna Height (ft)	Path Loss Exponent (n)	Standard Deviation (σ)
Horn	6	2.1453	10.2696
	25	2.2914	14.0143
	32	2.1587	12.2731
Discone	6	3.0839	11.5290
	25	2.7923	8.5745
	32	2.7788	10.8051

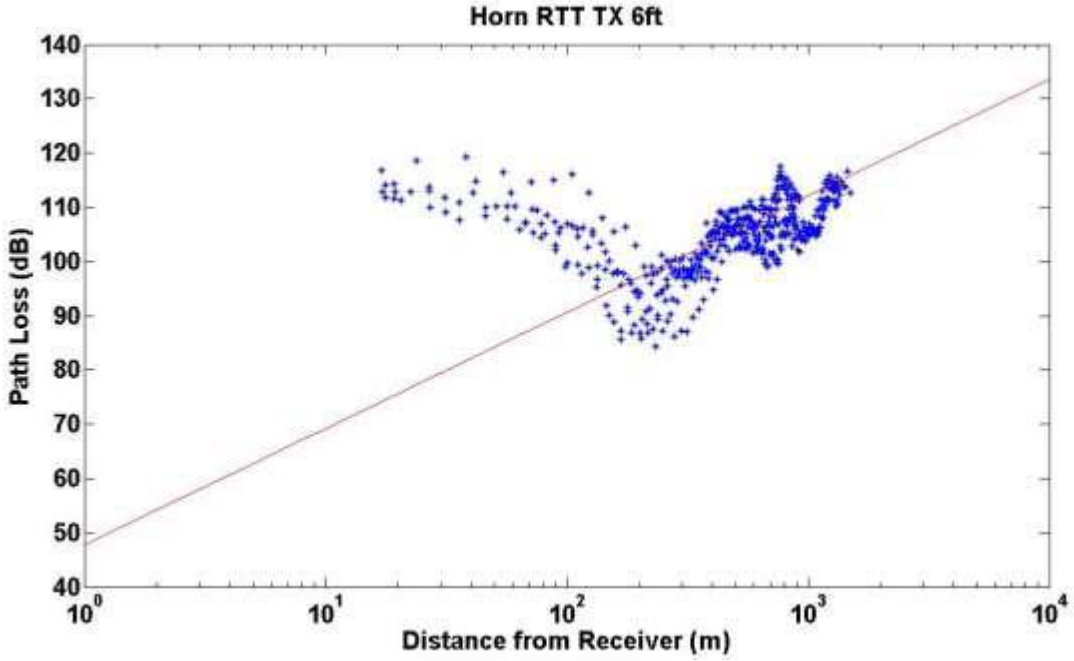

Figure 75 Path loss model for the horn antenna at a height of 6ft

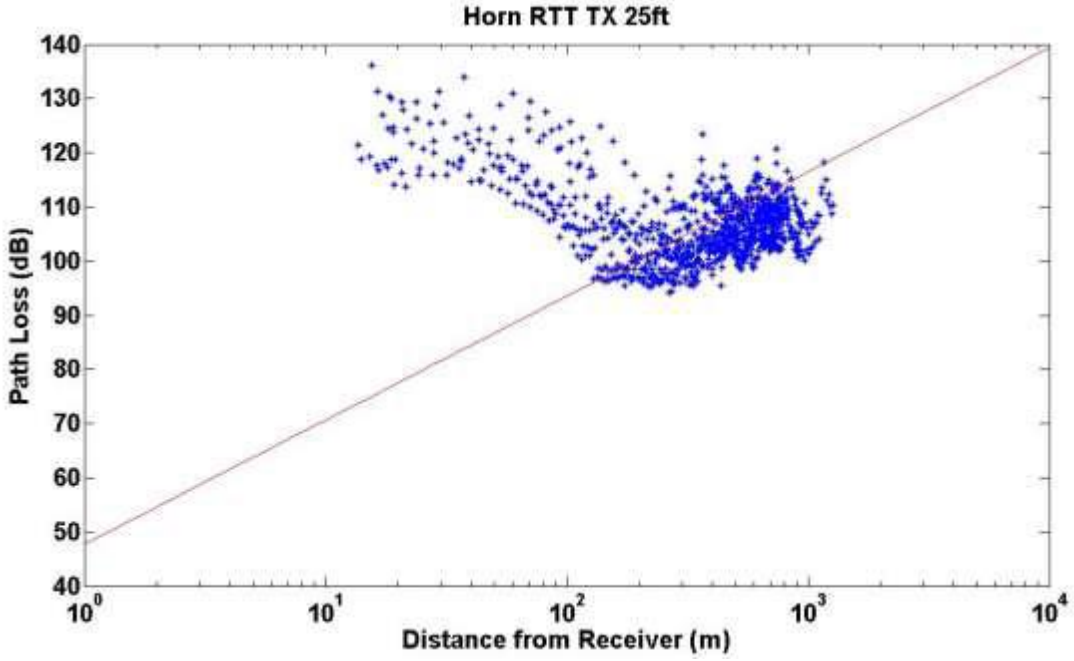

Figure 76 Path loss model for the horn antenna at a height of 25ft

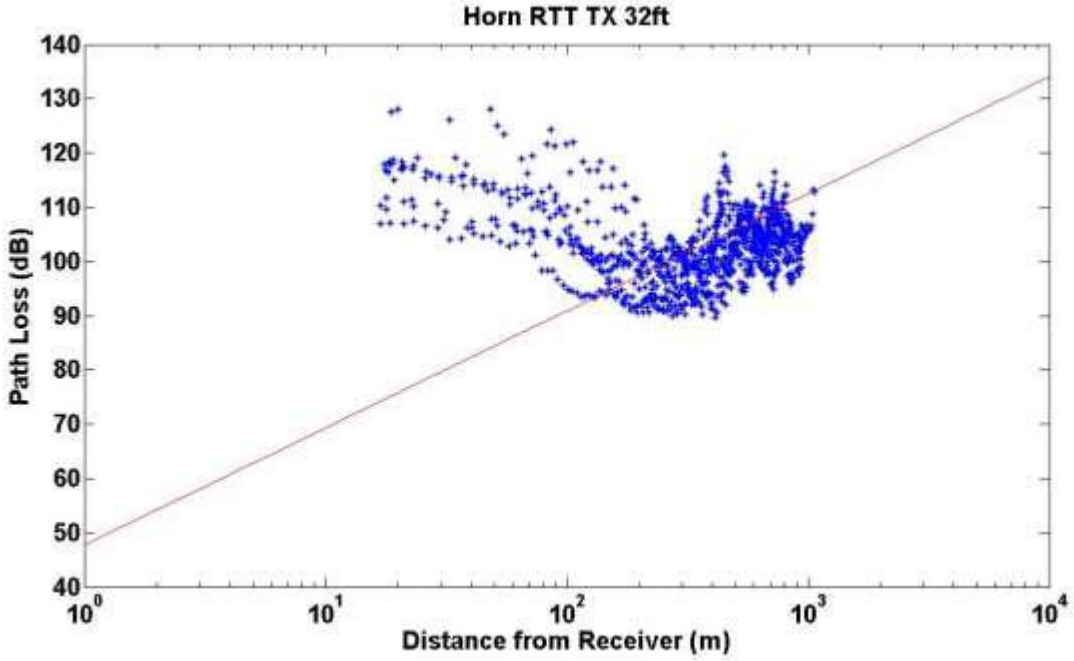

Figure 77 Path loss model for the horn antenna at a height of 32ft

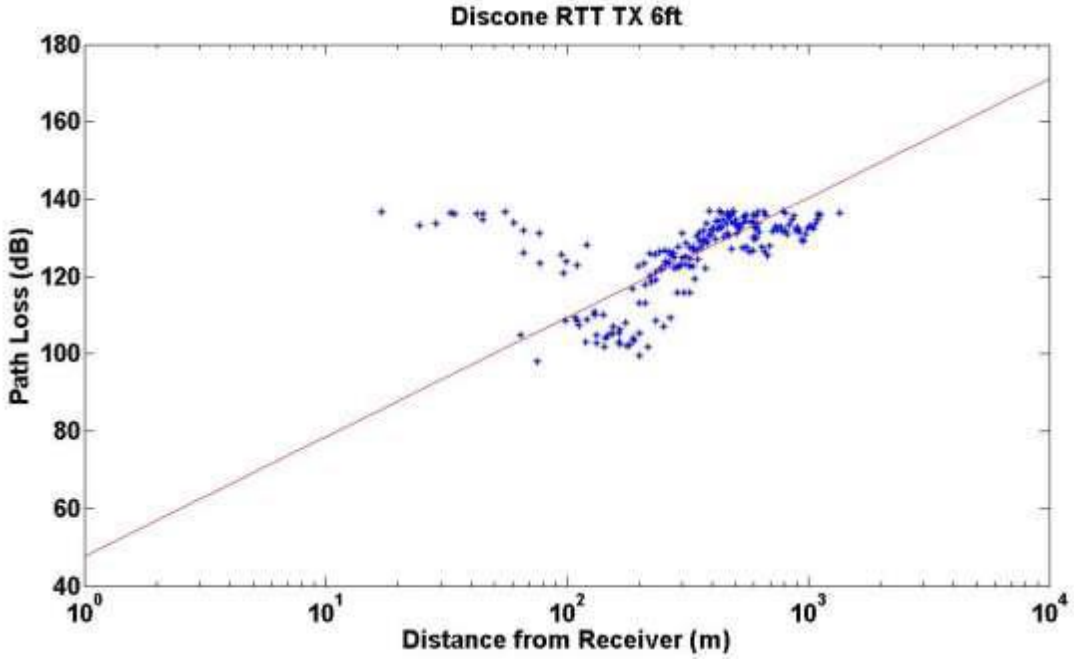

Figure 78 Path loss model for the discone antenna at a height of 6ft

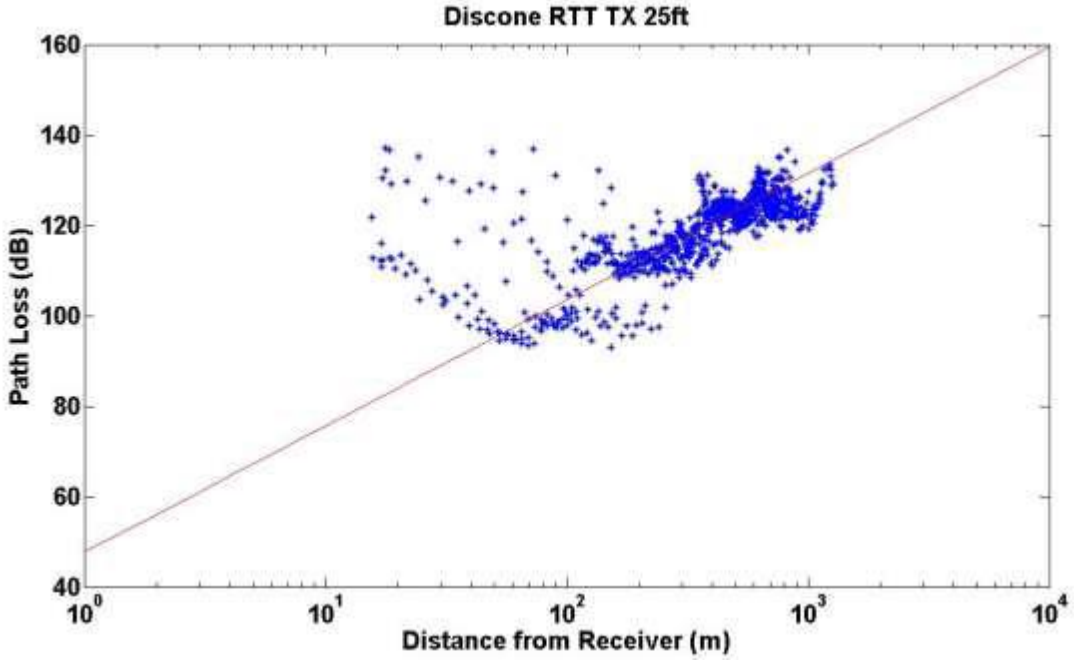

Figure 79 Path loss model for the discone antenna at a height of 25ft

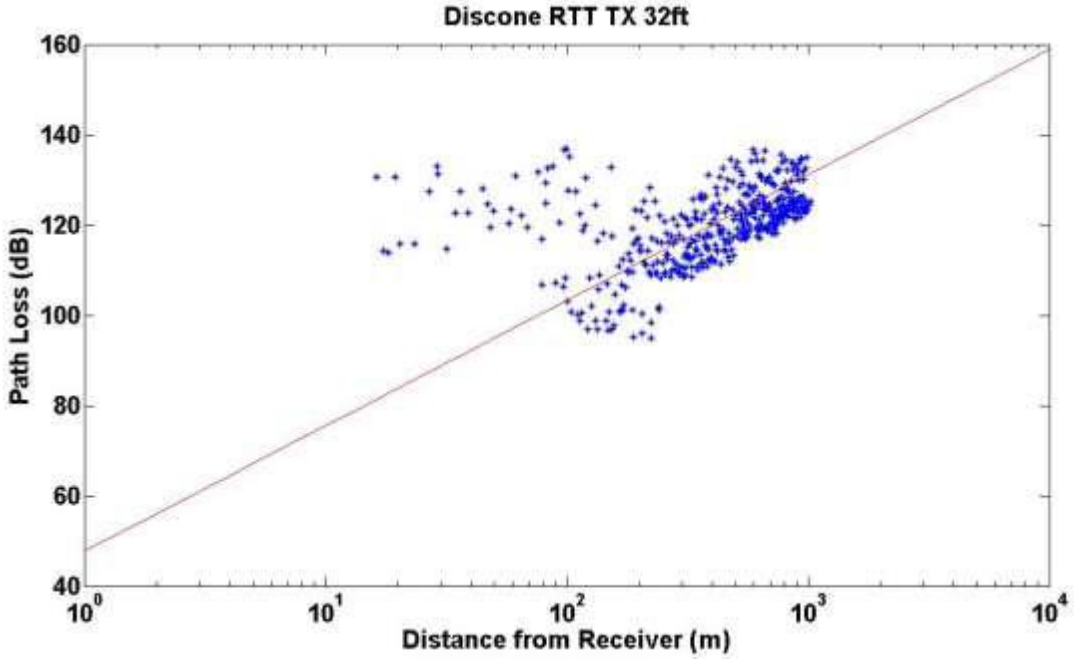

Figure 80Path loss model for the discone antenna at a height of 32ft

A.4 PTT Channel Modelling Results

The calculated path loss exponents fall in the expected range of between 2 and 3, this time falling closer to 3. These results are expected because the system was operating under a more cluttered, urban-like environment. These path loss models are also based on an estimated receiver location, since the GPS location of the receiver was not recorded. Consequently, the plots could show up to 164 ft of error, due to the speed of the train and the estimated GPS location. The path loss models show that the path loss increases as the transmitter and receiver distance gets shorter. The increase occurs because the obstructions were placed only around the receiver, otherwise the transmitter was operating in an environment that was closer to free space but still had more obstructions than the RTT test site.

Table XIX PTT Path loss model summary

Antenna Type	Antenna Height (ft)	Path Loss Exponent (n)	Standard Deviation (σ)
Horn	6	2.1321	14.0539
	20	2.3273	12.6482
	40	2.4806	15.1446
Discone	6	2.7613	12.2964
	20	2.5898	10.6355
	40	2.8026	9.1178

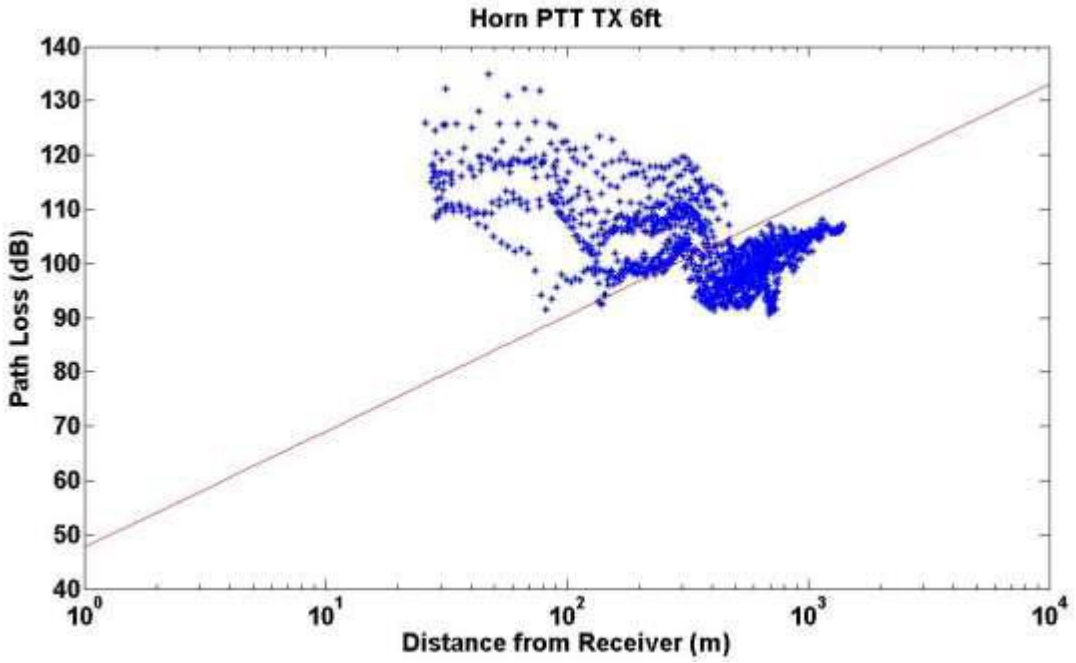

Figure 81 Path loss model for the horn antenna at 6ft

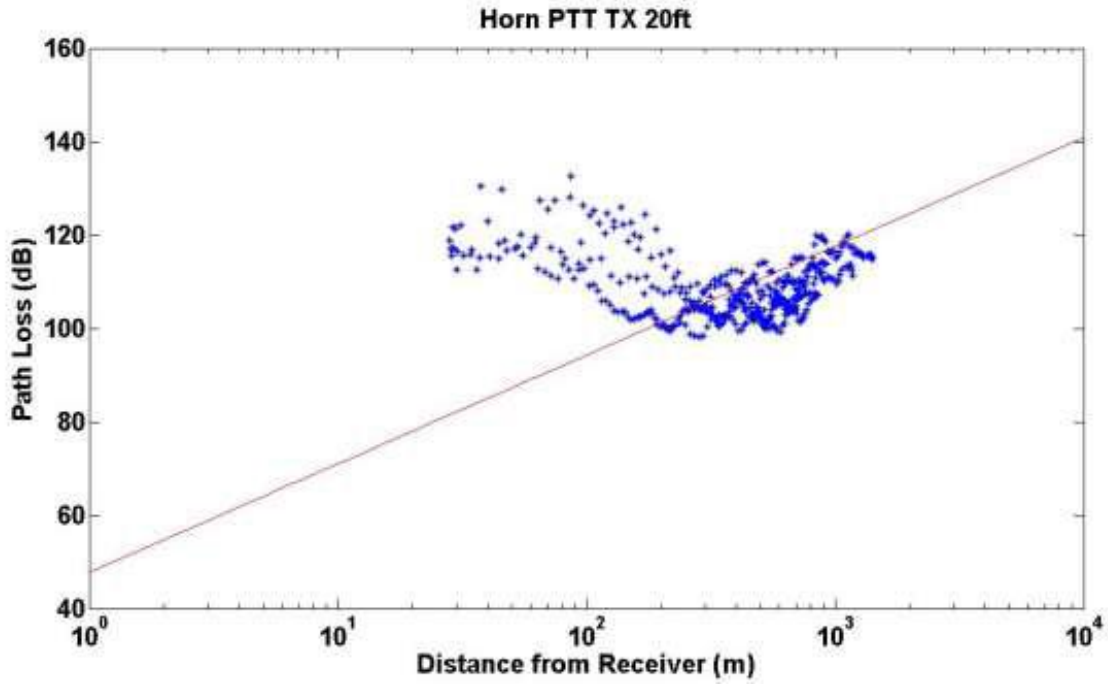

Figure 82 Path loss model for the horn antenna at 20ft

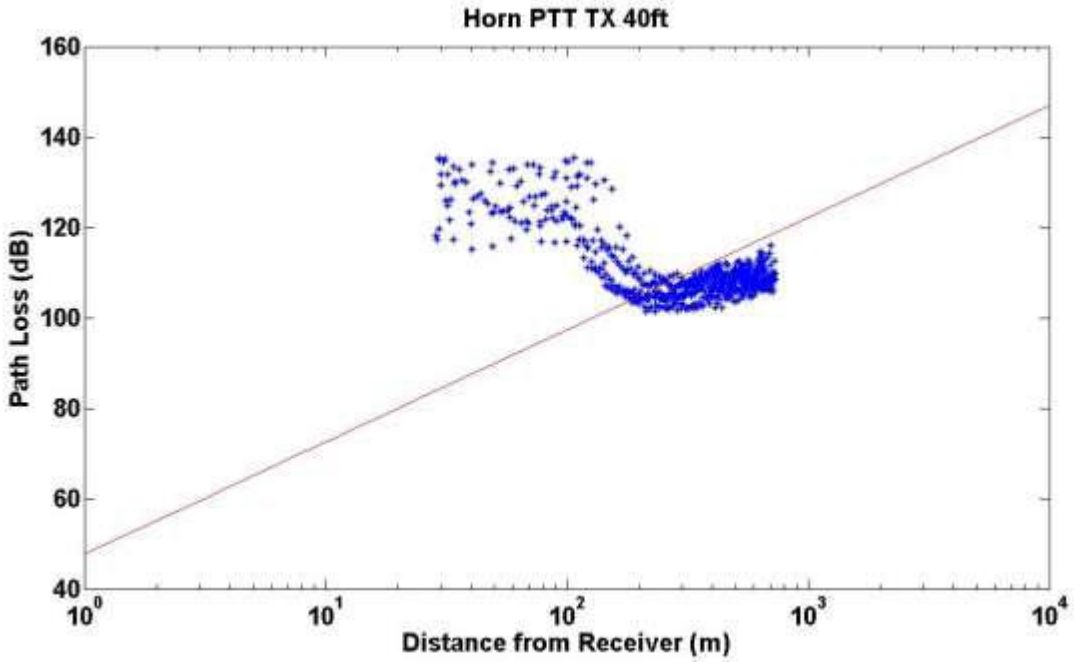

Figure 83 Path loss model for the horn antenna at 40ft

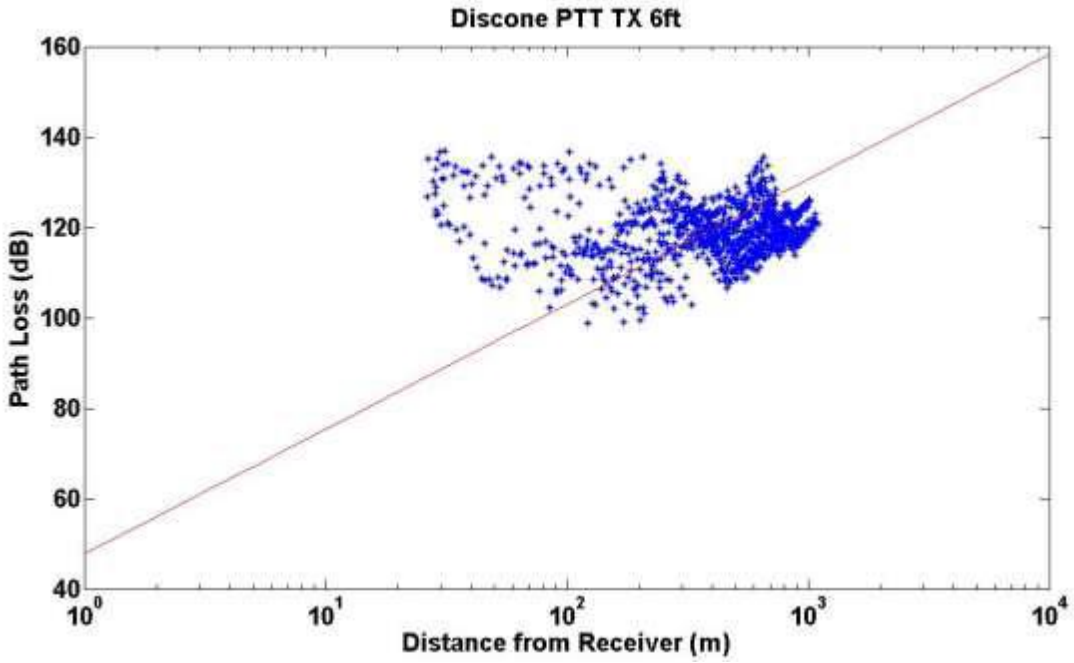

Figure 84 Path loss model for the discone antenna at 6ft

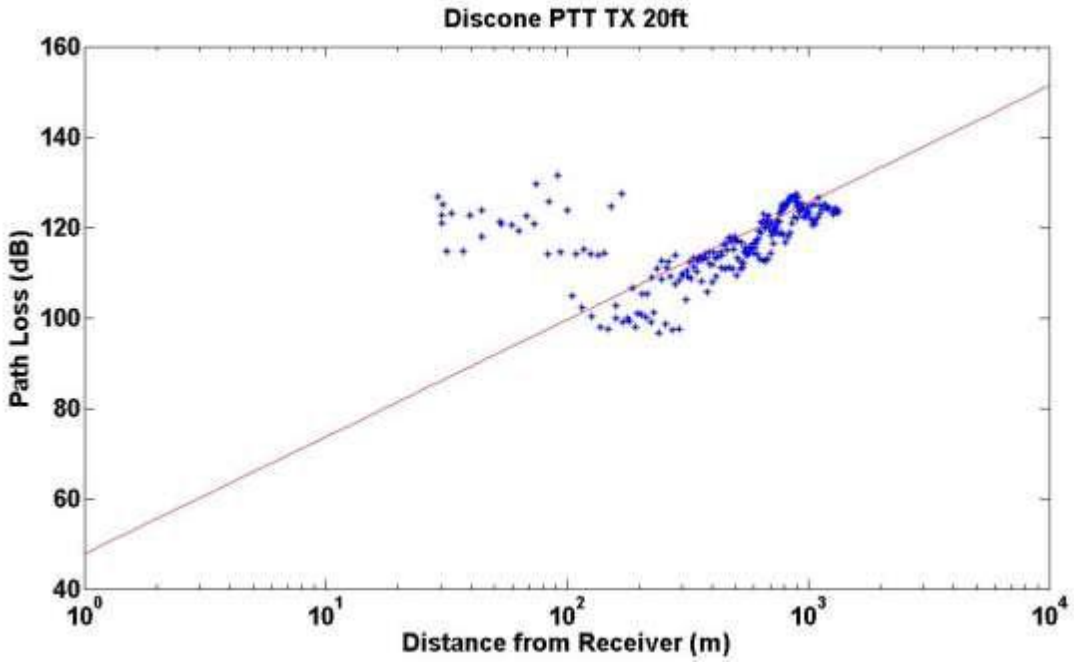

Figure 85 Path loss model for the discone antenna at 20ft

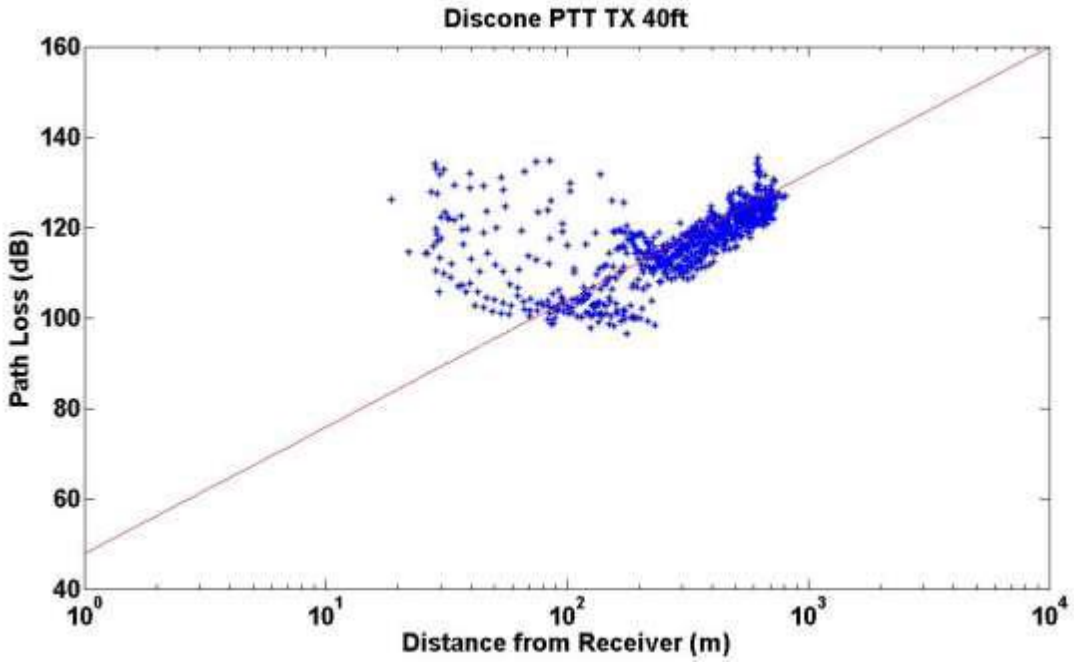

Figure 86 Path loss model for the discone antenna at 40ft

A.5 Small Scale Fading Model Results

Ricean models were chosen because the propagation environment did not show the severe fading effects where different K values were needed for different distances away from the receiver as suggested in literature. Instead the K values were generally consistent and were taken as an average for each speed of the conducted tests. The K values are generally consistent across the entire track that is made evident by the lack of change in color across the plots. The K-factors suggest that there is a line of sight component that is present which is expected because the RTT test site had minimal obstructions.

Table XX Average Ricean K-Factors (dB)

Antenna	20 mph	50 mph	79 mph
Discone	10.89	9.76	11.31
Horn	14.00	11.01	10.70

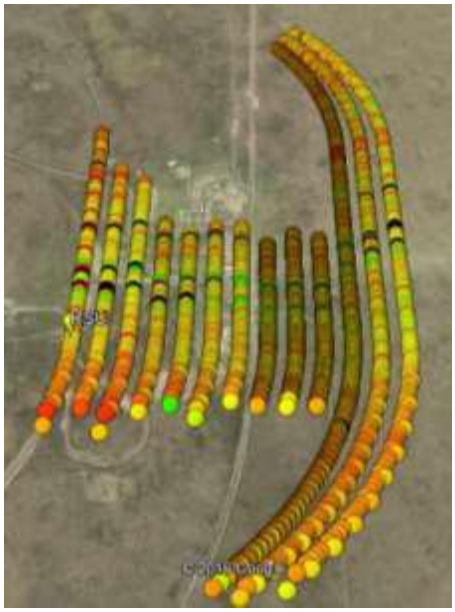

Figure 87 Google Earth plot of K values in dB

Appendix B: TTCI RSU PER Results

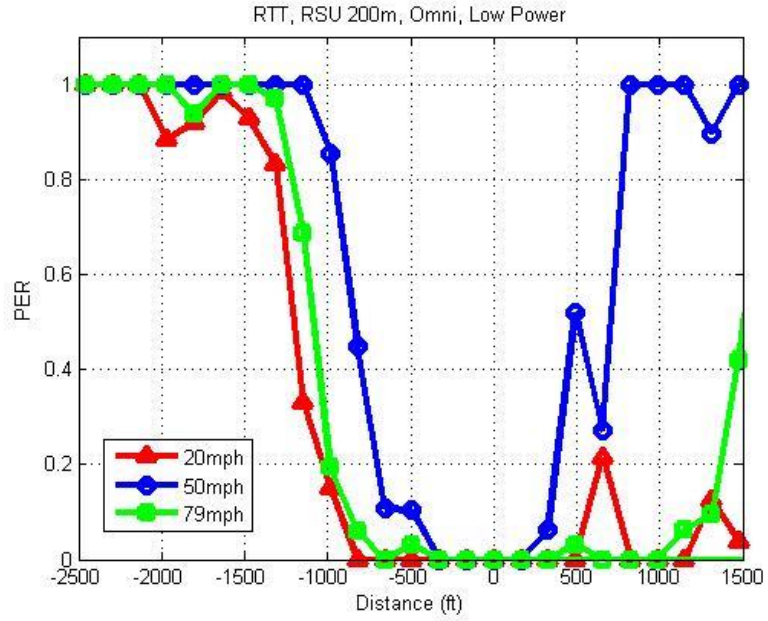

Figure 88 RTT RSU Omnidirectional Low Power 200m from crossing

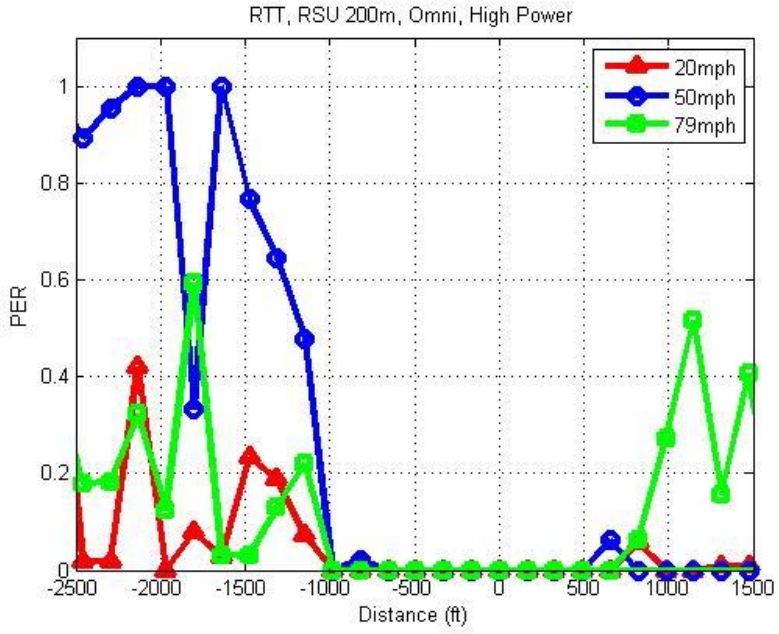

Figure 89 RTT RSU Omnidirectional High Power 200m from crossing

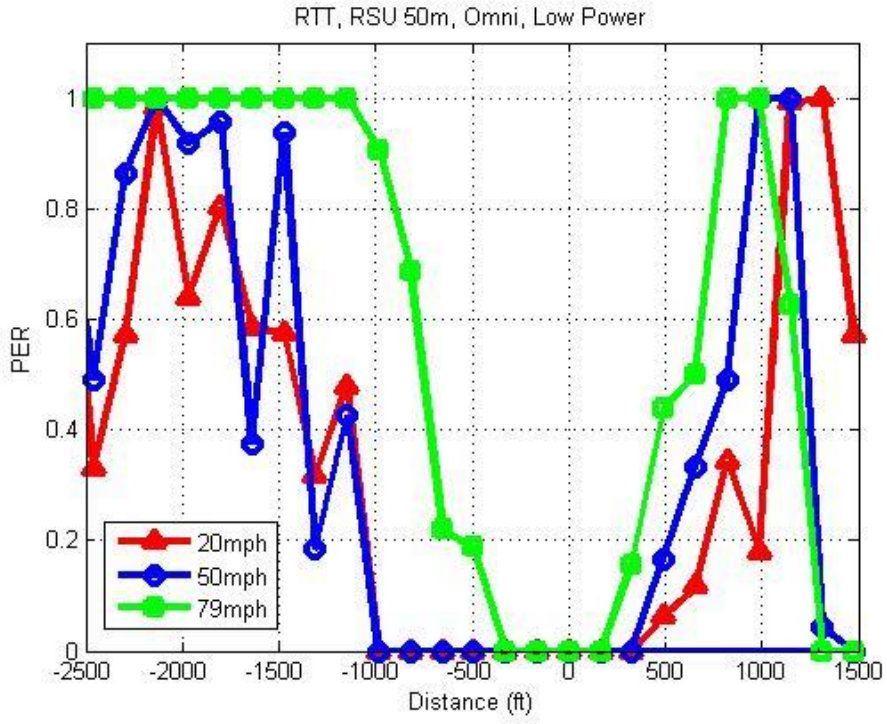

Figure 90 RTT RSU Omnidirectional Low Power 50m from crossing

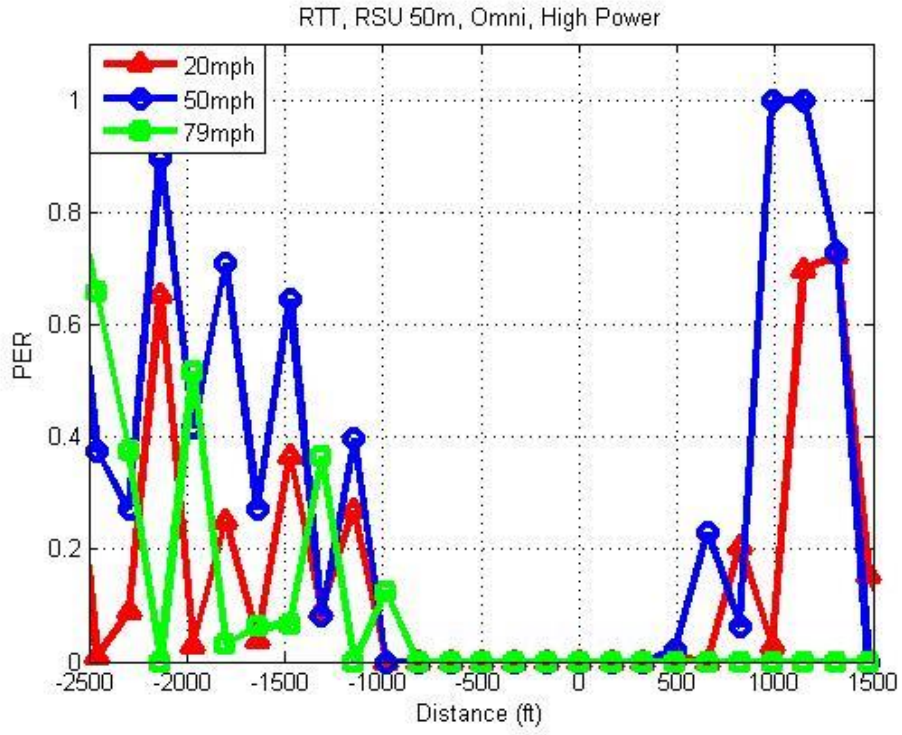

Figure 91 RTT RSU Omnidirectional High Power 50 m from crossing

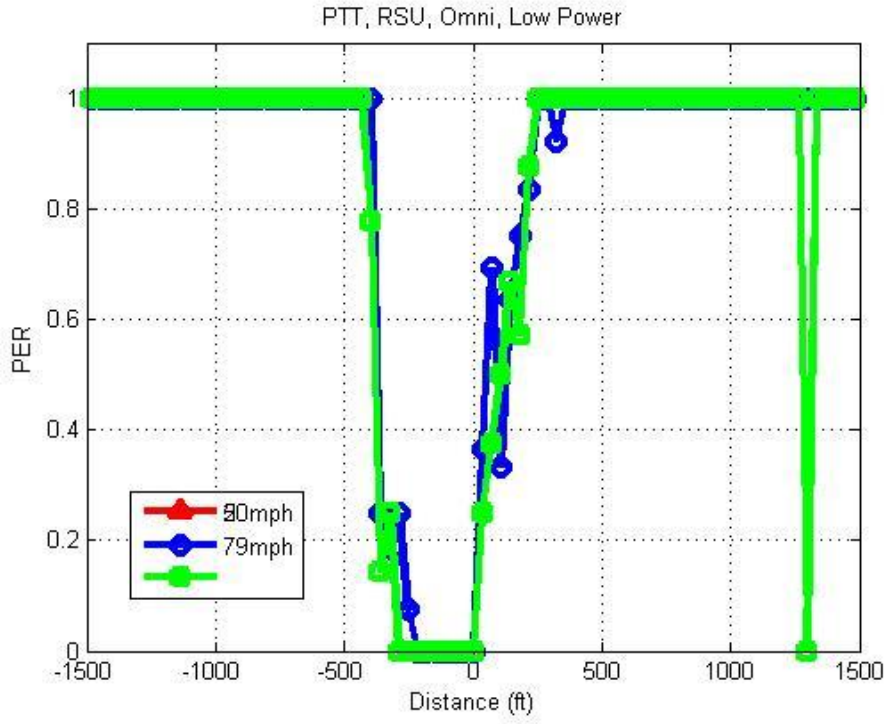

Figure 92 PTT RSU Omnidirectional Low Power

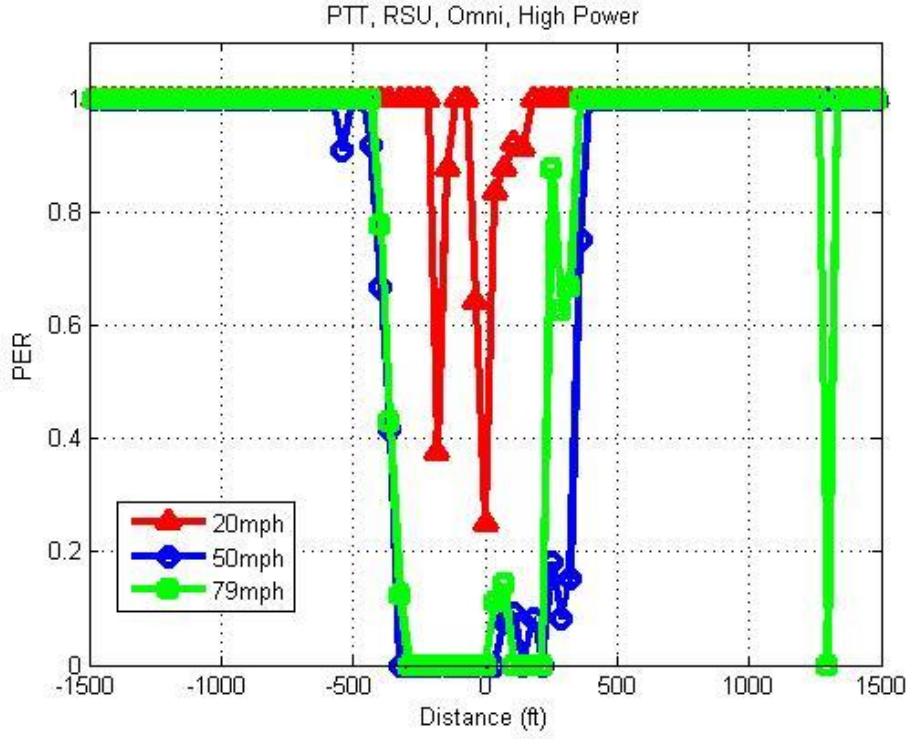

Figure 93 PTT RSU Omnidirectional High Power

Appendix C: Validations of DSRC and Interference Signals

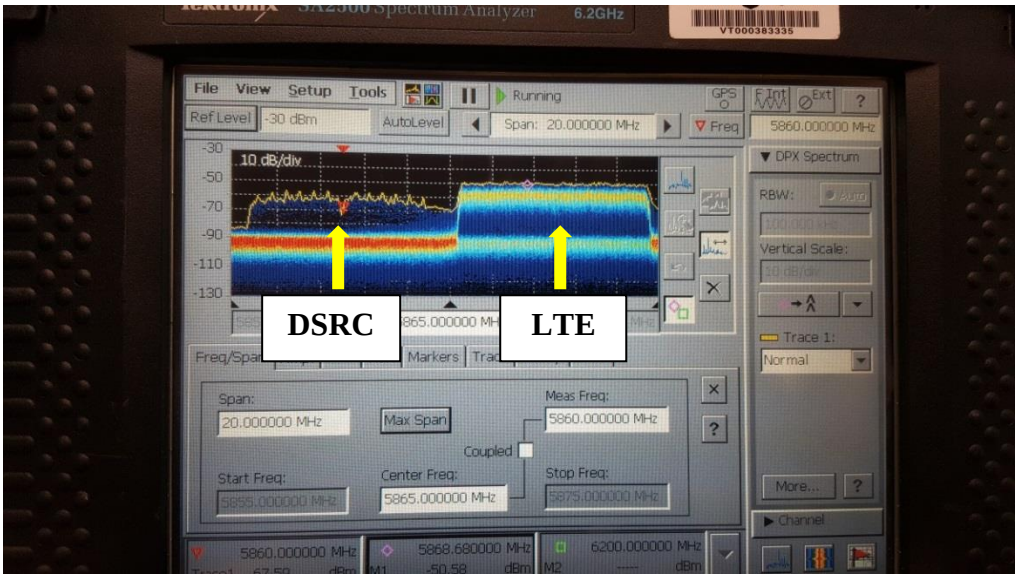

Figure 94 Spectrum Analyzer Photo for DSRC Signal (ch 172) and LTE Signal (ch 174)

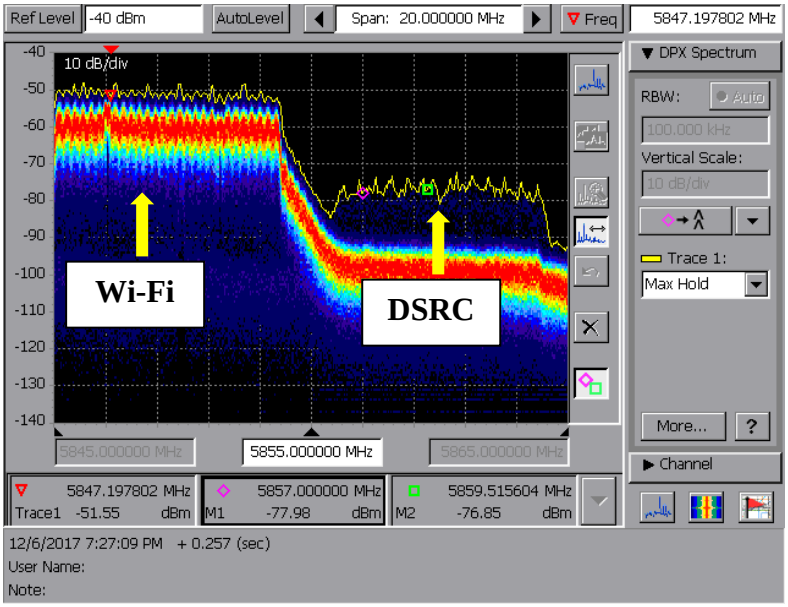

Figure 95 Validation of 20 MHz Wi-Fi and DSRC Signal

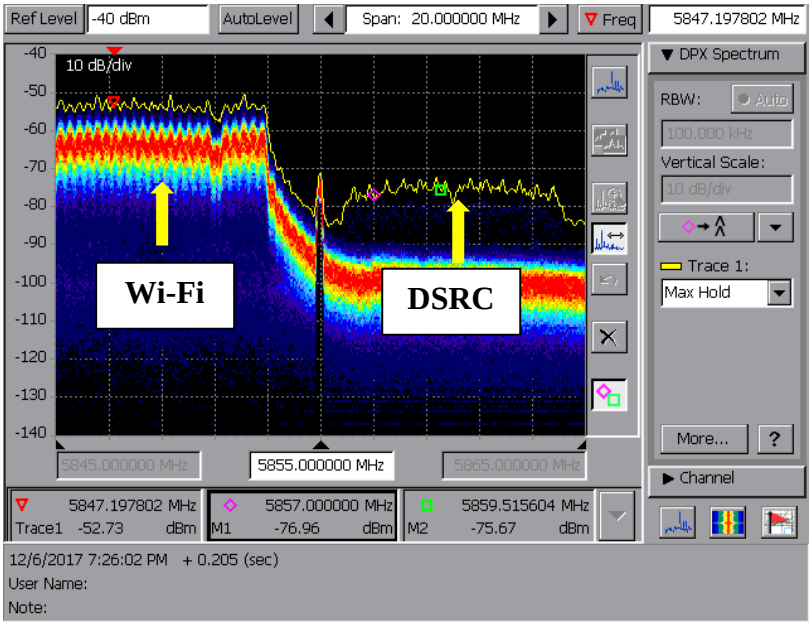

Figure 96 Validation of 40 MHz Wi-Fi and DSRC Signal

Appendix D: Propagation channel characteristics for each crossings

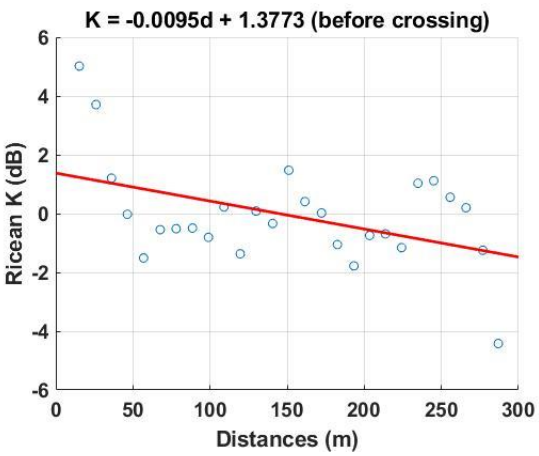

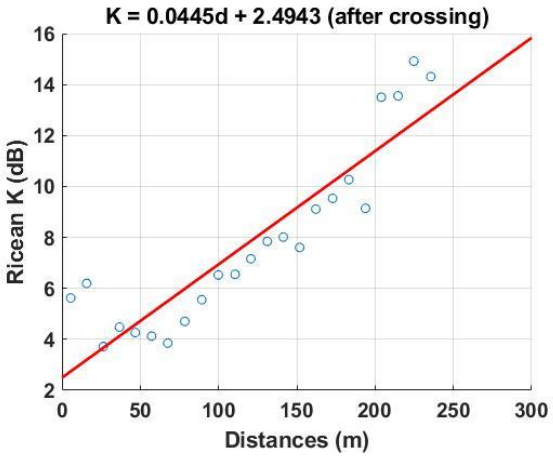

Figure 97 Ricean K for before/after Crossing #3

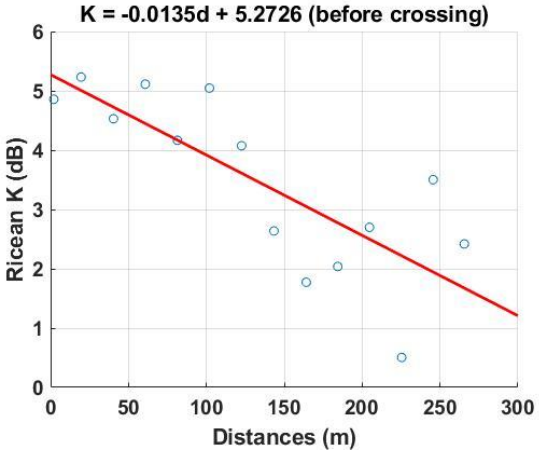

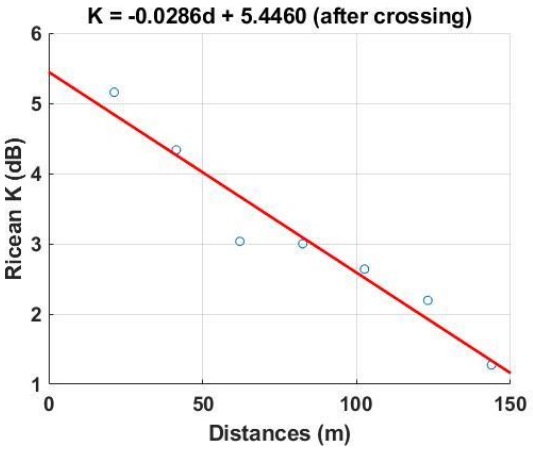

Figure 98 Ricean K for before/after Crossing #4

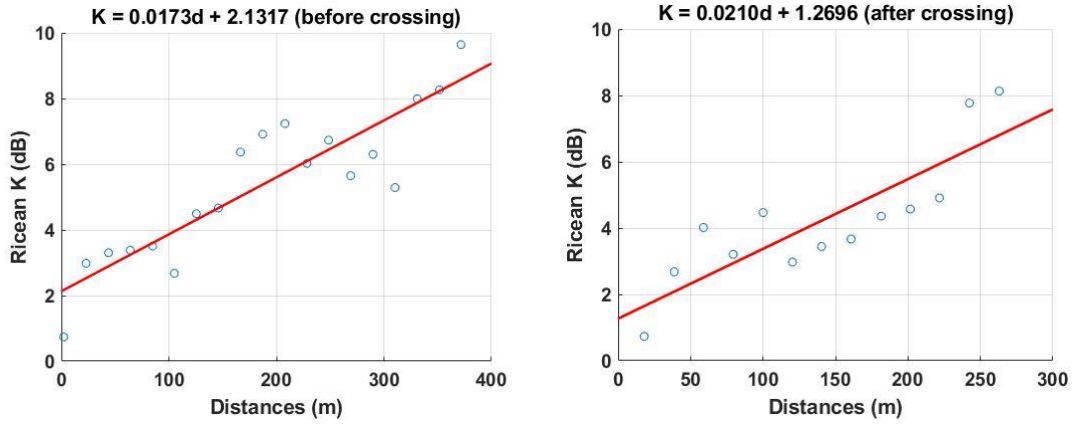

Figure 99 Ricean K for before/after Crossing #6

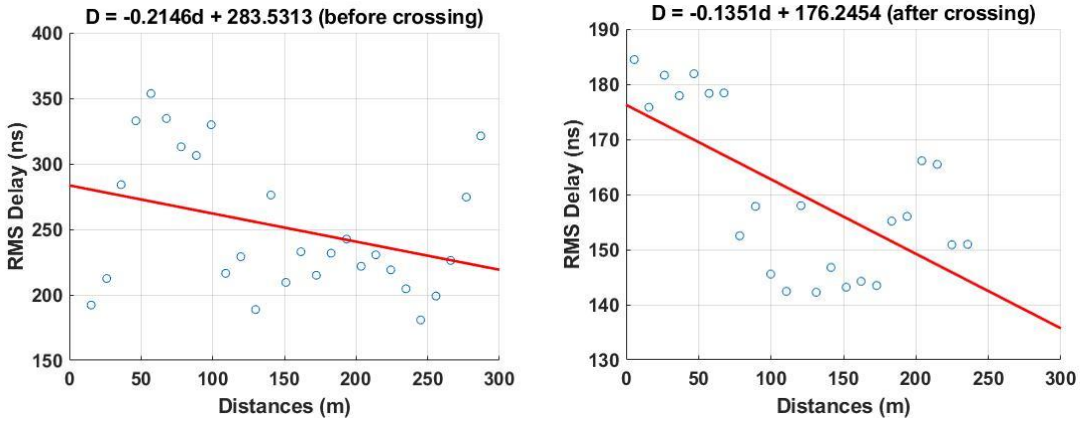

Figure 100 RMS delay for before/after Crossing #3

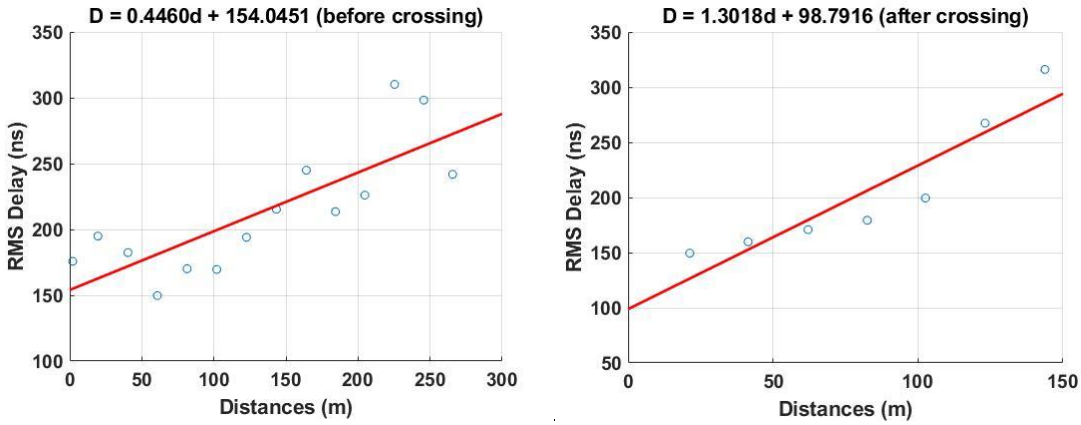

Figure 101 RMS delay for before/after Crossing #4

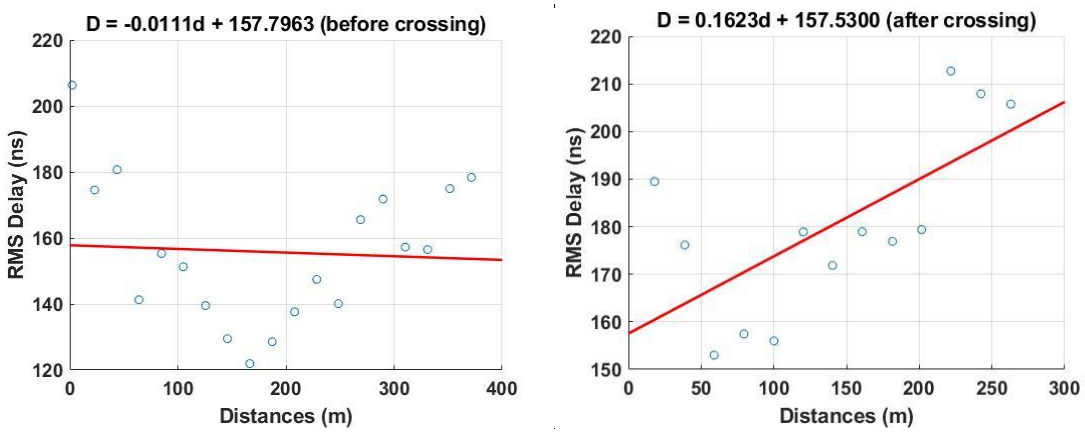

Figure 102 RMS delay for before/after Crossing #6

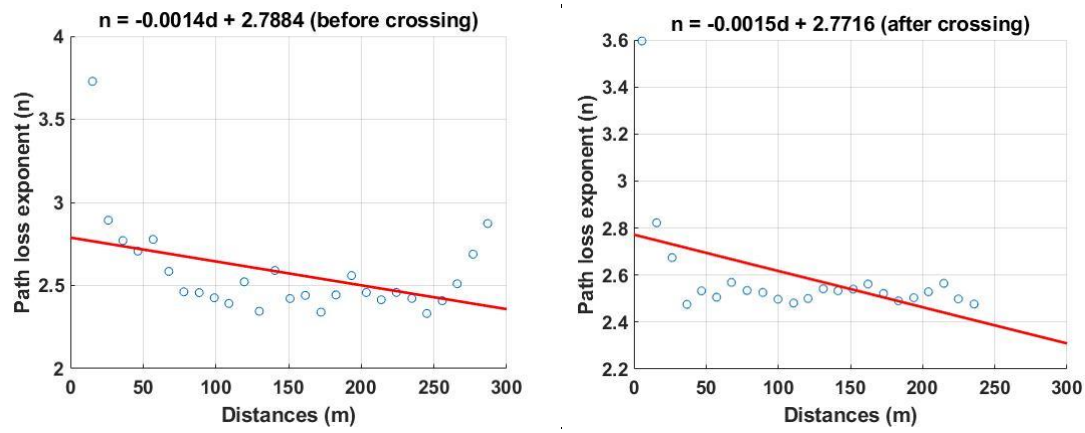

Figure 103 Path loss exponent for before/after Crossing #3

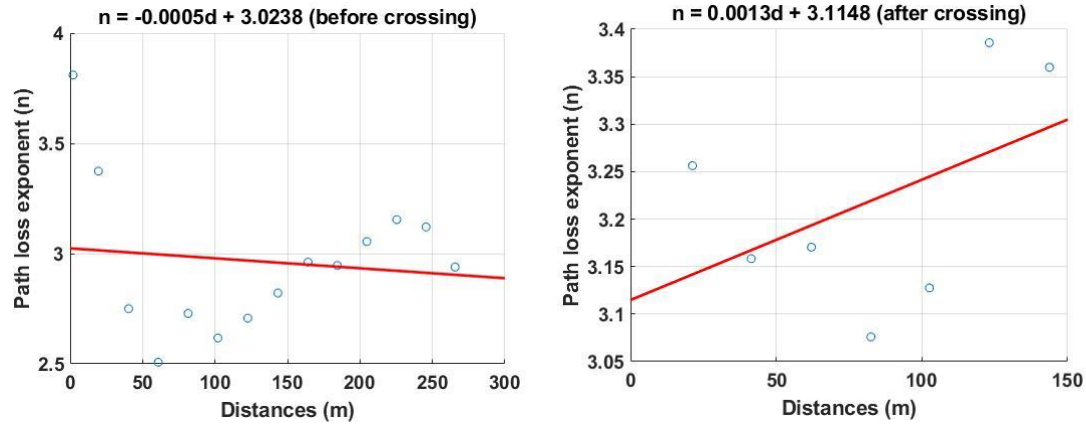

Figure 104 Path loss exponent for before/after Crossing #4

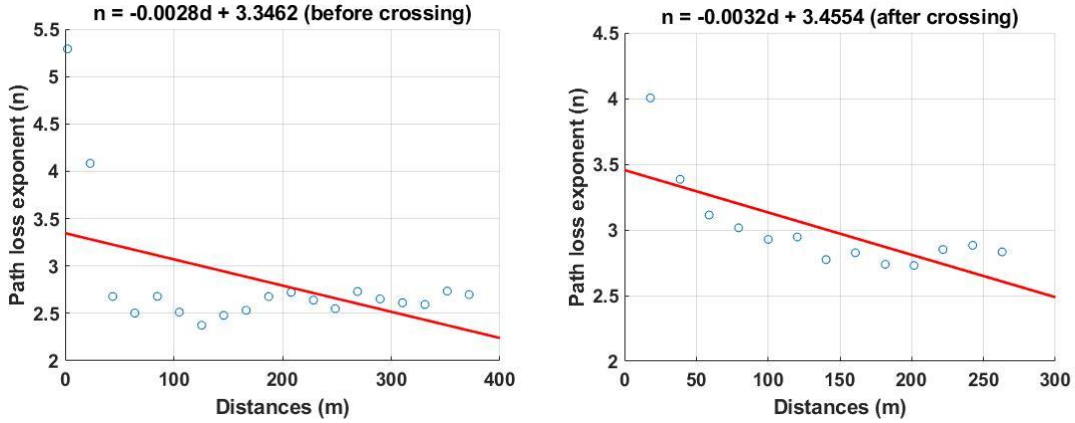

Figure 105 Path loss exponent for before/after Crossing #6

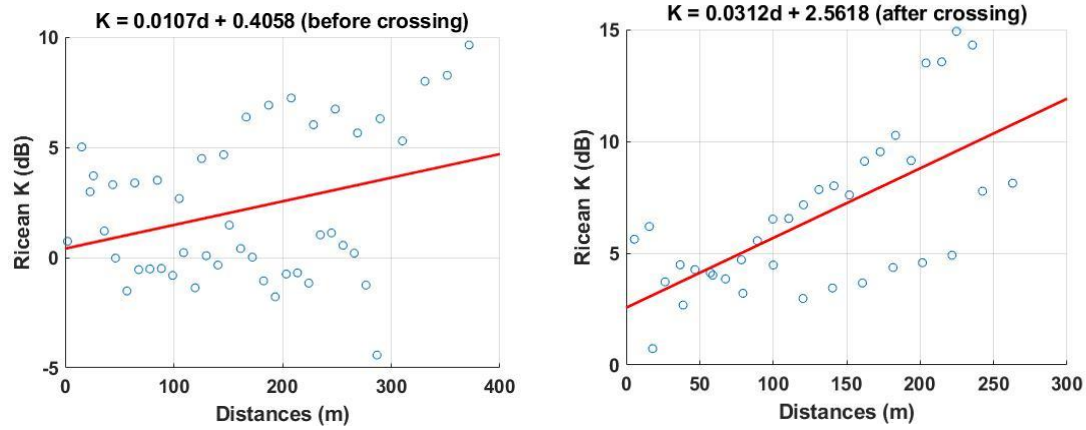

Figure 106 Ricean K for before/after rural crossings

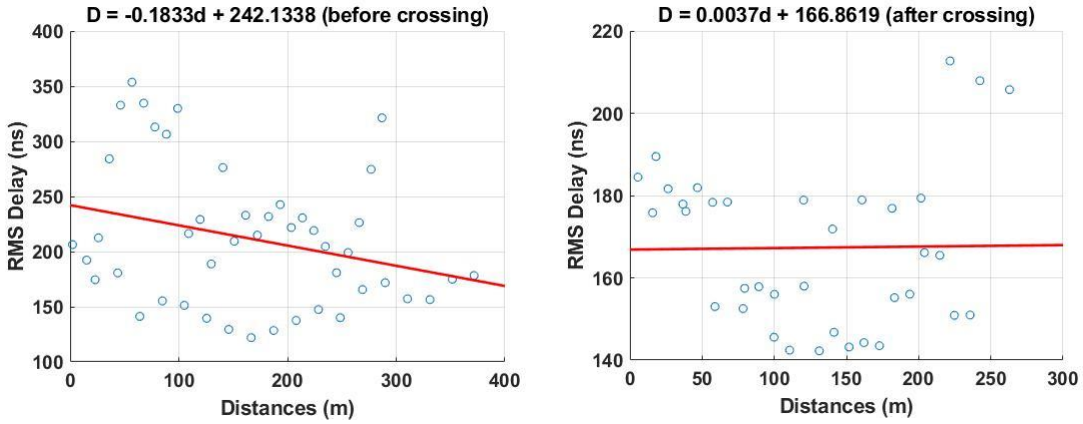

Figure 107 RMS delay for before/after rural crossings

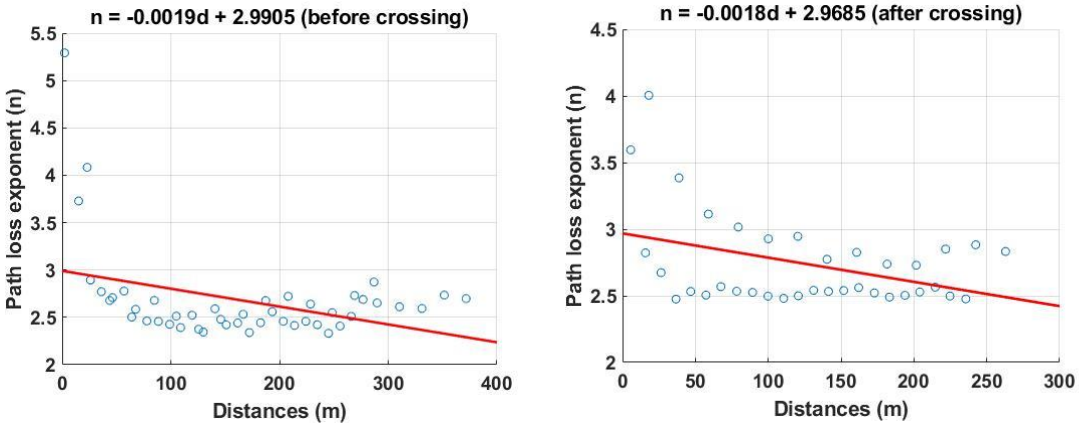

Figure 108 Path loss exponent for before/after rural crossings